SANDIA REPORT
SAND2019-15372
Printed December 2019

Sandia National Laboratories

Big Wheel Farm: Farmland Scour Reduction

Sterling S Olson, Chris C Chartrand, and Jesse D Roberts

Prepared by
Sandia National Laboratories
Albuquerque, New Mexico
87185 and Livermore,
California 94550

Issued by Sandia National Laboratories, operated for the United States Department of Energy by National Technology & Engineering Solutions of Sandia, LLC.

Available to DOE and DOE contractors from
U.S. Department of Energy
Office of Scientific and Technical Information
P.O. Box 62
Oak Ridge, TN 37831

Telephone: (865) 576-8401
Facsimile: (865) 576-5728
E-Mail: reports@osti.gov
Online ordering: http://www.osti.gov/scitech

Available to the public from
U.S. Department of Commerce
National Technical Information Service
5301 Shawnee Rd
Alexandria, VA 22312

Telephone: (800) 553-6847
Facsimile: (703) 605-6900
E-Mail: orders@ntis.gov
Online order: https://classic.ntis.gov/help/order-methods/

ABSTRACT

Flood irrigation benefits from low infrastructure costs and maintenance but the scour near the weirs can cause channeling of the flow preventing the water from evenly dispersing across the field. Using flow obstructions in front of the weir could reduce be a low cost solution to reduce the scour. The mitigation strategy was to virtually simulate the effects of various geometric changes to the morphology (e.g. holes and bumps) in front of the weir as a means to diffuse the high intensity flow coming from the gate. After running a parametric study for the dimensions of the shapes that included a Gaussian, semi-circle, and rectangle; a Gaussian hole in front of the gates showed the most promise to reduce farm field shear-stresses with the added benefit of being easy to construct and implement in practice. Further the simulations showed that the closer the Gaussian-hole could be placed to the gate the sooner the high shear stress could be reduced. To realize the most benefit from this mitigation strategy, it was determined that the maximum depth of the Gaussian-hole should be 0.5 m. The width of the hole in the flow direction and the length of the Gaussian hole normal to the flow should be 0.5 m and 3 m respectively as measured by the full width at half maximum.

ACKNOWLEDGEMENTS

The researchers would like to acknowledge the Small Business Assistance Program for the support and funding to complete this work as well as the guidance and support from Daniel Hutchison, owner and proprietor of Big Wheel Farm.

CONTENTS

LIST OF FIGURES

LIST OF TABLES

This page left blank

EXECUTIVE SUMMARY

This study focused on low cost solutions to help a New Mexico farm reduce scour near the discharge of flood irrigation gates at the head of a crop field. The study investigated several mitigation strategies to diffuse the flow out of the gates and reduce scour inducing shear stresses. The investigations included simulations of various obstructions placed in front of the irrigation gates. Ultimately, do to ease of implementation as wells as its effectiveness, three different geometric depression or hole shapes (e.g. rectangle, semi-circle, and Gaussian) were simulated in detail to better understand their shear stress reducing effectiveness. These shapes were placed in front of the gates to the field and a parametric study was run on the hole shape and location free parameters which included distance in front of the gate, depth or height of the feature, width in the direction of flow, and length in the direction normal to flow.

The results of this study provide guidance on the placement of various types, sizes, and location of obstructions near the discharge of flood irrigation gates for scour reduction. It was shown that the feature should not protrude from the ground but rather be a hole. The semi-circle and Gaussian shapes provided better shear reduction than the rectangle. The Gaussian shape was chosen as it is easier to construct with a backhoe compared to a semi-circle. Further the natural curve into the Gaussian is safer for humans and cattle to navigate, making it less likely to fall into the hole and cause injury. The hole should be placed as close as possible to the gate but not so close as to interfere with the earthen dam. The depth of the hole should be at least 0.5 m deep, 0.5 wide in the direction of flow, and 3 m long in the direction normal to the flow. These minimum dimensions may be increased but show diminishing returns for the increases in the size of the holes.

Lastly the results of a uniquely shaped field were presented which in addition to the scour reduction needed help moving the water to the opposite side of the field from the location of the gates. In this case the same Gaussian solution was applied as before this time rotating the shape 45 degrees counter-clockwise from the y-axis. The results of this simulation showed that it both decreased the shear stress and helped spread water to the previously dry part of the field.

The work presented here is limited in that it focuses on changes to water flow speed, resultant shear stress, and overall water coverage in a farm field caused by changes in depression shapes near the discharge of the irrigation gates. This study does not investigate the dynamics of sediment transport with respect to the field or the earthen dams. These transient effects may lead to observations of different results than those simulated here. Further the simulations are limited as the earthen damns are treated as areas of no flow such that the shear stress on the walls of the dams was not measured. The issue of scour on the dams is a known issue and if considered in further studies, could help derive an optimal solution to this challenging problem.

Future work could investigate sediment transport using Delft 3D's sediment transport module and utilize the water power technologies staff's expertise in this area. Further investigations into the effects on the earthen dams could be studied in detail. These developed models could be further utilized and improved by considering soil infiltration rates to measure the water received by the front of the field and back of the field to optimize infiltration rates.

ACRONYMS AND DEFINITIONS

Abbreviation	Definition
FWHM	Full Width at Half Maximum
QoI	Quantity of Interest
2D, 3D	Two-dimension, three-dimension

1. PROJECT OVERVIEW

The goal of the Big Wheel Farm project was to optimize the flood irrigation system to reduce scour near the front of the weirs. The proprietor completed one season using current flood irrigation system. The flood irrigation system is a common design to multiple fields featuring to 6' by 6' gates supplying 150' wide by 100s of feet long fields. During the season scour was observed near the flood gates as can be seen in **Figure 1-1**. In **Figure 1-1** left the flooding out of one of the 6' x 6' gates can be seen to from the gate which is raised 1' from the bottom creating a 1'x6' flow opening. Each field has two identical weirs, the second one in **Figure 1-1** (left) can be seen by looking for the grey tarp further back in the picture. The high flow out of the gate causes scour which creates ruts in the land as is shown in **Figure 1-1** (right) by the pooling of water near the gate. This process repeated over time creates channels in the ground and prevents the water from dispersing evenly across the 150' wide fields.

Figure 1-1. Picture of flooding from irrigation system (left) and scouring of the land in front of the gates (Provided by Big Wheel Farm)

1.1. Flood Irrigation Procedure

Big Wheel Farm totals 60 acres with 20 gates serving about 10 crop fields as shown in **Figure 1-2**.

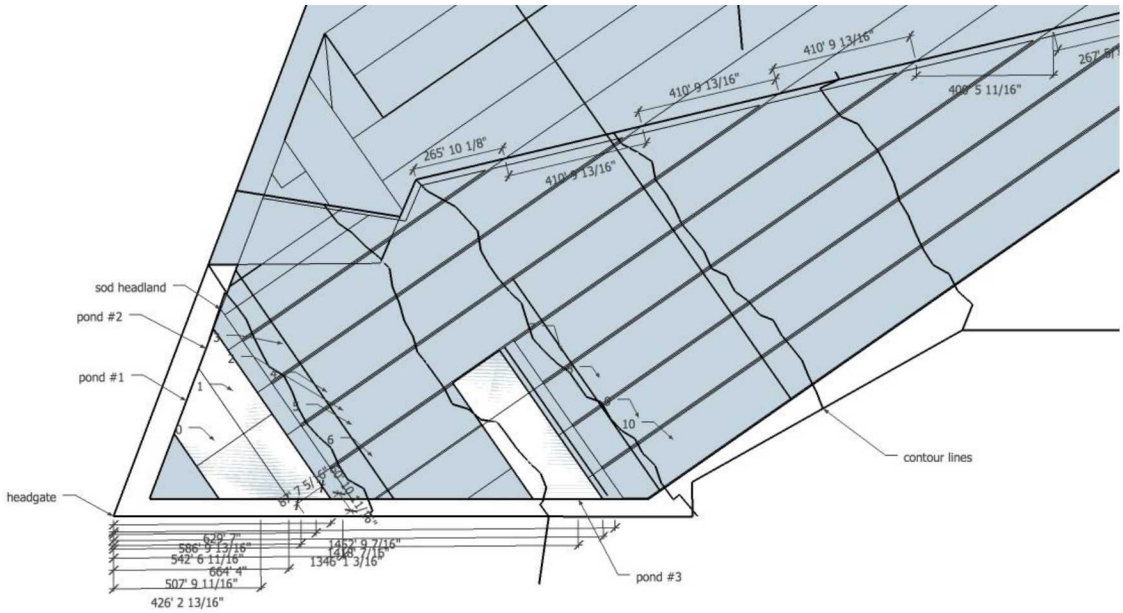

Figure 1-2. Plan View of Farm (Provided by Big Wheel Farm)

The flood irrigation system for the farm works for one field at a time by opening the two gates (**Figure 1-3**) that feed into the desired plot of land. The two gates are each connected to pond #2 (**Figure 1-2**) and which lift from the bottom up. Pond #2 has 20" (0.5 m) of head and the gates are raised up 1' (0.3 m) from the bottom. The head in pond #2 is maintained constant at 20" by opening the gates from pond #1 until pond #1 depletes the water source which takes about 30 minutes.

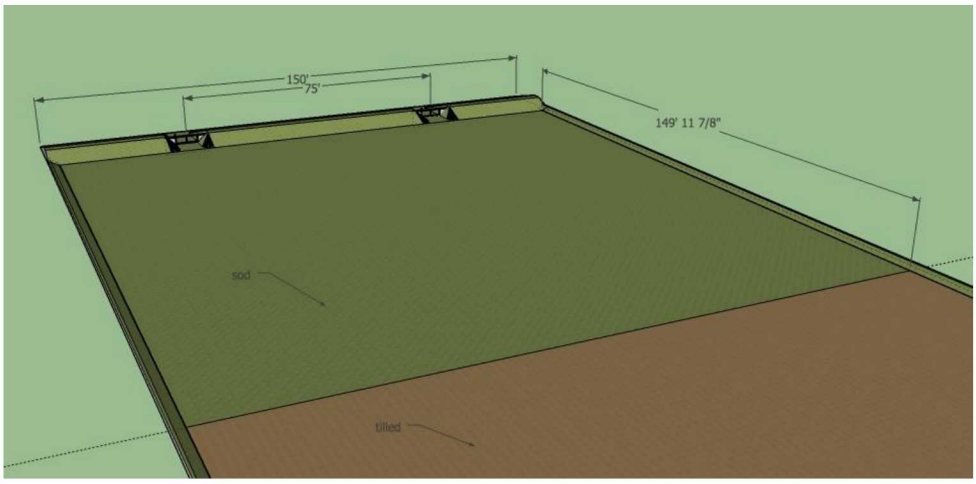

Figure 1-3. Isometric view of representative farm channel (Provided by Big Wheel Farm)

In addition to the standard square plot there was a plot of land with a two-gate flood irrigation system with a modification to the standard configuration as shown in **Error! Reference source not found.**. In this variation scour near the gates was an issue but diffusion of the water across the 150' wide field was an additional issue. The embankment comes off the south end of the earthen dam holding the gates at a 45-degree angle.

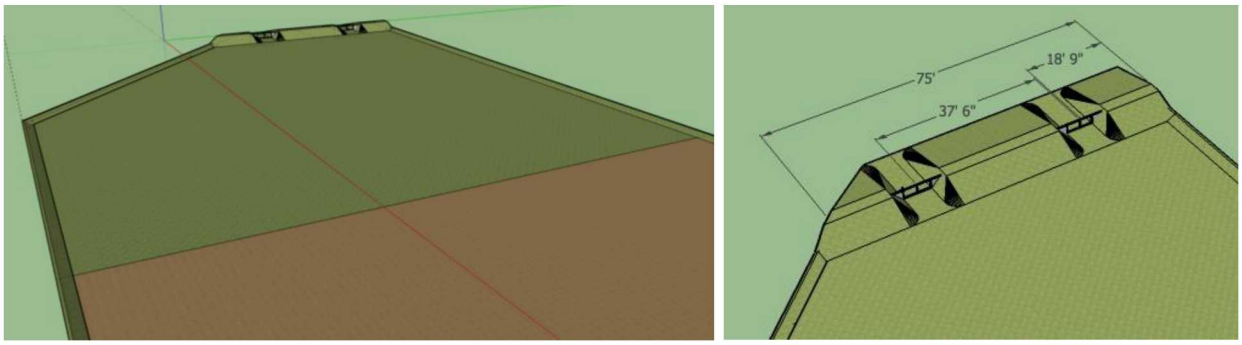

Figure 1-4. Isometric view of variation of the standard configuration (Provided by Big Wheel Farm)

1.2. Solution Approach

The goal of this project was to test the effects of scour reduction features near the outlet of the flood irrigation gates using computational fluid dynamics (CFD). CFD was chosen for its ability to quickly and cheaply iterate proposed solutions. The proprietor proposed an initial solution of a small channel in front of the irrigation gates. This solution was inspired by a tractor wheel which became stuck in the rut in front of the gate creating a small trench normal to the direction of flow. The team was asked to test different shape profiles, some potential solutions of interest were provided by the proprietor as shown in **Figure 1-5**.

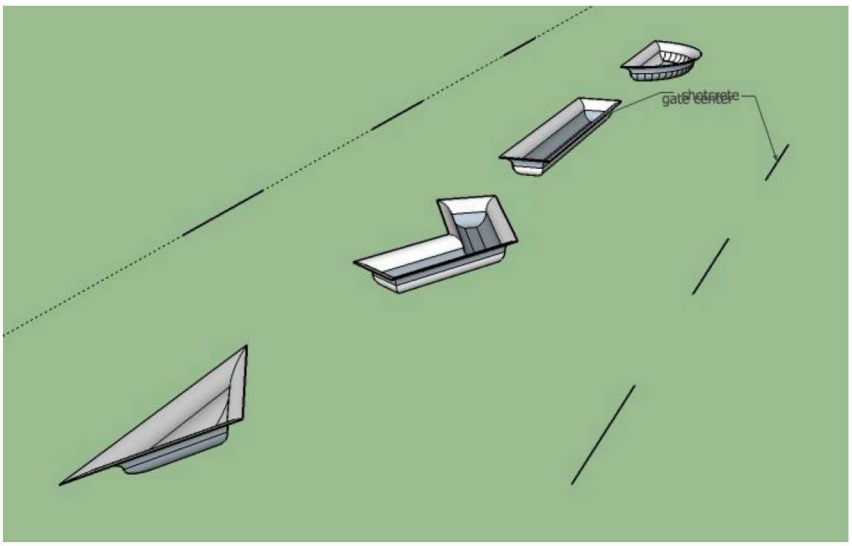

Figure 1-5. Isometric view of proposed flow obstructions for shear stress reduction to placed in the ground in front of the gates (Provided by Big Wheel Farm).

The chosen CFD software was the environmental modeling tool Delft-3D. Delft-3D is a hydrodynamic simulation program developed by Deltares [3]. It is a fully integrated computer software suite for a multi-disciplinary approach for 1D, 2D and 3D computations for coastal, river and estuarine areas. It can carry out simulations of hydrodynamic flow, waves, water quality and ecology. Key features of the software include:

- River flow simulations.

- Rural channel networks
- Time varying sources and sinks (e.g., river discharges)
- Robust simulation of drying and flooding of inter-tidal flats and river winter beds
- Non-linear iterations in the solver can be enabled for accurate flooding results.
- Optional facility for special structures such as pumping stations, bridges, fixed weirs and controllable barriers (1D, 2D and 3D)
- Domain partitioning for parallellized runs on MPI-based High Performance Computing clusters.

2. METHODOLOGY & MODEL SETUP

This section details the setup and definitions of the computational model. This includes the simplifications and choices taken to represent the "real world" in a computer simulation. The farm was represented as a two-dimension (2D) model of the "sod area" (**Figure 1-3**) with a 10 m (38.2') area behind the gate representing pond #2 (**Figure 1-2**). The left side of the pond was held constant at 0.508 m (20"). The width of the farmland was modeled in the y-direction as a 46m (150'). The gates were modeled using Delft-3D's built in fixed-gate feature defined as 6' (1.83 m) high by 6' wide with a 1' (0.3048 m) opening at the bottom. The earthen dams between the gates holding the water (**Figure 1-1**) were modeled as "Dry Areas" which allowed no flow through the grid cells within the defined area. Finally, a constant grade of 1.5% was applied starting at the gate to the end of the field in the direction of flow (x-axis) as specified by the proprietor. Lastly on the right-hand side of the domain a constant gradient boundary condition was applied such that flow could exit the domain.

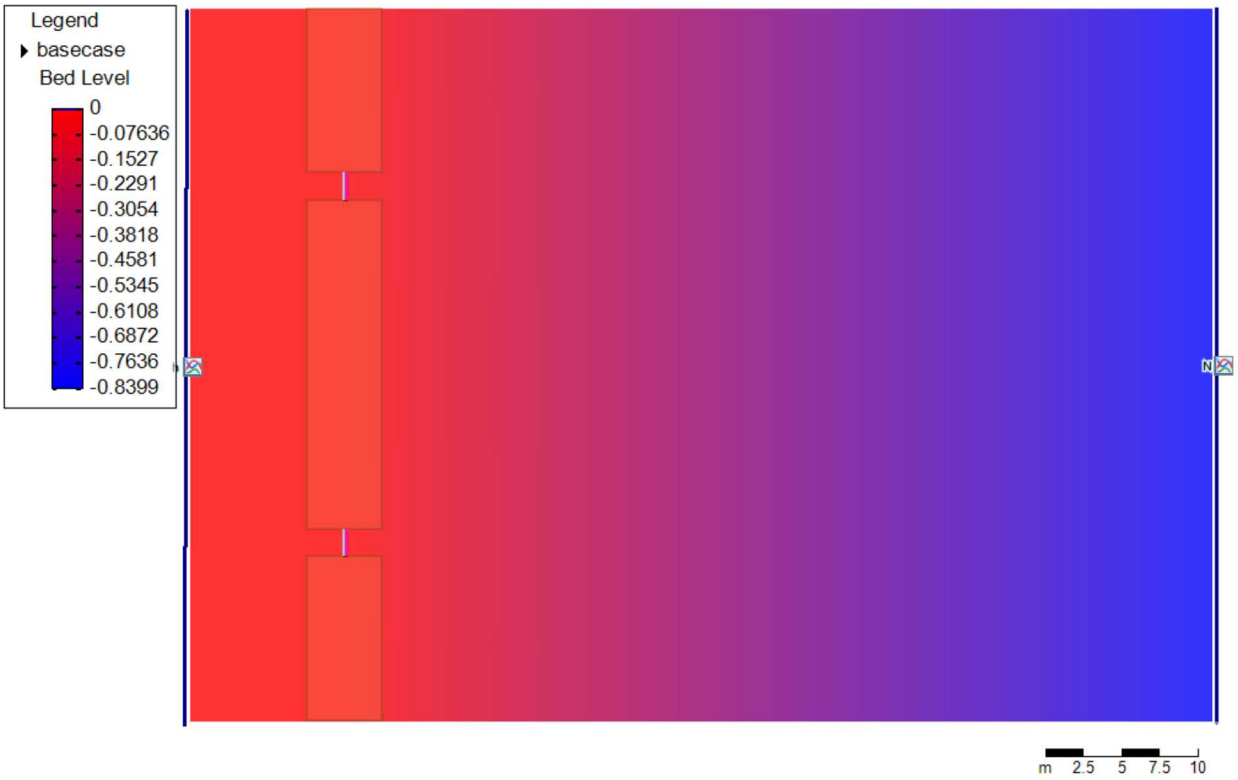

Figure 2-1. Delft-3D model view showing boundary conditions (constant water height left, constant gradient right), gates (2 white lines), Dry Areas (3 yellow boxes), and contour of 1.5% Grade applied to the field starting at the gate location.

The discretized domain was constructed to enable scour reduction testing in front of the gates through the modification of the bathymetry. Therefore, the area of the gate and directly in front of it was identified as the area of interest and was discretized to be have the highest resolution. The original domain was constructed to be 56 m by 46 m with an unstructured grid created in a cartesian shape with a 0.5 m discretization. A two-times (2x) grid refinement was applied three times, each time nested into a slightly smaller area as shown in **Figure 2-2**. This created a largest to smallest grid discretization of 0.5 m, 0.25 m, 0.125 m and finally 0.0625 m in the area around the gate. The higher

resolution around the gate allowed for study of highly defined diffusion structures and resolution of the water in in that area.

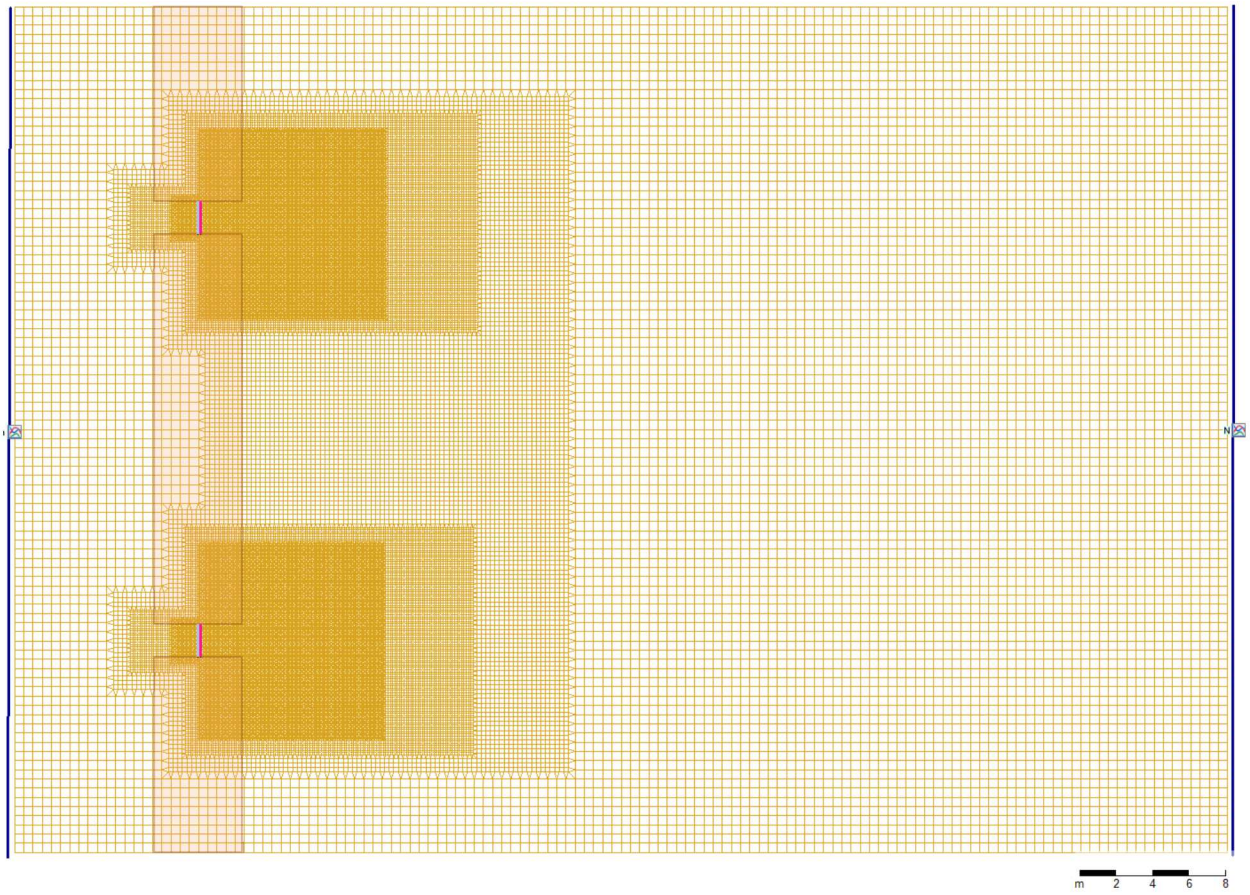

Figure 2-2. Delft-3D Model grid showing 4 levels of discretization with the smallest discretization of 0.0625 m and largest of 0.5 m

A similar procedure was followed for the edge case shown in **Figure 2-3** and **Figure 2-4**. In this case the boundary conditions are the same with a 20" (0.508 m) constant water height on the left side of the domain, and a constant gradient on the right side of the domain. The two 6' by 6' gates are shown as white lines in **Figure 2-3** surrounded on either side by no flow areas marked by yellow rectangular boxes. The edge on the south side of domain comes off as a 45-degree angle from the edge of the earthen dam. The proprietor specified the grade for the edge case field to be 1% and this grade was applied starting at the gates.

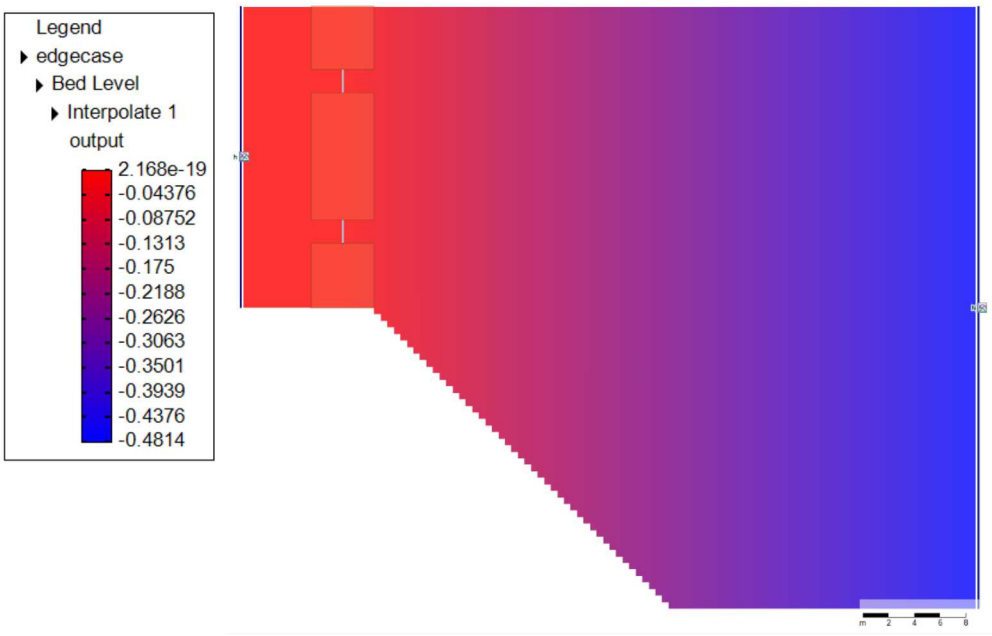

Figure 2-3. Delft-3D edge case model showing boundary conditions (constant water height left, constant gradient right), gates (2 white lines), Dry Areas (3 yellow boxes), and contour of 1.0% grade applied to the field starting at the gate location.

The solution approach was to determine the shape of the design using the standard case and then modify that design for the edge case. Therefore, the grid here was slightly less discretized because this model domain was run after determining the necessary dimensions on the base case. Here the discretization approach was similar in that it was initialized with a constant 0.5 m discretization in both the a and y-directions. Then a series of two nested 2x refinements were performed near the gate locations resulting in even grid discretization of 0.5 m, 0.25 m, and 0.125 m for the three zones visible in **Figure 2-4**

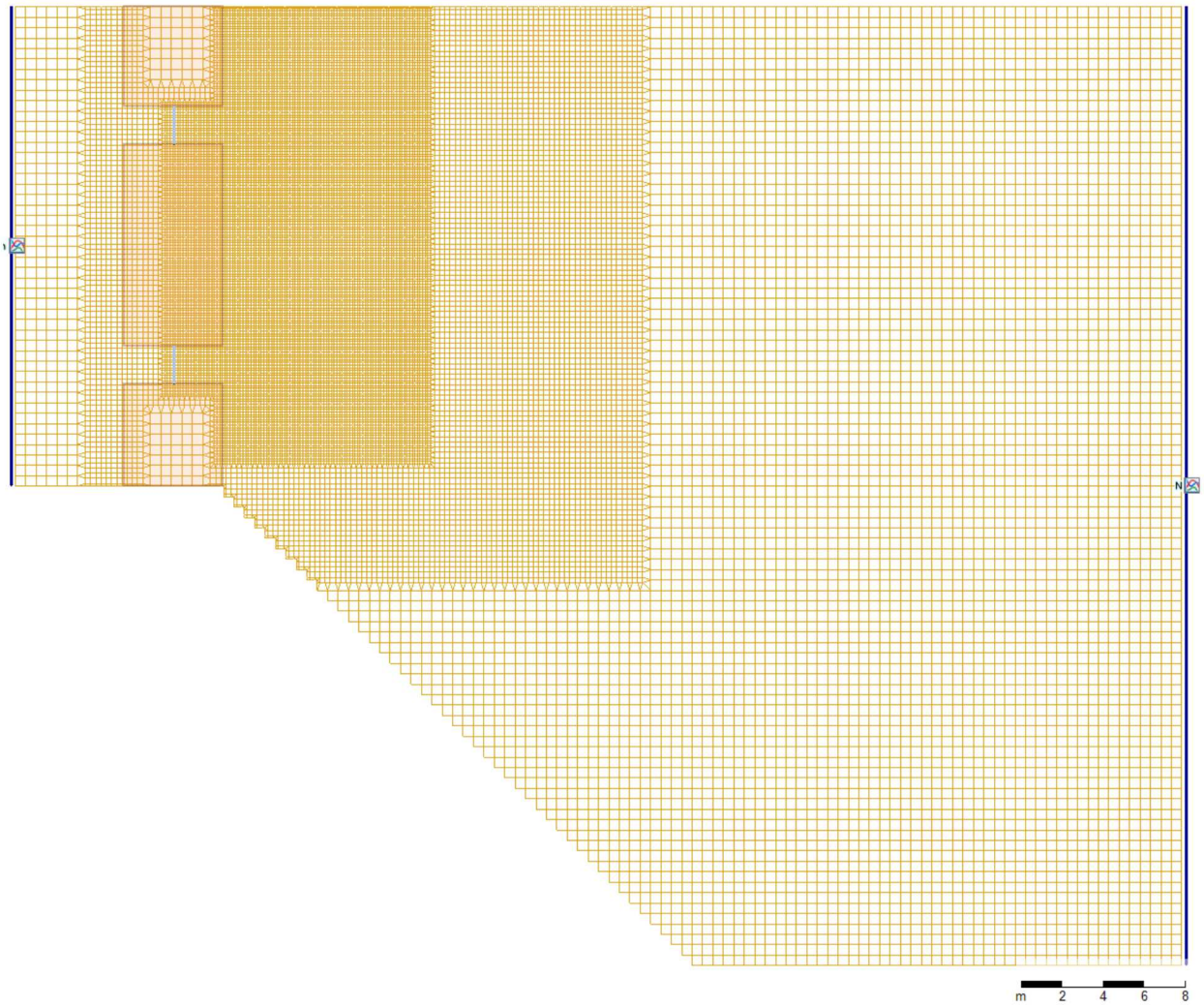

Figure 2-4. Delft-3D edge case grid showing 3 levels of discretization with the smallest discretization of 0.125 m and largest of 0.5 m

3. INITIAL MODEL RESULTS

The initial model results for both the base case and edge case are present in this section as a reference point for modifications going forward. The quantities of interest (QoIs) presented in the results are water depth, magnitude of water velocity (speed), and bed shear stress. Ideally the water will spread to a thin even layer at a low enough speed to not cause significant shear stress. Effects not captured by the model are the unevenness of the tilled farmland which will increase the spreading of the water. The model incorporated a bed roughness using a Manning coefficient of 0.035 typical of floodplains/ pasture farmland [2]. The QoIs for the base case are presented in **Figure 3-1** through **Figure 3-6** as contours and cross-sections of the contours.

Figure 3-1 shows the base case water depth [ft] results for the farm field at 99 seconds into the simulation. This time was approximately when the water reached the end of the modeled domain. Looking to the end of the modeled field (right side) the round shape caused by the diffusion out of the gates can still be observed in the corners and middle as 0 ft water depth (dark blue). Moving backwards from end of the field the typical water depth is about 2". In the area on the right of and nearest to the earthen dams (3 brown rectangles) the water can be seen not meeting along the centerline between the two dams until approximately 30' down the field. **Figure 1-1** (left) shows this to be an invalid result. However, the model is demonstrating the expected behavior as the ground here should be thought of more as a sloped parking with a very rough surface. Coming out of the two gates the water mostly moves with the grade of the land but diffuses laterally some due to the height of the water and roughness of the land. The reality of the non-constant nor homogenous surface observed in **Figure 1-1** (right) is not captured by the model. However, for the purposes of this exercise it does not need to as the focus is on reducing shear stress near the gates.

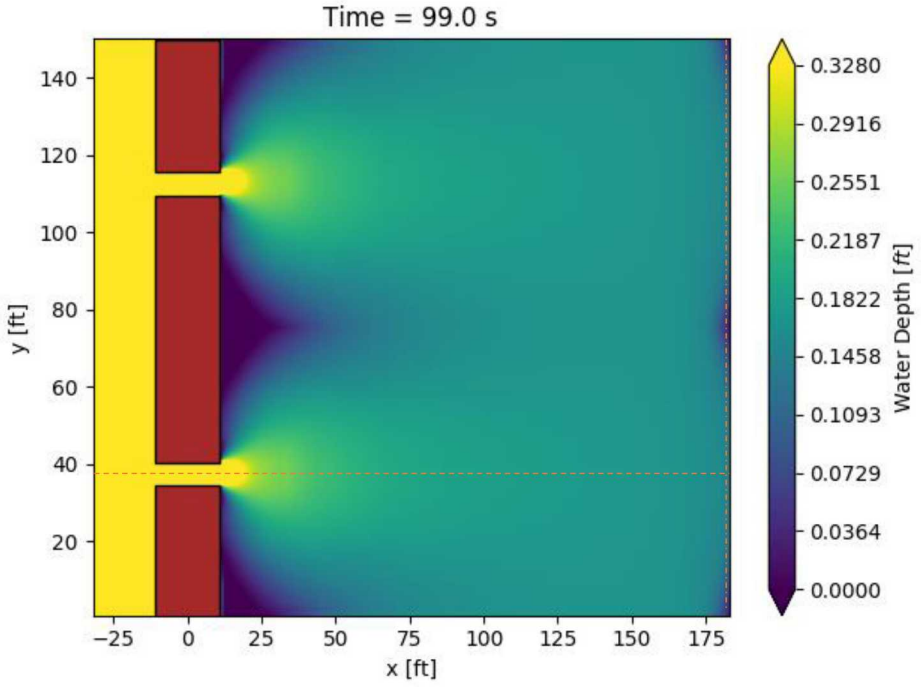

Figure 3-1. Base case simulated results for water depth [ft] prior to shear stress reduction techniques. Orange dashed lines represent cross-sections shown in Figure 3-2.

Two cross-section views of the data in **Figure 3-1** were plotted through the south gate location (y = 37.7', orange dashed line) and at the end of the field (x = 183', orange dash dot line). The water depth results along the orange lines are shown in **Figure 3-2**. The left cross-section shows the development of the water depth down the field through the gate. Prior to exiting the gate, the boundary condition specifies the pond height to be a constant 20" (0.508 m). The water depth drops as it approaches the gate at x = 0', then slowly decreases for the first 10' out of the gate. After 10' the water decreases more quickly from 0.8' to 0.3' after which the water depth slowly decreases to 0.16'. The right cross-section of **Figure 3-2** shows what the front part of the water flow out of the gate 183' down field is predicted to behave by the simulation. The water depth is not predicted to be uniform.

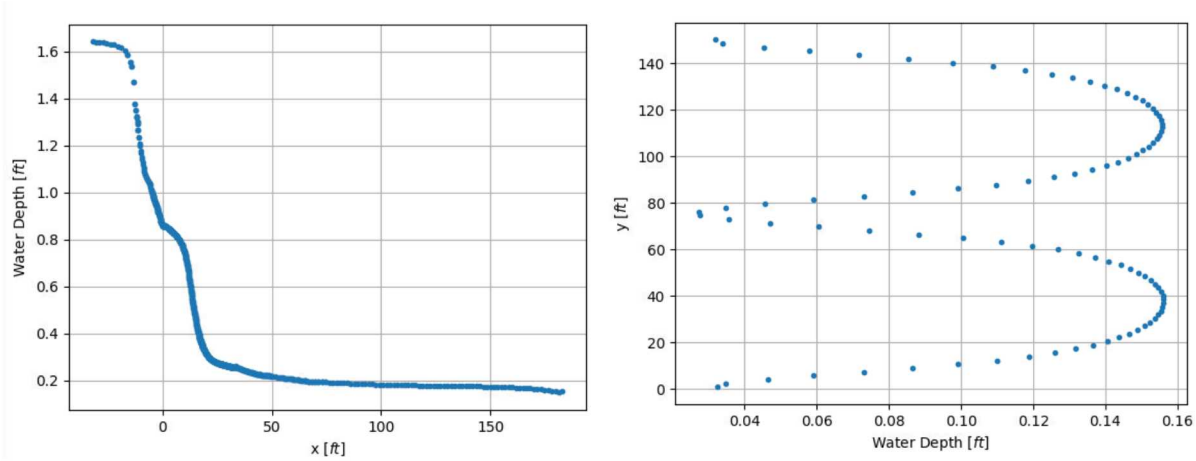

Figure 3-2. Base case water depth cross-section at y =37' (left) and x = 183' (right) as shown in Figure 3-1 as an orange dashed line and orange dash-dot line respectively.

The velocity magnitude is shown in **Figure 3-3** at the same time (99 seconds) as **Figure 3-1**. The plot shows that the velocity is highest near the exit of the gates and decreases to an even speed of about 2 ft/s at about 100' downstream.

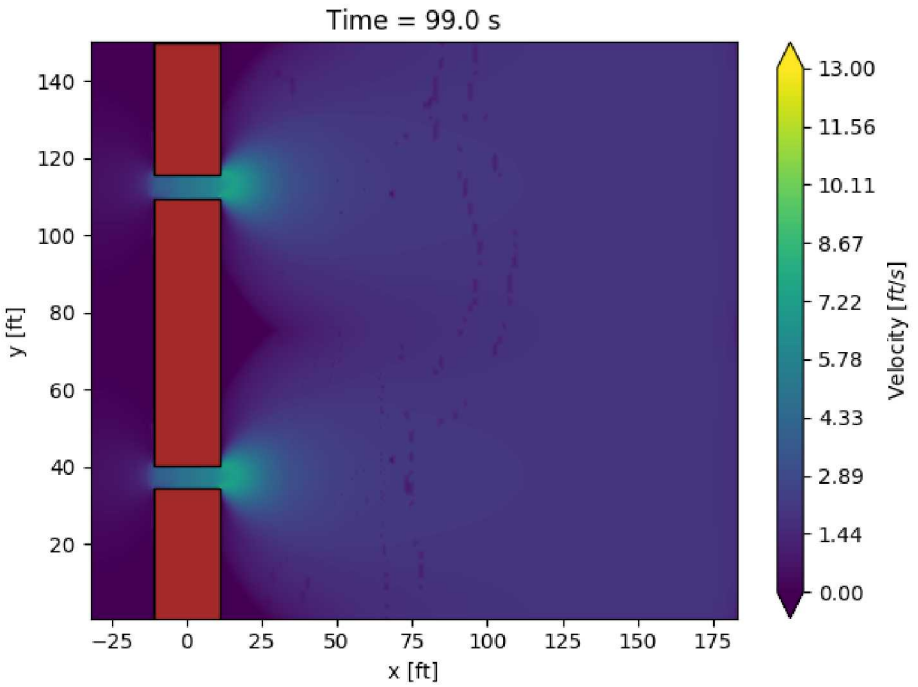

Figure 3-3. Base case showing simulated water speed results prior to shear stress reduction techniques.

The cross-section of velocity is shown in **Figure 3-4** at the same locations as those shown by the orange lines in **Figure 3-1**. The cross-section moving through the gate and down the field (left) shows that out of the gate the water is moving at about 5 ft/s (1.5 m/s) and the increases to 7 ft/s (2.1 m/s) as the water spills out of the earthen dam area. The velocity cross-section on the right shows that the velocity is generally traveling at 1.75 ft/s at the front of the water column moving down the field.

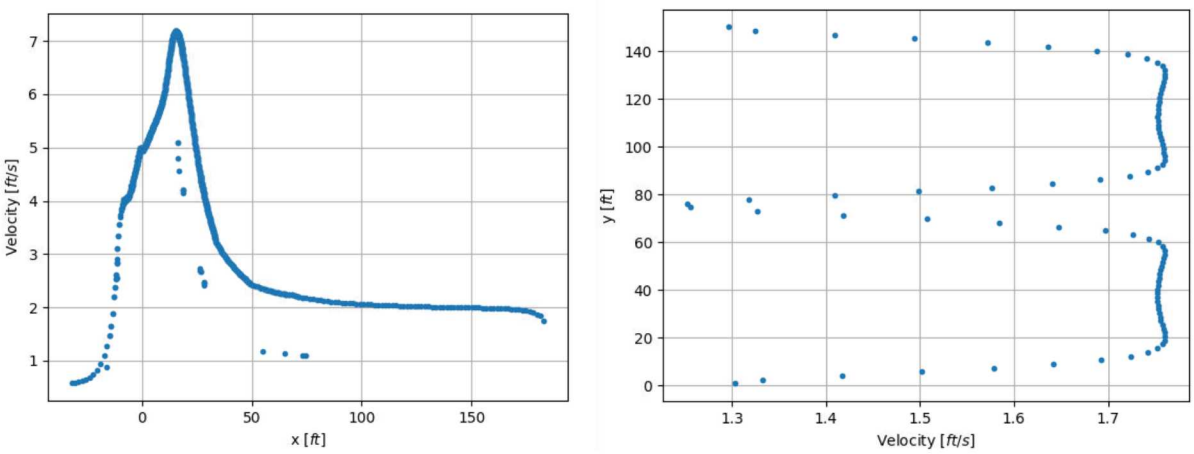

Figure 3-4. Base case water velocity cross-section at y =37' (left) and x = 183' (right) as shown in Figure 3-1 as an orange dashed line and orange dash-dot line respectively.

Lastly, the bed shear stress is shown for in **Figure 3-5** which shows the highest shear stress to not be directly out of the gates but where the water is allowed to diffuse laterally at the end of the

earthen dams. This will be the focus area for reducing shear stress. The maximum shear stress can be observed in **Figure 3-6** (left) which shows a maximum value near 1.8 lb/ft^2 (78 Pa). Down the field this value reduces to about 0.2 lb/ft^2 (8.7 Pa). At the front of the water channel (**Figure 3-6** right) the shear stress value is slightly lower at 0.15 lb/ft^2 (6.5 Pa).

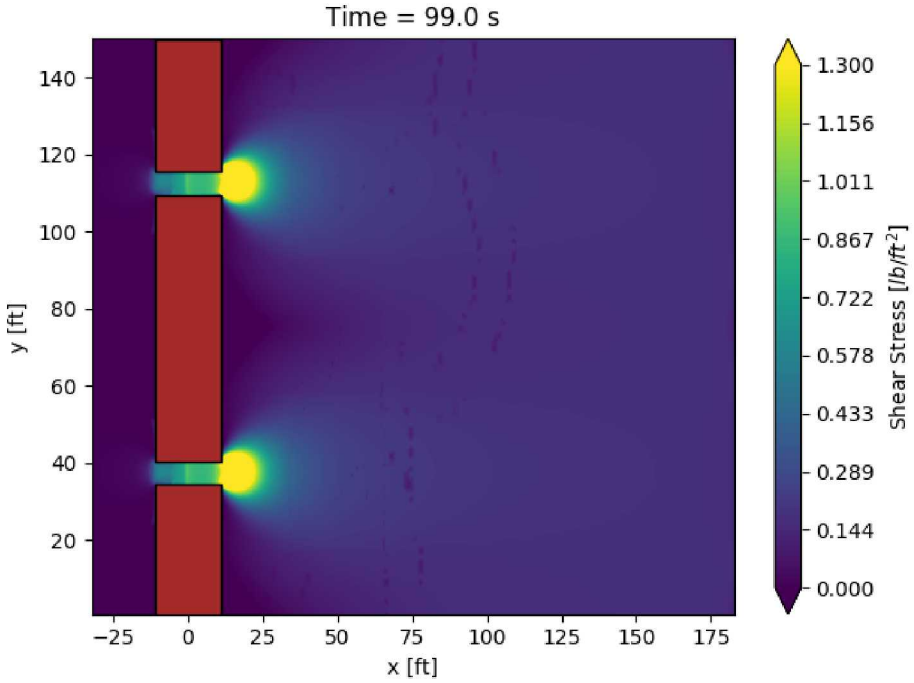

Figure 3-5. Base case showing simulated bed shear stress results prior to shear stress reduction techniques.

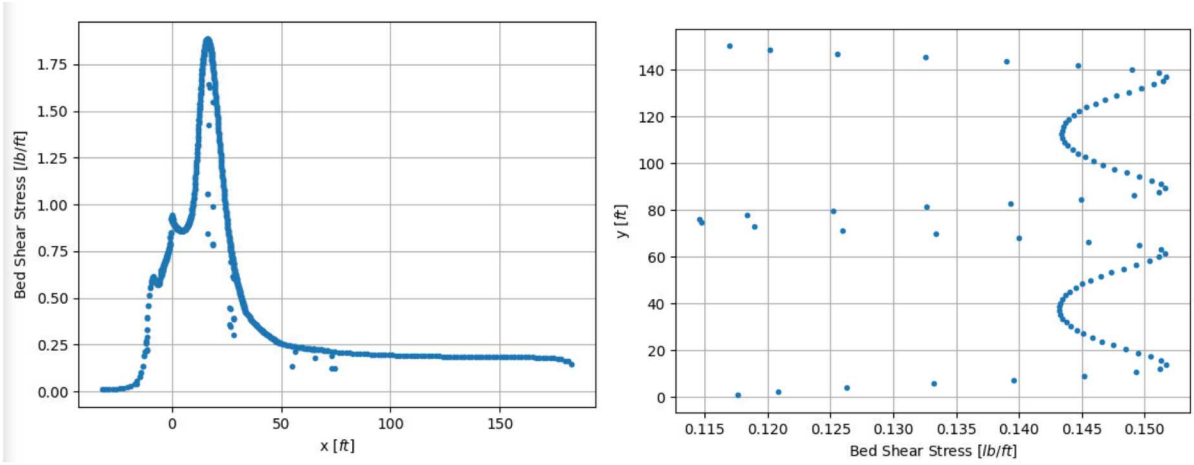

Figure 3-6. Base case bed shear stress cross-section at y =37' (left) and x = 183' (right) as shown in Figure 3-1 as an orange dashed line and orange dash-dot line respectively.

4. SHEAR STRESS REDUCTION APPROACH

Shear stress reduction approaches focused on creating obstructions to flow following the guidance laid out by the proprietor (**Figure 1-5**). The obstruction shapes studied here were a rectangle, a semi-circle, and a Gaussian curve. In addition to overall shear stress reduction other factors considered in determining the correct solution were ease of construction and safety of humans and cattle (e.g. potential to fall into any created hole). The following section will layout the parameters and values chosen to investigate.

Starting first with the rectangle the parameters included distance in front of the gate to the center of the left edge of the rectangle (x_0), the height (positive up) of the rectangular hole (z), and the length of sides x and y with respect to the model domain (x, y). For the rectangular parametric test case the values varied are listed in Table 4-1 for each respective parameter. A single test case consisted of a combination of the four parameters and each distinct value of any parameter was compared against all variations of the other parameters. This created a total of 16 test cases which are attached in the appendix in full.

Table 4-1. Parametric rectangular values test matrix defined by the combination of any four distinct values listed (e.g. {x_0, z, x, y})

Parameter	Values [m]
Distance in front of Gate (x_0)	3.5
Height (z)	-0.1, -0.15, -0.3, -0.75
Length of Side X (x)	0.5, 1
Length of Side Y (y)	3, 6

The semi-circle cases reduced the number of studied parameters to three namely distance in front of the gate to the straight side of the semi-circle (x_0), height (positive up) of the semi-circle (z), and radius (r). This parametric study created a total of 8 cases.

Table 4-2. Parametric semi-circle values test matrix defined by the combination of any three distinct values listed (e.g. {x_0, z, r})

Parameter	Values [m]
Distance in front of Gate (x_0)	3.5
Height (z)	-0.1, -0.15, -0.3, -0.75
Radius (r)	3, 6

The last flow obstruction shape investigated was a Gaussian shape. The initial effort focused on creating a Gaussian "speed bump" on top of the land to slow the flow. However, it was found that the inverse "speed bump" that went into the ground produced greater ease of construction and shear stress reduction. Creating a positive "speed bump" with the desired results would have required fine tuning the shape to the flow which would require a validated model for design success. The Gaussian "speed bump framework" is laid out below and is shown as positive but has identical description for a negative amplitude.

Figure 4-1 (left) shows the shape of a 2D Gaussian curve with a maximum value of f_{max}. The end points of a Gaussian approach zero at infinity but never reaches zero. Therefore, the width of a

Gaussian curve is defined here using a proxy method which the distance at which half of maximum amplitude is observed. This metric is known as full-width at half-maximum (FWHM). In the farmland case a 3D gaussian is of interest therefore two FWHM values are needed one to describe the width of the Gaussian in both the flow direction (x) and normal to the flow direction (y). An example 3D gaussian shape is shown in **Figure 4-1** (right) for a positive z, zero grade domain. The slope of the farmland was modeled as a constant 1.5% grade from the gate location to the end of the field in the flow direction. To model the Gaussian curve Equation 1 was applied to the 1.5% grade.

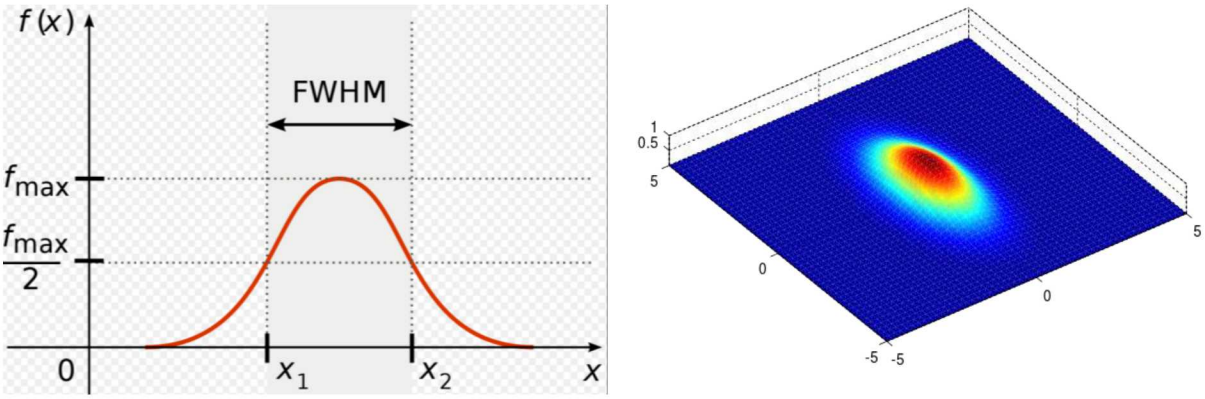

Figure 4-1. Gaussian parameters shown in 2D (left) and a resultant 3D Gaussian speed bump (right)

In Equation 1 the height at some location in the domain (x,y) is calculated by adding the Gaussian approximation to the current height at that spatial point as defined by the initial 1.5% grade. The Gaussian approximation is scaled by the amplitude z referred to as f_{max} in **Figure 4-1** left. This amplitude is the value shown in dark red of **Figure 4-1** (right). This maximum amplitude is placed at some location x_0 and y_0 refer. x_0 is defined by the distance in front of a gate and y_0 is the center location of either gate. Lastly, the FWHM is defined for both the x and y direction in the domain. This process is applied to every point in the domain two times, once for each gate (y_0) to determine the final field height values.

Equation 1: Gaussian curve approximation applied to the farm land grade

$$height = height(x,y) + z \cdot exp\left(-4\,log(2) * \left(\frac{(x-x_0)^2}{FWHM_x^2} + \frac{(y-y_0)^2}{FWHM_y^2}\right)\right)$$

The parameter values chosen for the study are listed in Table 4-3. Similar to the previous study every combination of the parameters was run resulting in a total of 16 cases.

Table 4-3. Parametric Gaussian values test matrix defined by the combination of any three distinct values listed (e.g. {x_0, z, $FWHM_X$, $FWHM_Y$})

Parameter	Values [m]
Distance in front of Gate (x_0)	2.5, 4
Depth (z)	-0.75, -0.15, 0.15, 0.75
$FWHM_X$	0.5
$FWHM_Y$	3, 6

5. RESULTS

5.1. General Parameter Influence

Independent of the shape chosen it was observed that the closer the shear reduction object was placed to the high shear stress area in front of the gate the sooner the higher shear stress could be reduced. The proprietor has discussed issues with scour of the earthen dam sides near the outlet of the gate (observe the gray tarps in **Figure 1-1** (left). Due to the potential of this scour any chosen reduction shape must not cause increased scour near these areas. This effect was outside the scope of this initial investigation and has been identified as a potential area for future investigation.

The next primary parameter that was varied what the height of the shape. The shape was found to need to be near about 0.5 deep to significantly reduce the shear stress. Further for the Gaussian case positive as well as negative values were simulated. The positive values were observed to increase the shear stress due to forcing the water around the structure. While it would be possible to design the height and shape of the structure such that shear stress was not increased in simulation, in practice this design would likely require experimental iteration and validation of the design.

The next parameter of interest is the width of the shape in the direction of flow (x-axis). For this axis 0.5 m was found to be sufficient for shear stress reductions independent of the chosen shape. Further increases to 1 m were found to have a relatively small reduction on the shear stress for the doubling of the size of the hole. Lastly the length of the shape normal to the flow (y-axis) was found to require a 3 m minimum. Additional increases in length to the 6 m again showed relatively small reduction on the overall shear stress. In summary this report found that the shear stress reduction device should be place as near as possible to the gates without interfering with the earthen dams and have a depth of at least 0.5 m, 0.5m wide, and 3 m long.

Comparing all the cases the Gaussian and semi-circle cases reduced the shear stress more than the rectangular case. Between the Gaussian and semi-circle case the results were similar, but the Gaussian was chosen because the sloped sides were safer for humans and cattle to prevent falls into the hole and better for concrete construction. The results of a Gaussian reference case are presented below.

5.2. Gaussian Design

The Gaussian design presented in this section represents a Gaussian shaped flow obstruction with the minimum requirements to reduce shear stress. Shear stress may be increased by increase the obstruction size. The Gaussian presented here was placed 5 m in front of the gate, with a maximum height of -0.5 m, a $FWHM_X$ of 0.5 m, and a $FWHM_Y$ of 3 m. The results of this case are shown as contours in the second row of **Figure 5-1**. The first row of **Figure 5-1** shows the base case results previously presented for quick comparison. The rows are the three QoIs namely water depth, velocity magnitude, and shear stress. For a given QoI the color scale is identical between the two presented case results (e.g. the base case and the modified case).

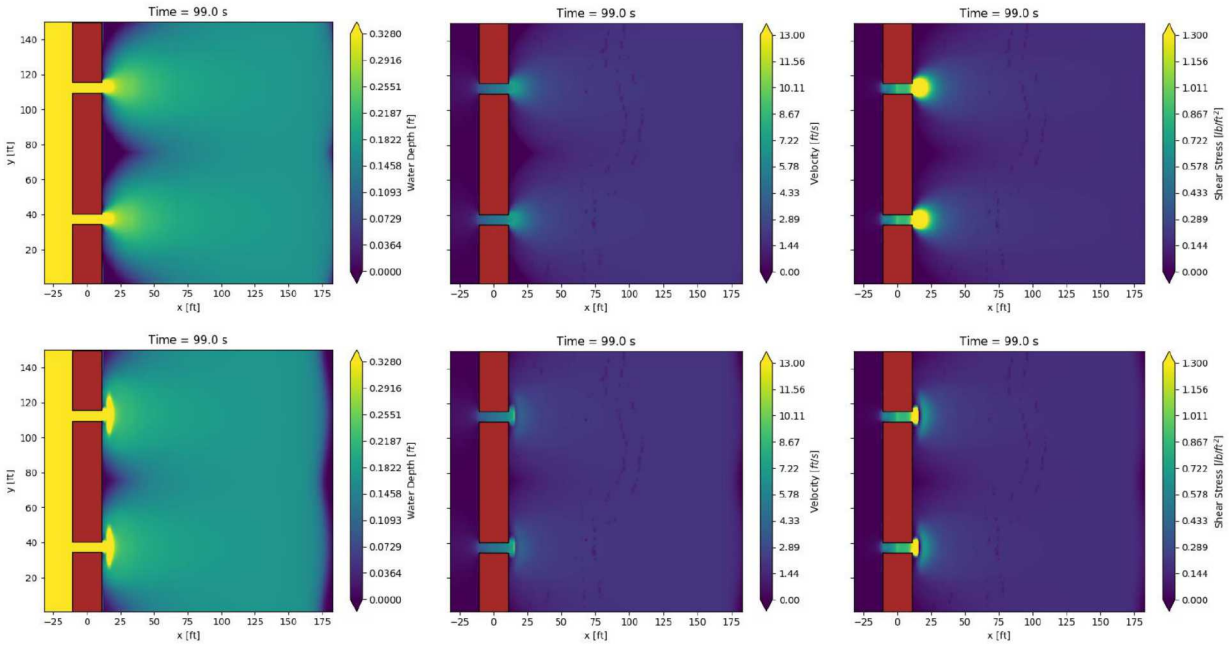

Figure 5-1. Top row base case. Bottom row Gauss x = 5m, height = -0.5m, FWHMx = 0.5m, FWHMy = 3m. Column 1: Water Depth, Column 2: Velocity Magnitude, Column 3: Bed shear stress

Looking to the first column in **Figure 5-1** it can be seen that the water has traveled a shorter distance in the 99s simulation. Further the Gaussian shape can be observed in the water depth plot near the gate through the spreading of the max value (yellow) as compared to the base case. Further, the water depth is dispersed more due to the Gaussian causing the two streams from each gate to meet sooner (e.g. 25' to 50'). This increased dispersion in the y direction should be kept in mind again to ensure that the shear on the earthen dam is not substantially increased in practice.

The second column in **Figure 5-1** shows a decrease in the velocity at the Gaussian shear stress reducer. Beyond the near gate speed reduction, the downstream results appear similar down the field. Lastly, looking to the third column the shear stress shows a sharp reduction at the gaussian location (e.g. the bright yellow suddenly ends) showing the success of the Gaussian shape at reducing shear stress.

Looking to a cross sectional view of each of the QoIs **Figure 5-2** shows that there is a small change in water depth following the Gaussian shape. The primary difference is observed in front of the gate as expected due to the placement of a maximum 0.5 m (1.64') hole. This hole causes the water depth to more quickly decrease to the constant value reached previously around 0.2' (0.6 m).

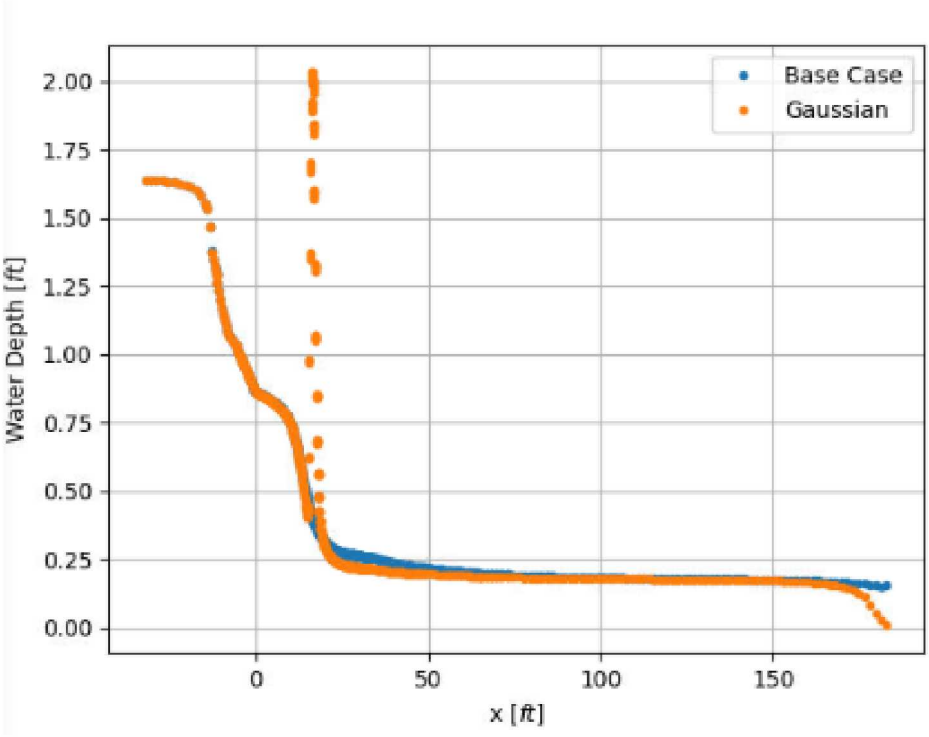

Figure 5-2. Compares the water depth between the base case and a Gaussian hole 5 m in front of the gate 0.5 m deep, 0.5 m $FWHM_X$, and 3 m $FWHM_Y$ down the farm field through the gate for a constant y-value = 37' (Figure 5-1)

The same centerline plot going through the south gate at y=37' (11.3 m, **Figure 5-2**) is shown for the velocity magnitude in **Figure 5-3**. Prior to the Gaussian hole the solutions between the two cases are nearly identical. At the Gaussian hole the solution diverges by showing a sudden increase in velocity then a rapid decrease to just under 4 ft/s (1.22 m/s) for the Gaussian solution. At this same location (x ~ 25' (7.6 m)) the base case can be seen to have a 7 ft/s (2.1 m/s) velocity. Downstream of the Gaussian hole the two solutions reach the same value at about 75' (22.7 m) to 100' (30.5).

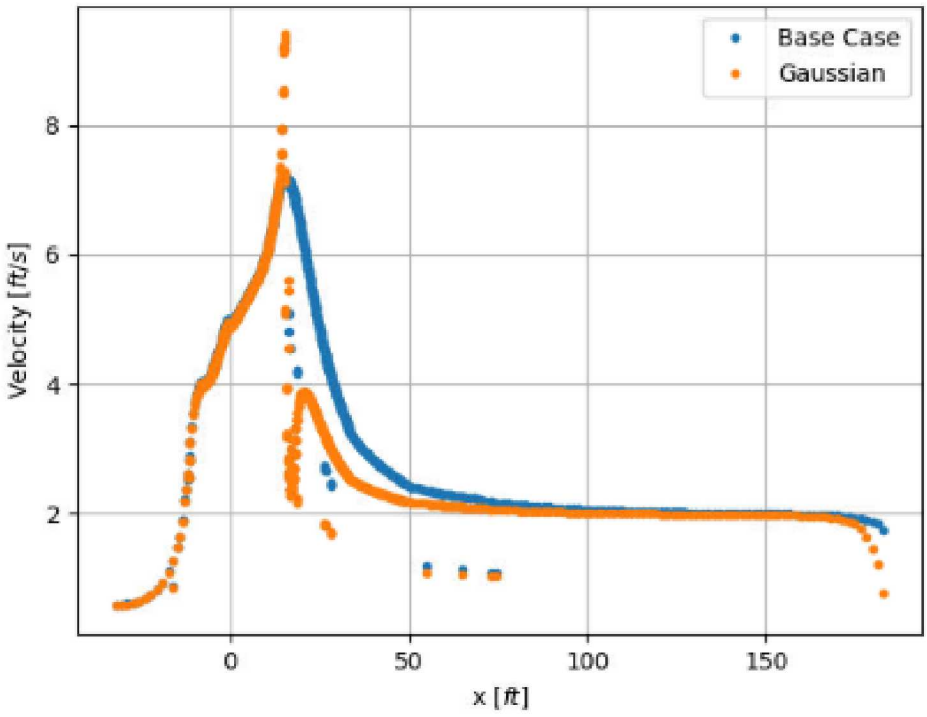

Figure 5-3. Compares the velocity magnitude between the base case and a Gaussian hole 5 m in front of the gate 0.5 m deep, 0.5 m $FWHM_X$, and 3 m $FWHM_Y$ down the farm field through the gate for a constant y-value = 37' (Figure 5-1)

Lastly, **Figure 5-4** shows a decrease in the shear stress caused by the Gaussian hole from 1.9 lb/ft^2 (82.7 Pa) to 0.7 lb/ft^2 (30.5 Pa) representing a 63% decrease in the shear stress at its maximum. Looking at the shear stress curve the location of the Gaussian is observed by the location where the shear stress suddenly rises and precipitously drops. This figure may help further clarify the guidance that the gaussian hole should be placed as close as possible to the gate so long as it does not interfere with the earthen dams.

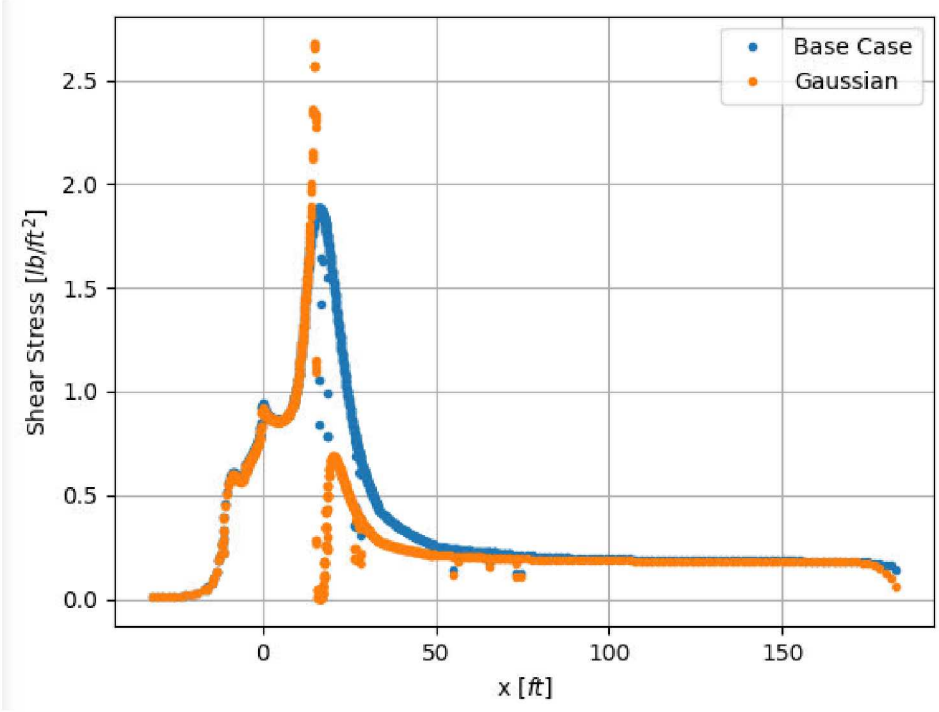

Figure 5-4. Compares the shear stress between the base case and a Gaussian hole 5 m in front of the gate 0.5 m deep, 0.5 m $FWHM_X$, and 3 m $FWHM_Y$ down the farm field through the gate for a constant y value = 37' (Figure 5-1)

5.3. Gaussian Design for the Edge Case

With the Gaussian design chosen as the solution for the base case the analysis shifted focus to the edge case. The edge case displayed high scour near the gates of the field and issues distributing the the water to the southern part of the field shown in **Figure 5-5**. The layout of the results is the same as described in **Figure 5-1** but this time the unmodified edge case is on the top row and the edge case with a Gaussian modification is on the bottom row. The water depth results of the unmodified case (top row first column) clearly shows the water failing to reach the southern part of the field. The water depth results for the modified result (second row first column) shows the results of placing a Gaussian hole 4 meters in front of the gate, which is 0.6 m deep, has a $FWHM_X$ of 0.5 m, and a $FWHM_Y$ of 4 m, and was shifted 45 degrees counter clockwise from the y-axis. The design forced the water to move more along the southern wall. Further the modified edge case shear stress results (second row third column) shows that the shear stress was significantly reduced as well.

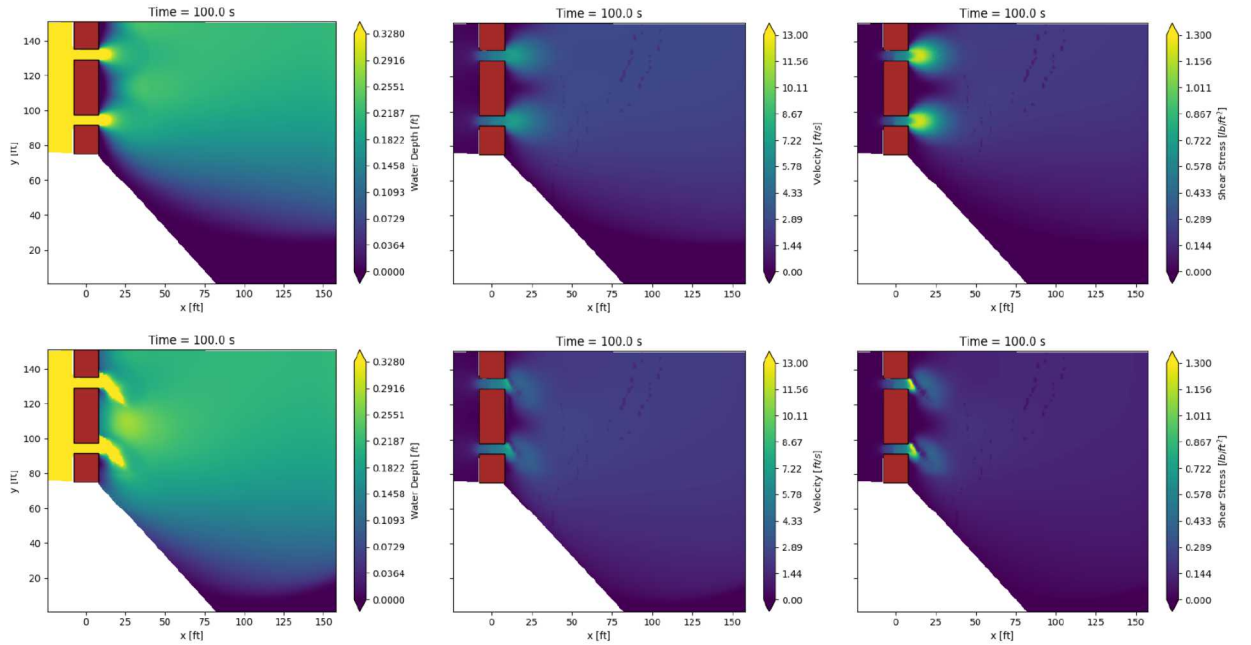

Figure 5-5. Top row edge case. Bottom row edge case with Gaussian at 4 m in front of the gate with a depth of 0.6 m, a FWHMx of 0.5m, a FWHMy of 4m, shifted 45 degrees counter-clockwise from the y-axis. Column 1: Water Depth, Column 2: Velocity Magnitude, Column 3: Bed Shear-stress

6. CONCLUSIONS

This study focused on low cost solutions to help a New Mexico farm reduce farmland scour near the flood irrigation gates to the field. The study investigated three shear stress reduction shapes e.g. rectangle, semi-circle, and Gaussian. These shapes were placed in front of the gates to the field and a parametric study was run on the free parameters for the shapes which included distance in front of the gate, depth or height of the feature, width in the direction of flow, and length in the direction normal to flow.

The results of this study provide guidance on the placement of a general shape for scour reduction. It was shown that the feature should not protrude from the ground but rather be a hole. The semi-circle and Gaussian shapes provided better shear reduction than the rectangle. The Gaussian shape was chosen as it is easier to construct with a backhoe compared to a semi-circle. Further the natural curve into the Gaussian is safer for human and cattle to prevent a fall into the hole. The hole should be placed as close as possible to the gate but not so close as to interfere with the earthen dam. The depth of the hole should be at least 0.5 m deep, 0.5 wide in the direction of flow, and 3 m long in the direction normal to the flow. These minimum dimensions may be increased but show diminishing returns for the increases in the size of the holes.

Lastly the results of a uniquely shaped field (here referred to as the edge case) were presented which in addition to the scour reduction needed help moving the water to the opposite side of the field from the location of the gates. In this case the same Gaussian solution was applied as before this time rotating the shape 45 degrees counter-clockwise from the y-axis. The results of this simulation showed that it both decreased the shear stress and help fill the previously dry part of the field.

6.1. Future Work

The work presented here is limited in the analysis in that it focuses on determining a shape to reduce the scour in a field. This case does not investigate the dynamics of sediment transport with respect to the field or the earthen dams. These transient effects may lead to observation of different results than those simulated here. Further the simulations are limited as the earthen damns are treated as areas of no flow such that the shear stress on the walls of the dams was not measured. The issue of scour on the dams is a known issue and needs to be considered as the solution is implemented.

Future work could investigate sediment transport using Delft 3D's sediment transport module and utilize the water power technologies staff's expertise in this area. Further investigations into the effects on the earthen dams could be studied in detail. These developed models could be further utilized and improved by considering soil infiltration rates to measure the water receive by the front of the field and back of the field to optimize the time spent water the field.

REFERENCES

[1] Yeomans, P. A. (2002). *Water for Every Farm: Yeomans Keyline Plan*. Keyline Designs.

[2] Engineering ToolBox, (2004). Manning's Roughness Coefficients. [online] Available at: https://www.engineeringtoolbox.com/mannings-roughness-d_799.html [09-12-2019].

[3] Deltares, D. (2019a). Delft3D-Flexible Mesh Suite: Delta shell, User Manual.

APPENDIX A. PARAMTERIC CASE STUDY RESULTS

A.1. Rectangular Cases

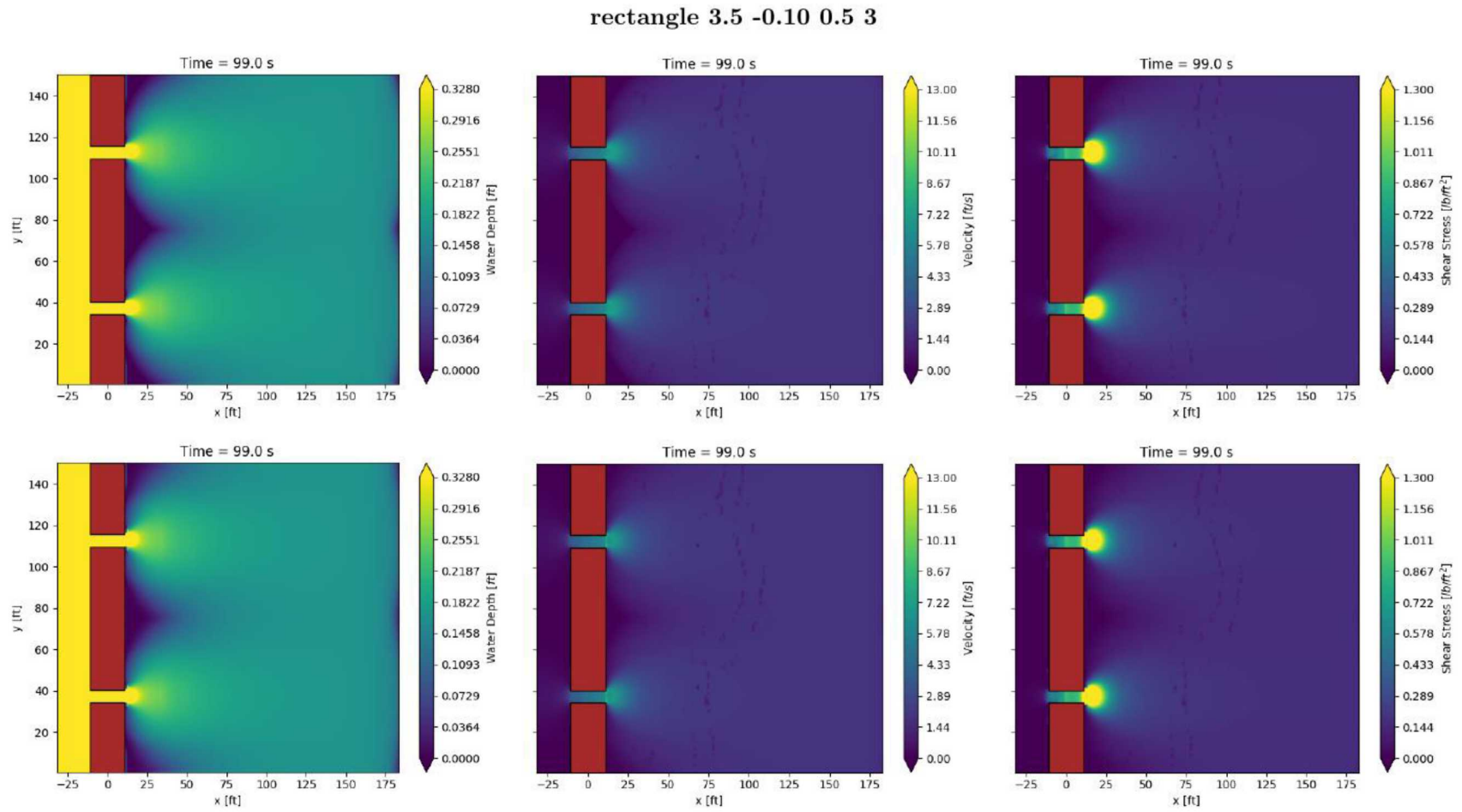

Figure 1: Top Row base case. Bottom Row rectangle x = 3.5m, depth = -0.10 m, length x = 0.5m, length y = 3m. Column 1: Water Depth, Column 2: Velocity Magnitude, Column 3: Bed Shear-stress

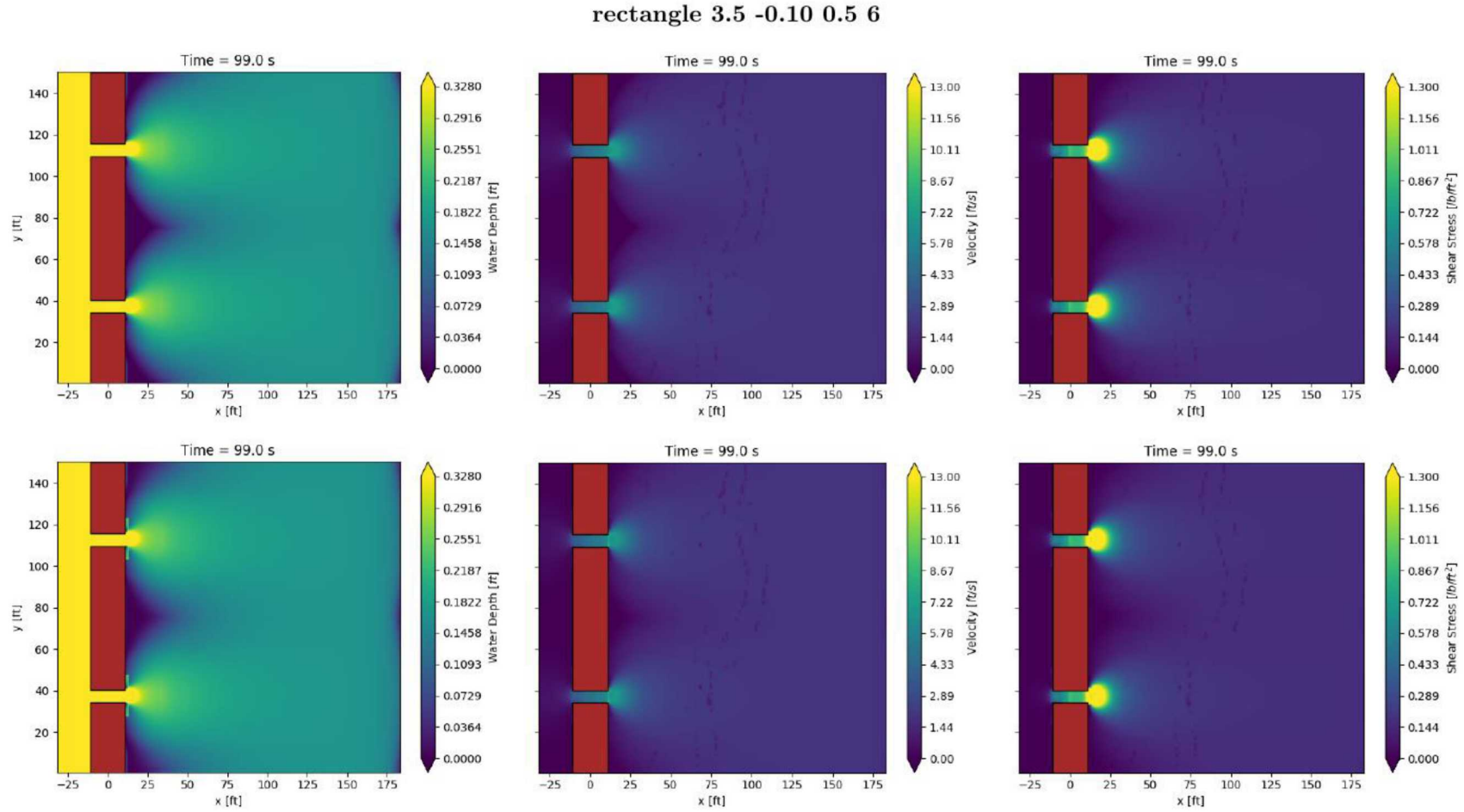

Figure 2: Top Row base case. Bottom Row rectangle x = 3.5m, depth = -0.10 m, length x = 0.5m, length y = 6m. Column 1: Water Depth, Column 2: Velocity Magnitude, Column 3: Bed Shear-stress

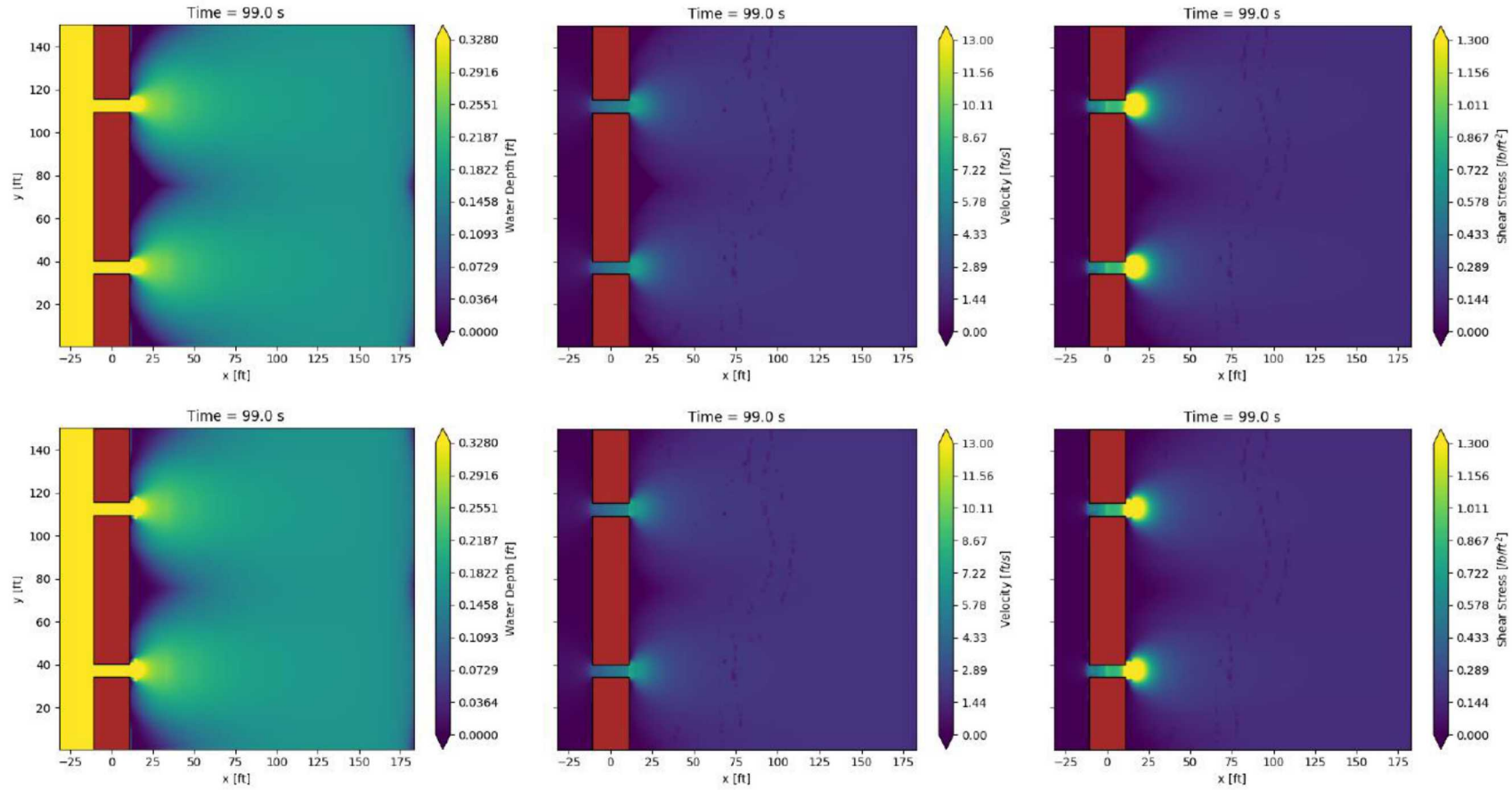

Figure 3: Top Row base case. Bottom Row rectangle x = 3.5m, depth = -0.10 m, length x = 1m, length y = 3m. Column 1: Water Depth, Column 2: Velocity Magnitude, Column 3: Bed Shear-stress

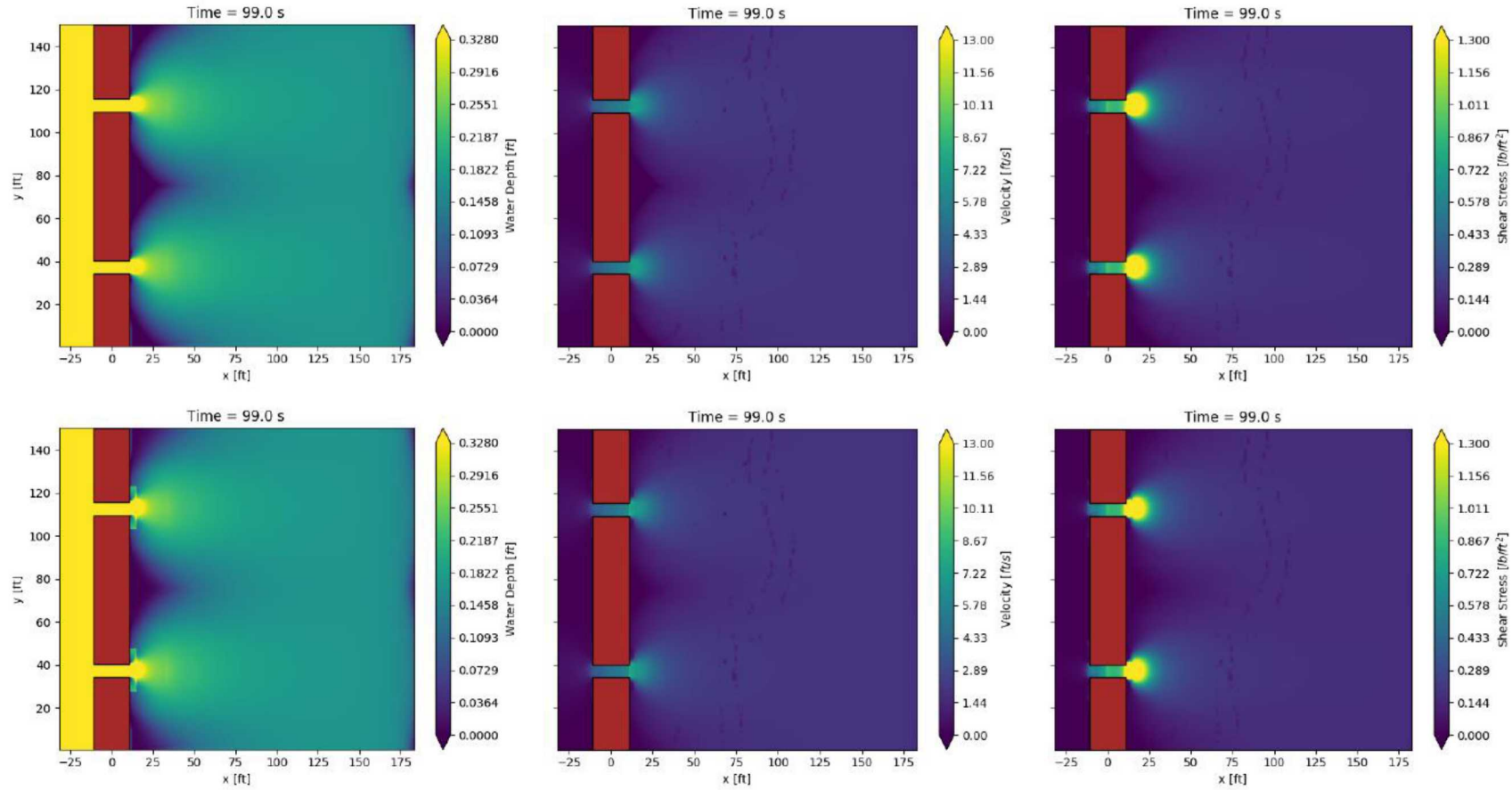

Figure 4: Top Row base case. Bottom Row rectangle x = 3.5m, depth = -0.10 m, length x = 1m, length y = 6m. Column 1: Water Depth, Column 2: Velocity Magnitude, Column 3: Bed Shear-stress

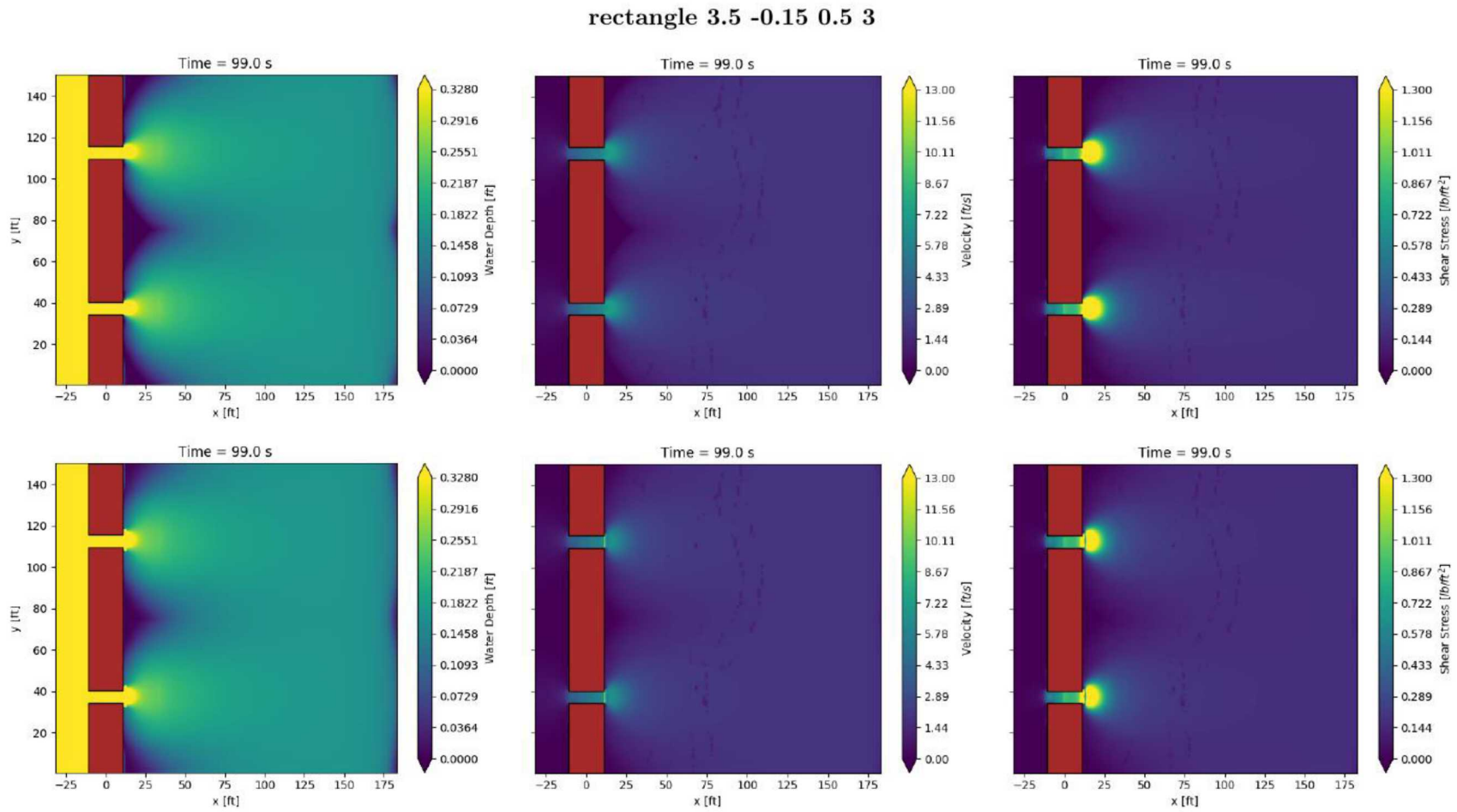

Figure 5: Top Row base case. Bottom Row rectangle x = 3.5m, depth = -0.15 m, length x = 0.5m, length y = 3m. Column 1: Water Depth, Column 2: Velocity Magnitude, Column 3: Bed Shear-stress

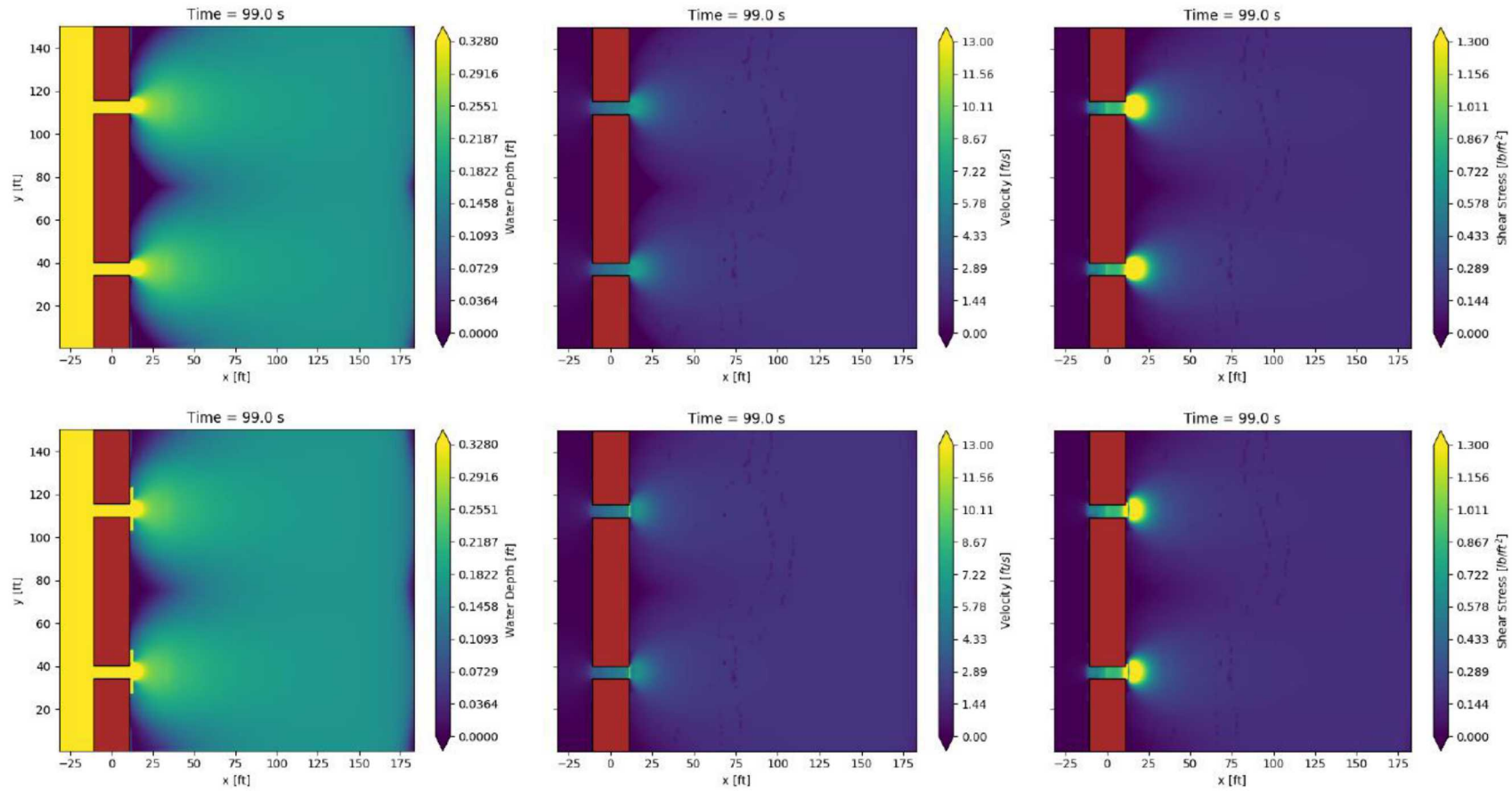

Figure 6: Top Row base case. Bottom Row rectangle x = 3.5m, depth = -0.15 m, length x = 0.5m, length y = 6m. Column 1: Water Depth, Column 2: Velocity Magnitude, Column 3: Bed Shear-stress

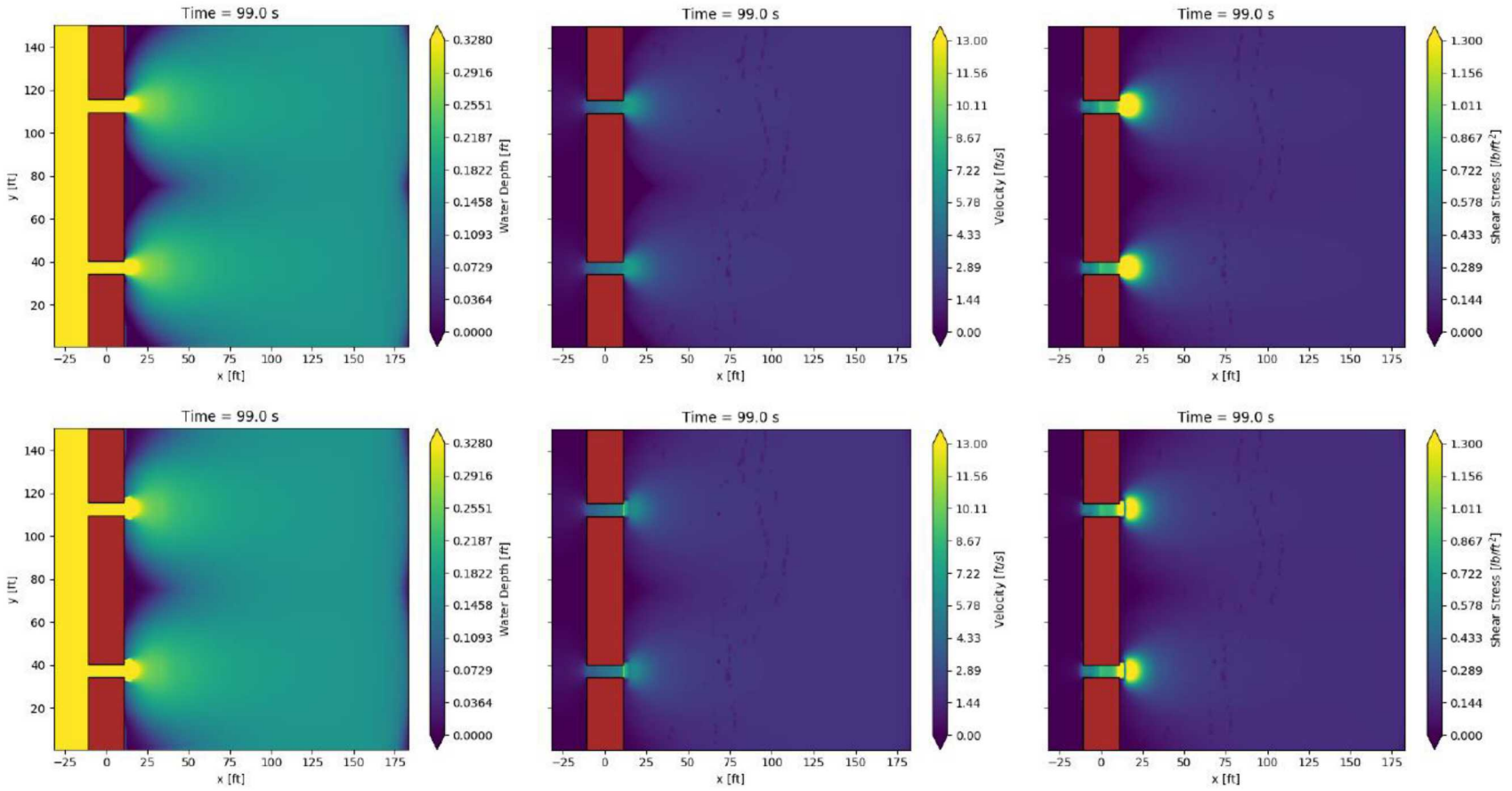

Figure 7: Top Row base case. Bottom Row rectangle x = 3.5m, depth = -0.15 m, length x = 1m, length y = 3m. Column 1: Water Depth, Column 2: Velocity Magnitude, Column 3: Bed Shear-stress

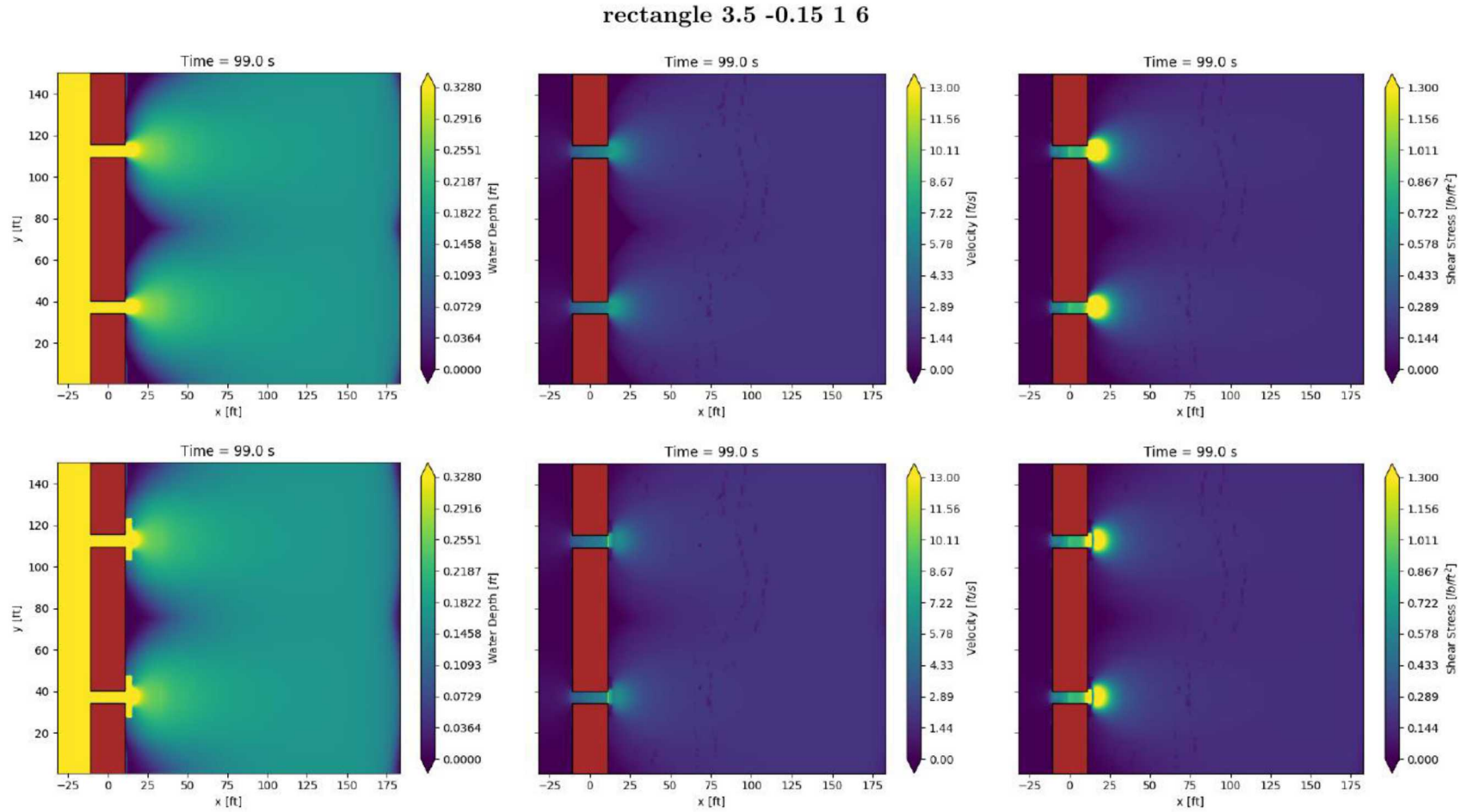

Figure 8: Top Row base case. Bottom Row rectangle x = 3.5m, depth = -0.15 m, length x = 1m, length y = 6m. Column 1: Water Depth, Column 2: Velocity Magnitude, Column 3: Bed Shear-stress

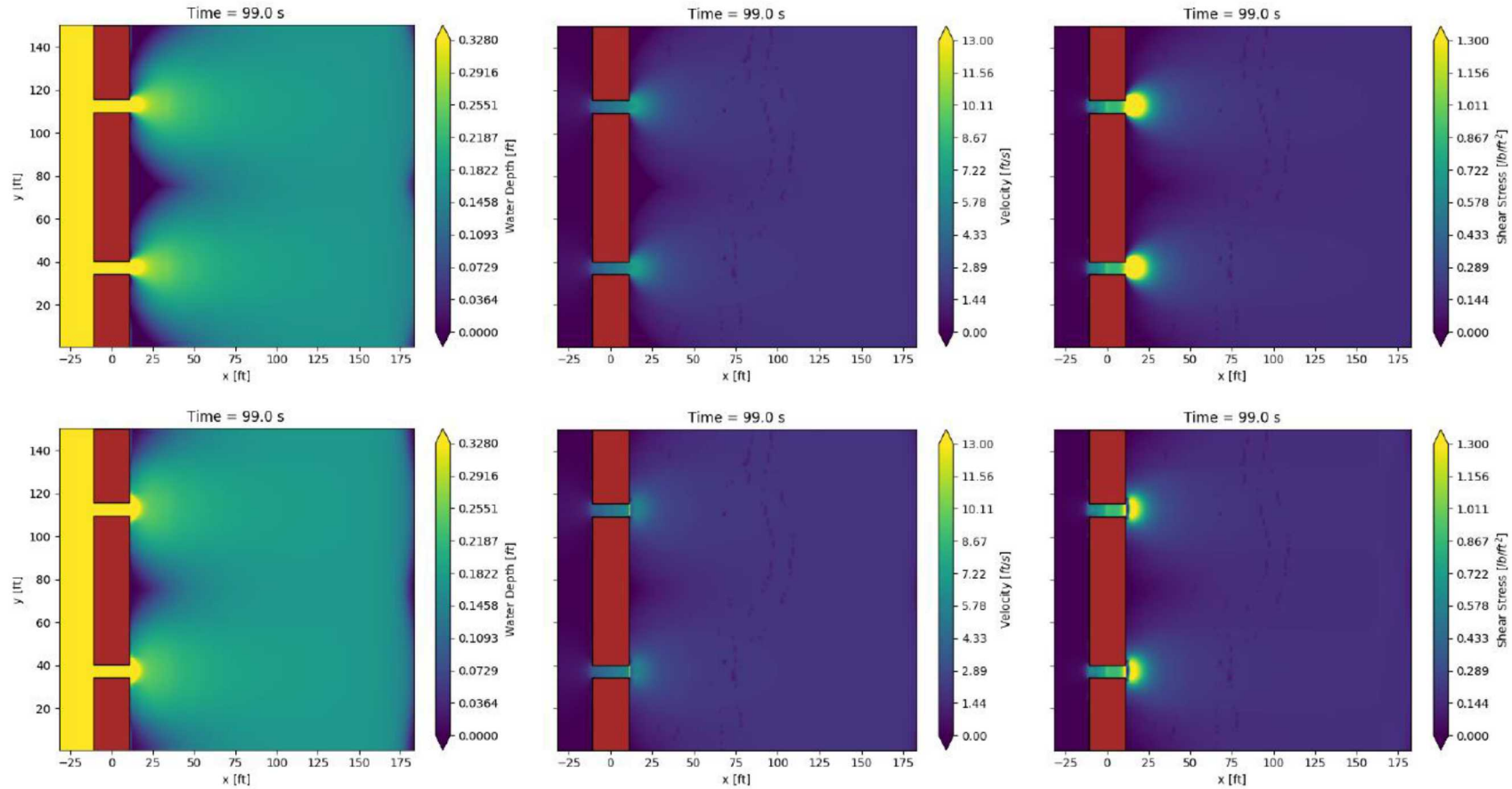

Figure 9: Top Row base case. Bottom Row rectangle x = 3.5m, depth = -0.30 m, length x = 0.5m, length y = 3m. Column 1: Water Depth, Column 2: Velocity Magnitude, Column 3: Bed Shear-stress

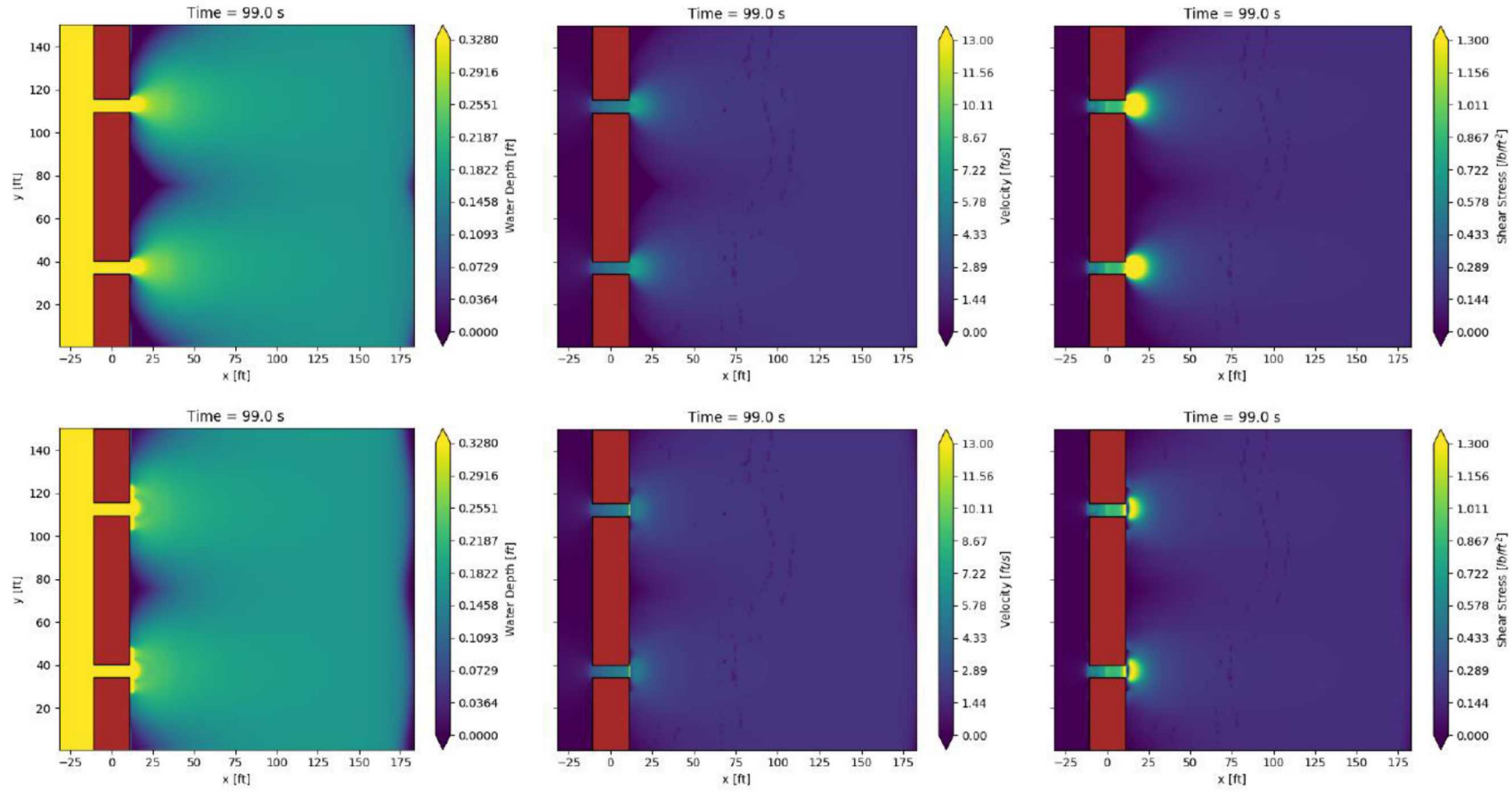

Figure 10: Top Row base case. Bottom Row rectangle x = 3.5m, depth = -0.30 m, length x = 0.5m, length y = 6m. Column 1: Water Depth, Column 2: Velocity Magnitude, Column 3: Bed Shear-stress

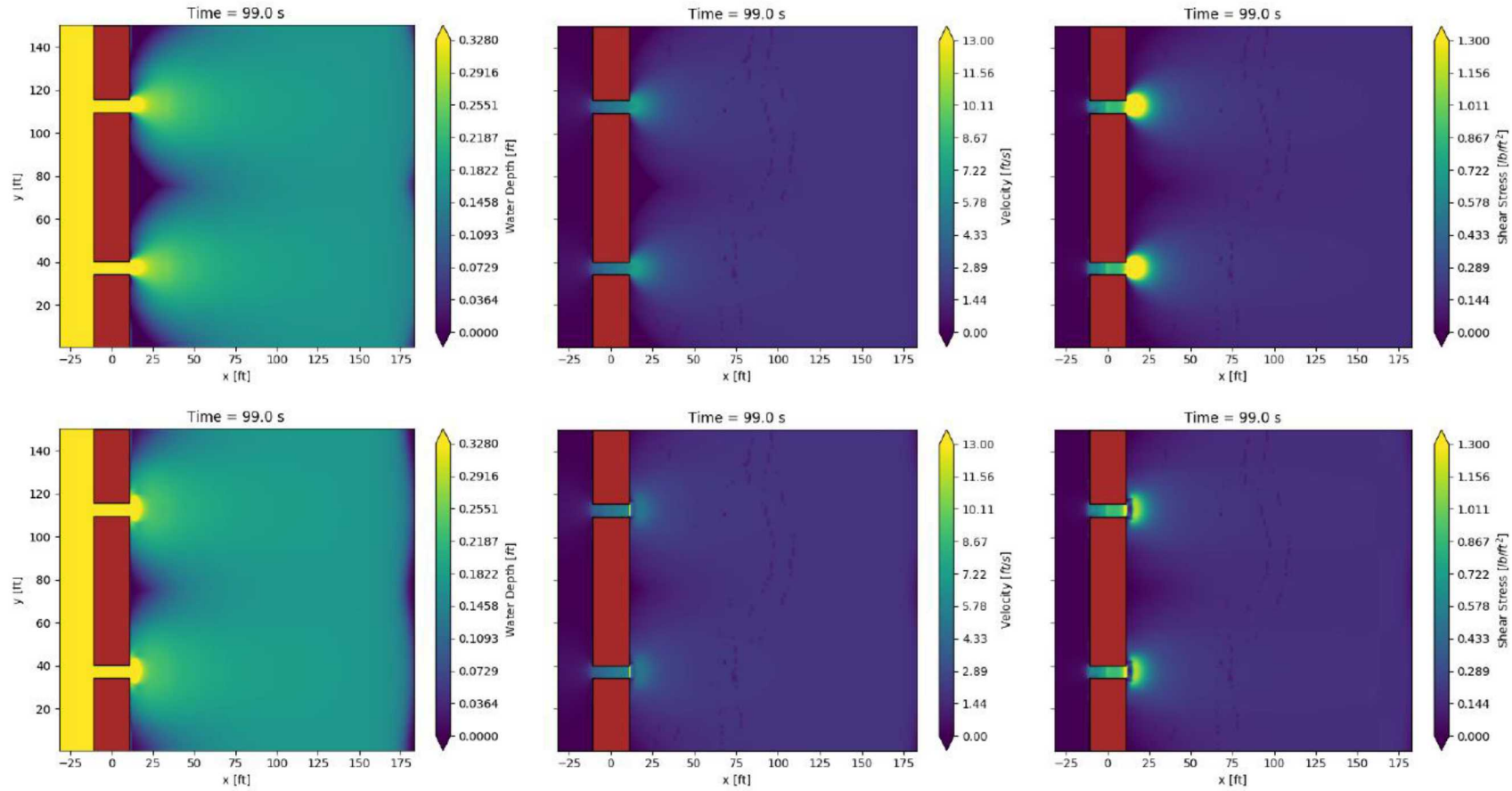

Figure 11: Top Row base case. Bottom Row rectangle x = 3.5m, depth = -0.30 m, length x = 1m, length y = 3m. Column 1: Water Depth, Column 2: Velocity Magnitude, Column 3: Bed Shear-stress

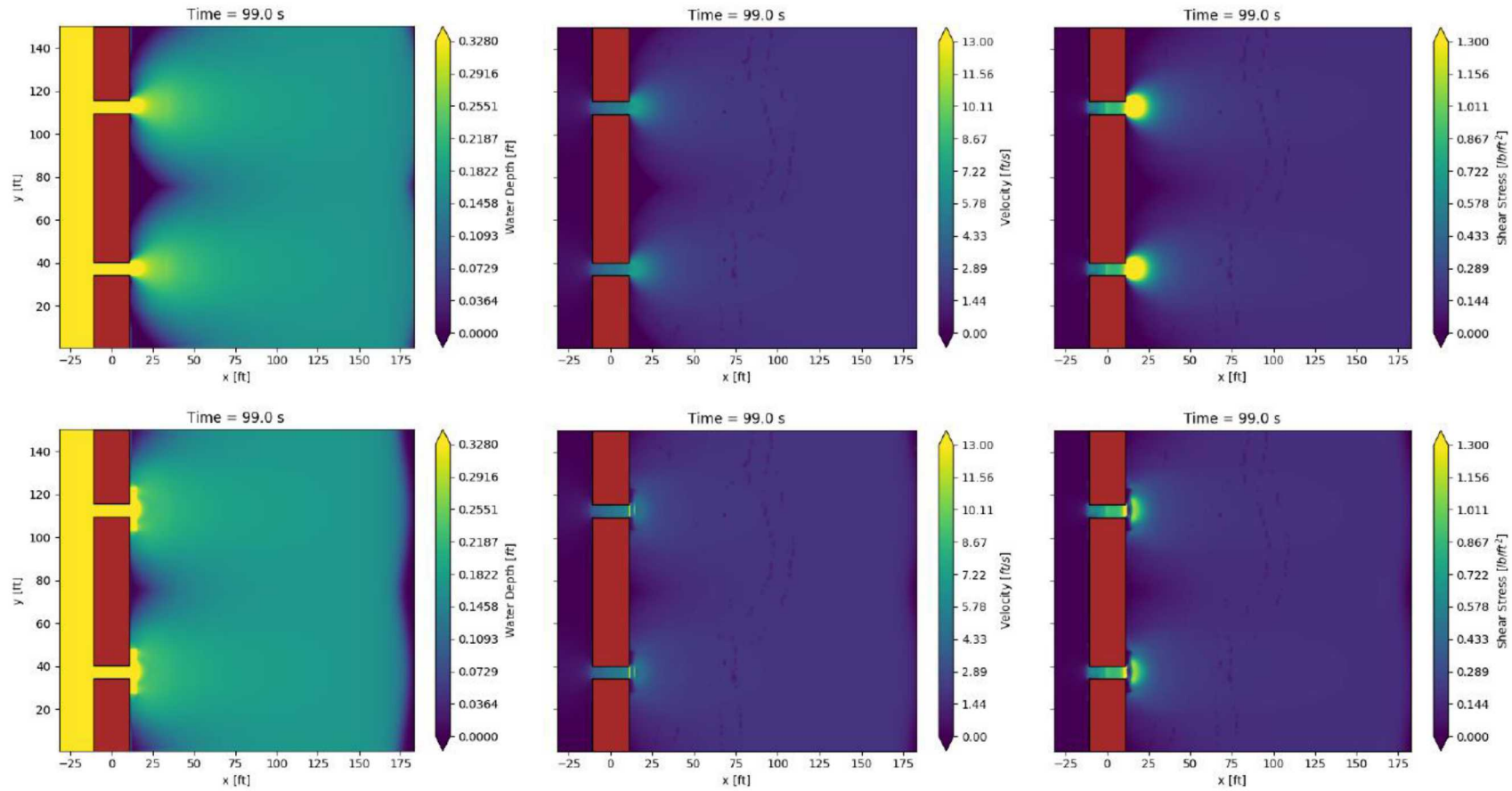

Figure 12: Top Row base case. Bottom Row rectangle x = 3.5m, depth = -0.30 m, length x = 1m, length y = 6m. Column 1: Water Depth, Column 2: Velocity Magnitude, Column 3: Bed Shear-stress

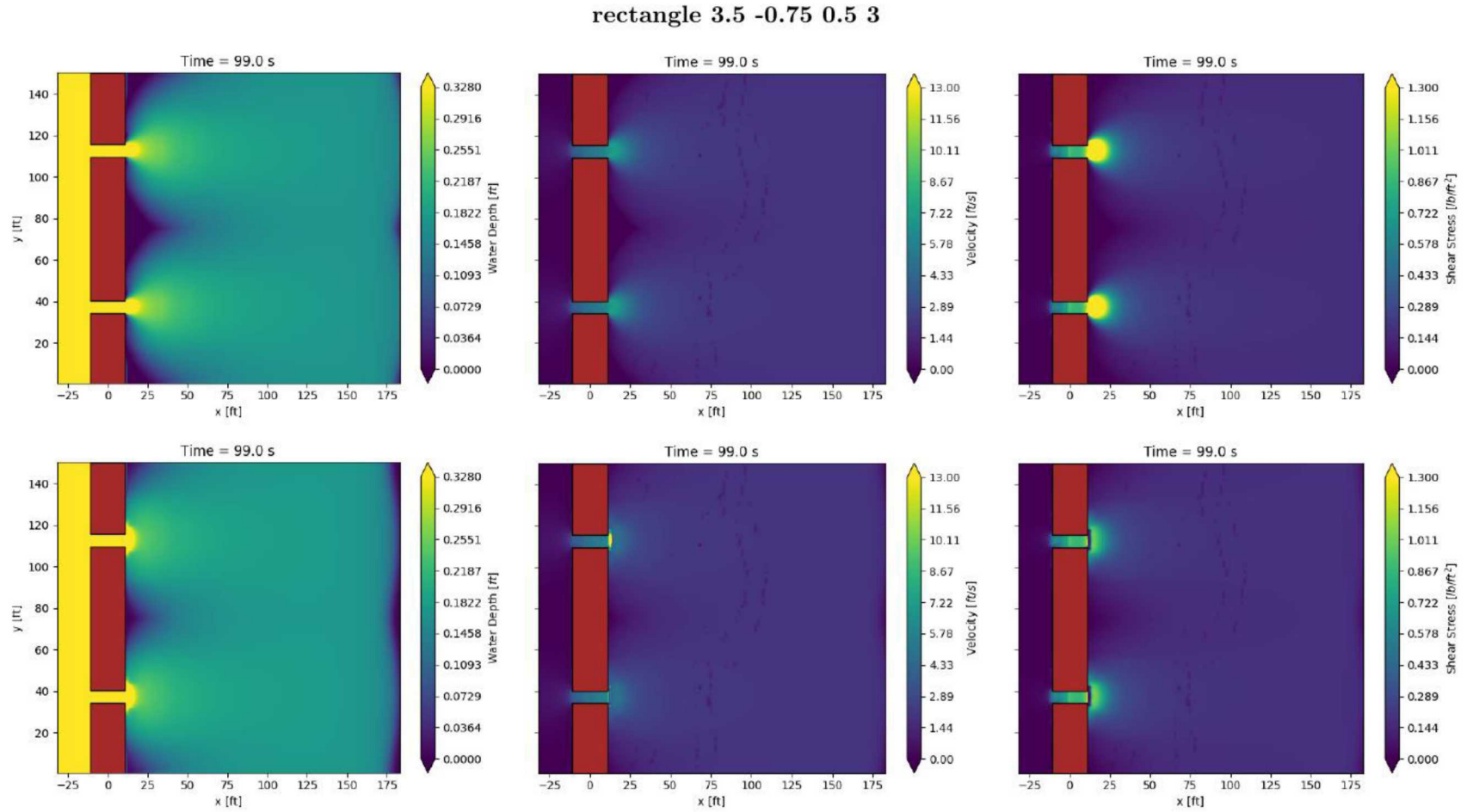

Figure 13: Top Row base case. Bottom Row rectangle x = 3.5m, depth = -0.75 m, length x = 0.5m, length y = 3m. Column 1: Water Depth, Column 2: Velocity Magnitude, Column 3: Bed Shear-stress

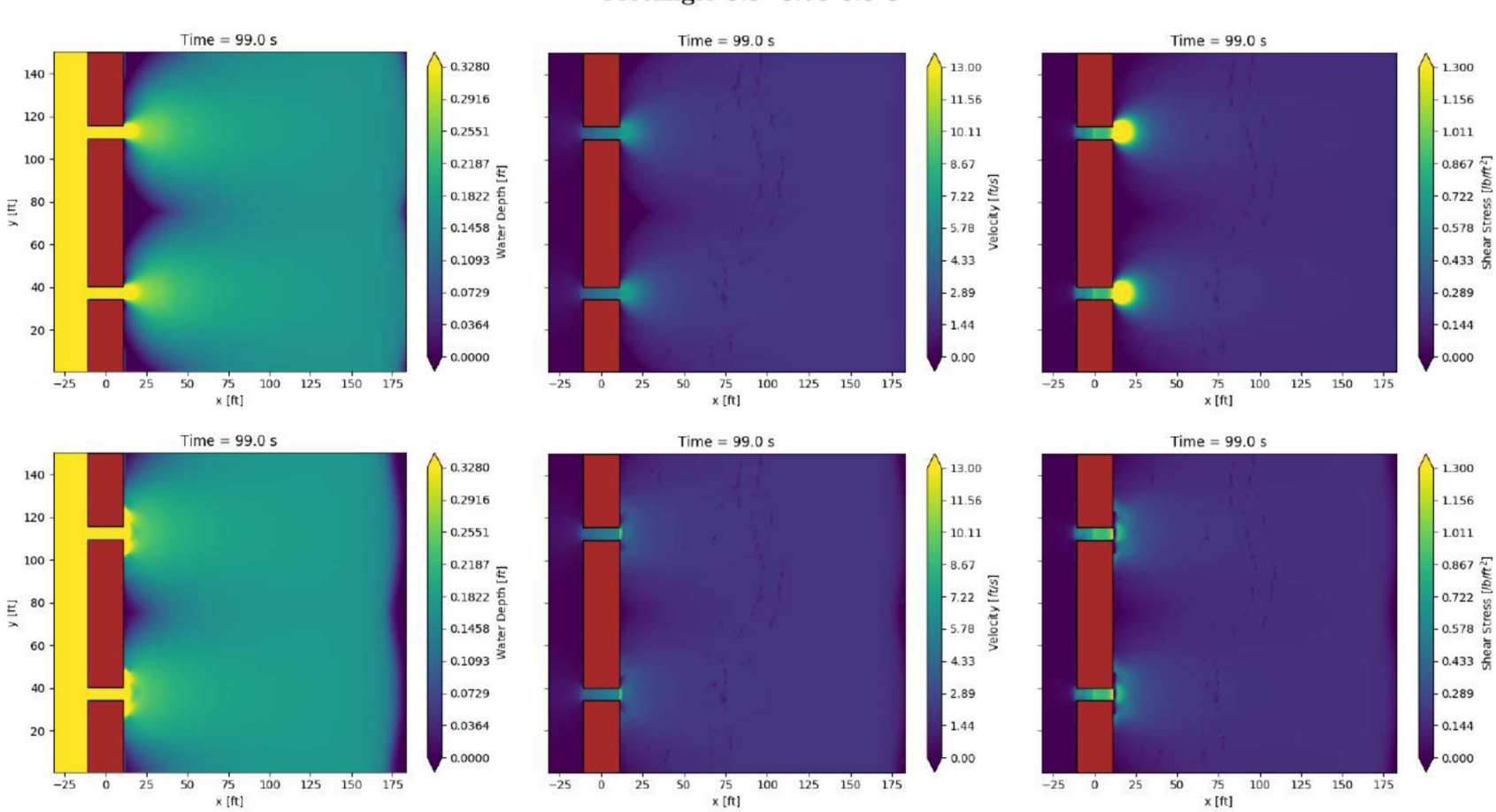

Figure 14: Top Row base case. Bottom Row rectangle x = 3.5m, depth = -0.75 m, length x = 0.5m, length y = 6m. Column 1: Water Depth, Column 2: Velocity Magnitude, Column 3: Bed Shear-stress

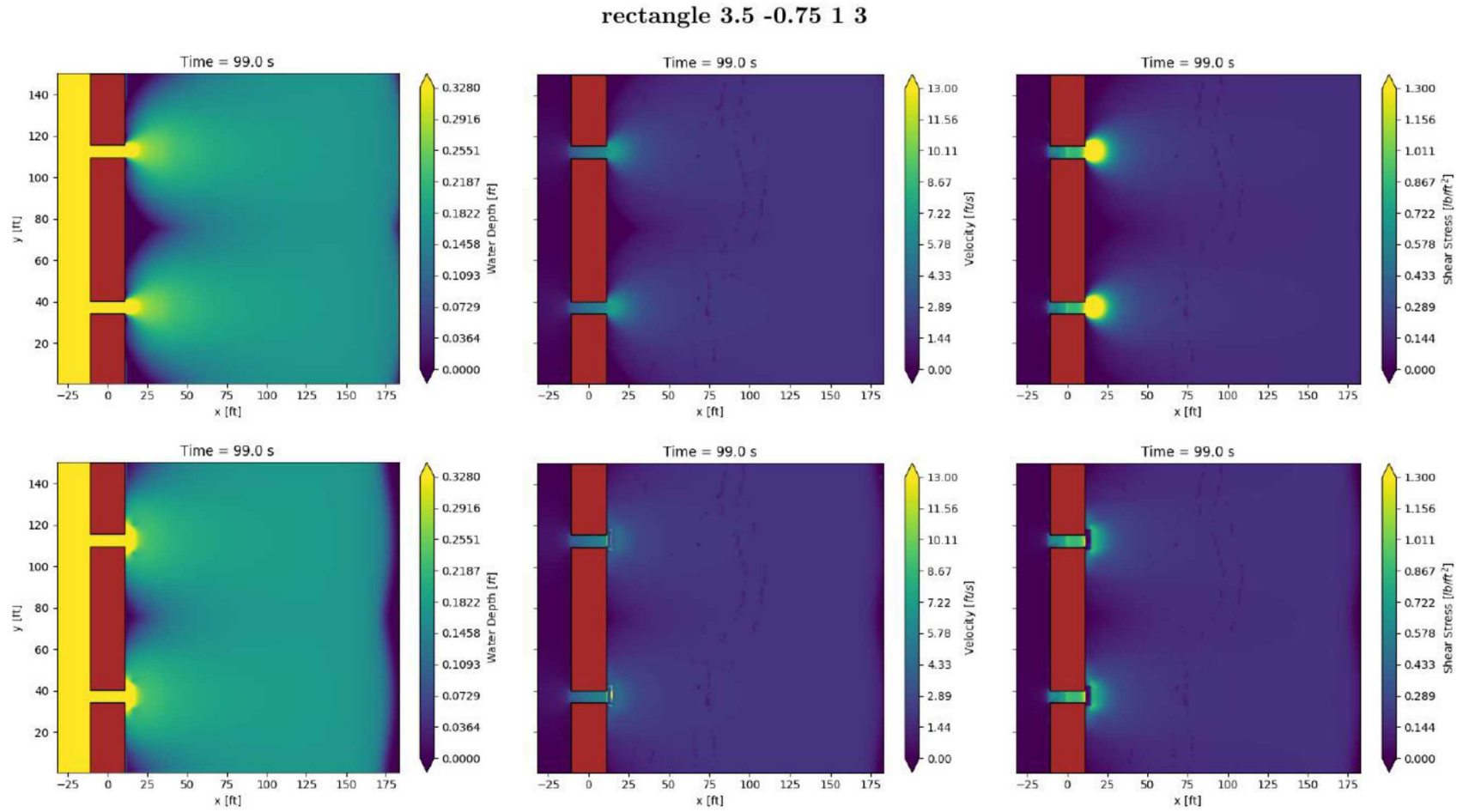

Figure 15: Top Row base case. Bottom Row rectangle x = 3.5m, depth = -0.75 m, length x = 1m, length y = 3m. Column 1: Water Depth, Column 2: Velocity Magnitude, Column 3: Bed Shear-stress

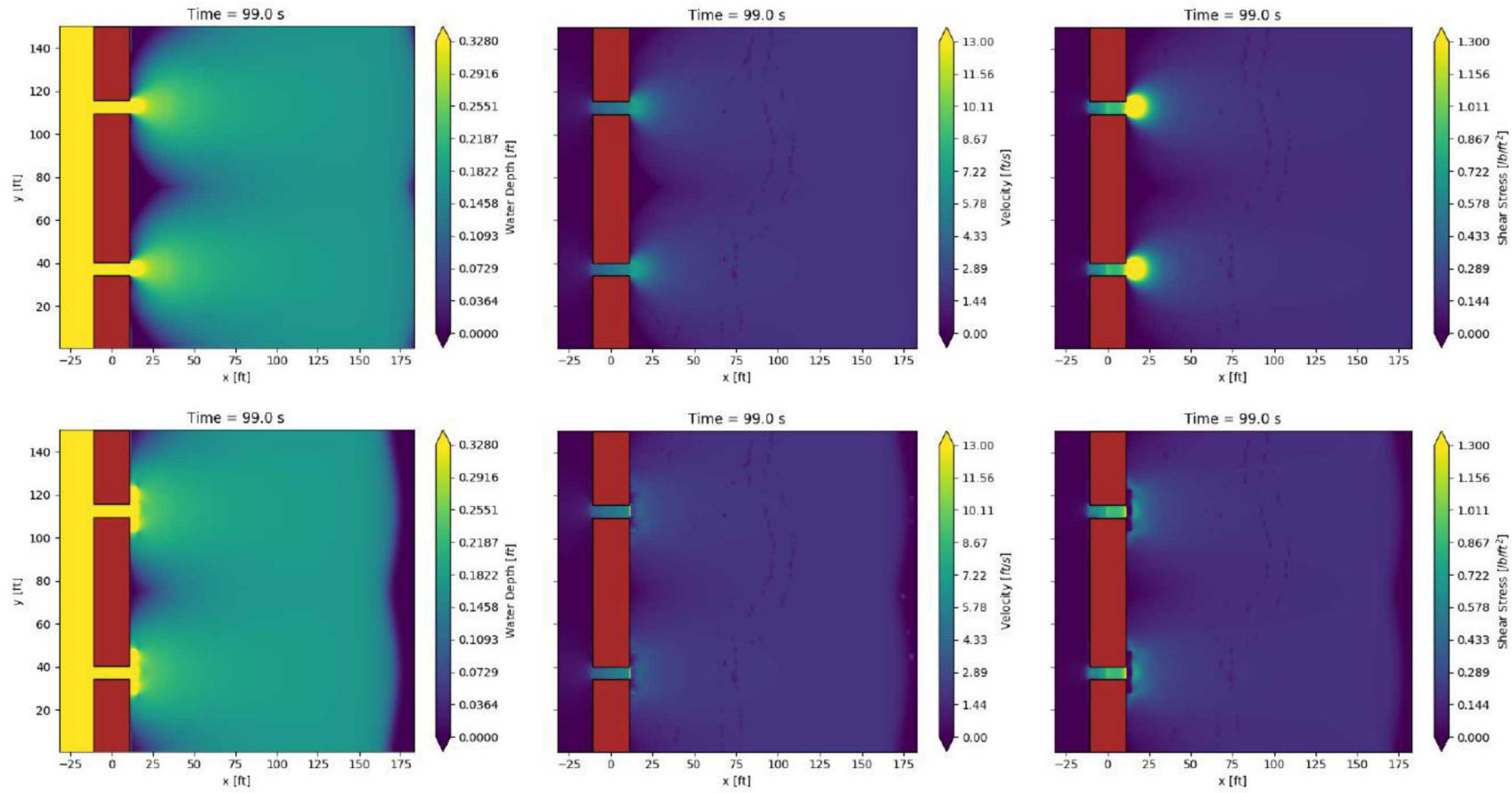

Figure 16: Top Row base case. Bottom Row rectangle x = 3.5m, depth = -0.75 m, length x = 1m, length y = 6m. Column 1: Water Depth, Column 2: Velocity Magnitude, Column 3: Bed Shear-stress

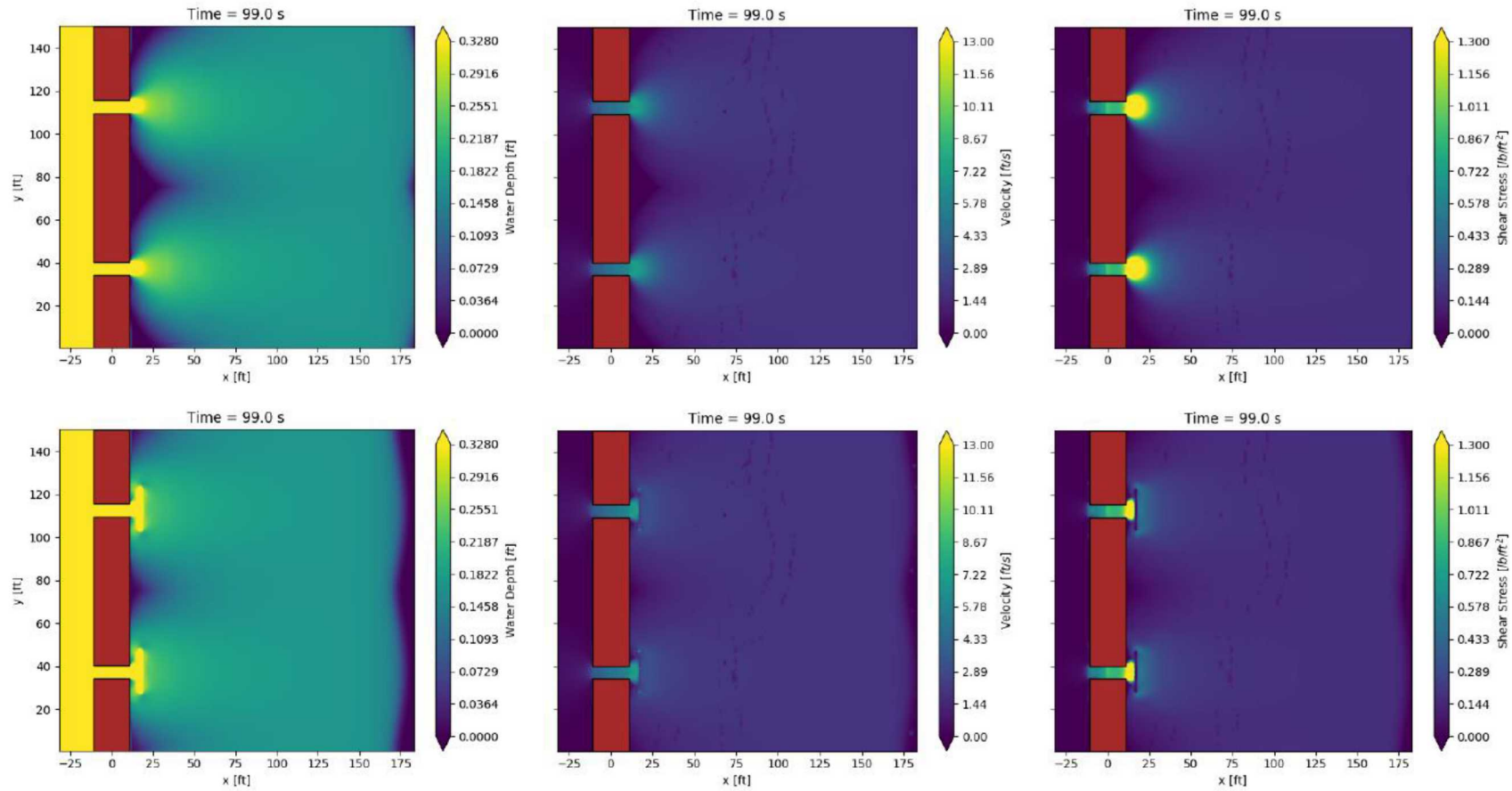

Figure 17: Top Row base case. Bottom Row rectangle x = 5m, depth = -0.70 m, length x = 0.5m, length y = 6m. Column 1: Water Depth, Column 2: Velocity Magnitude, Column 3: Bed Shear-stress

A.2. Semi-Circle Cases

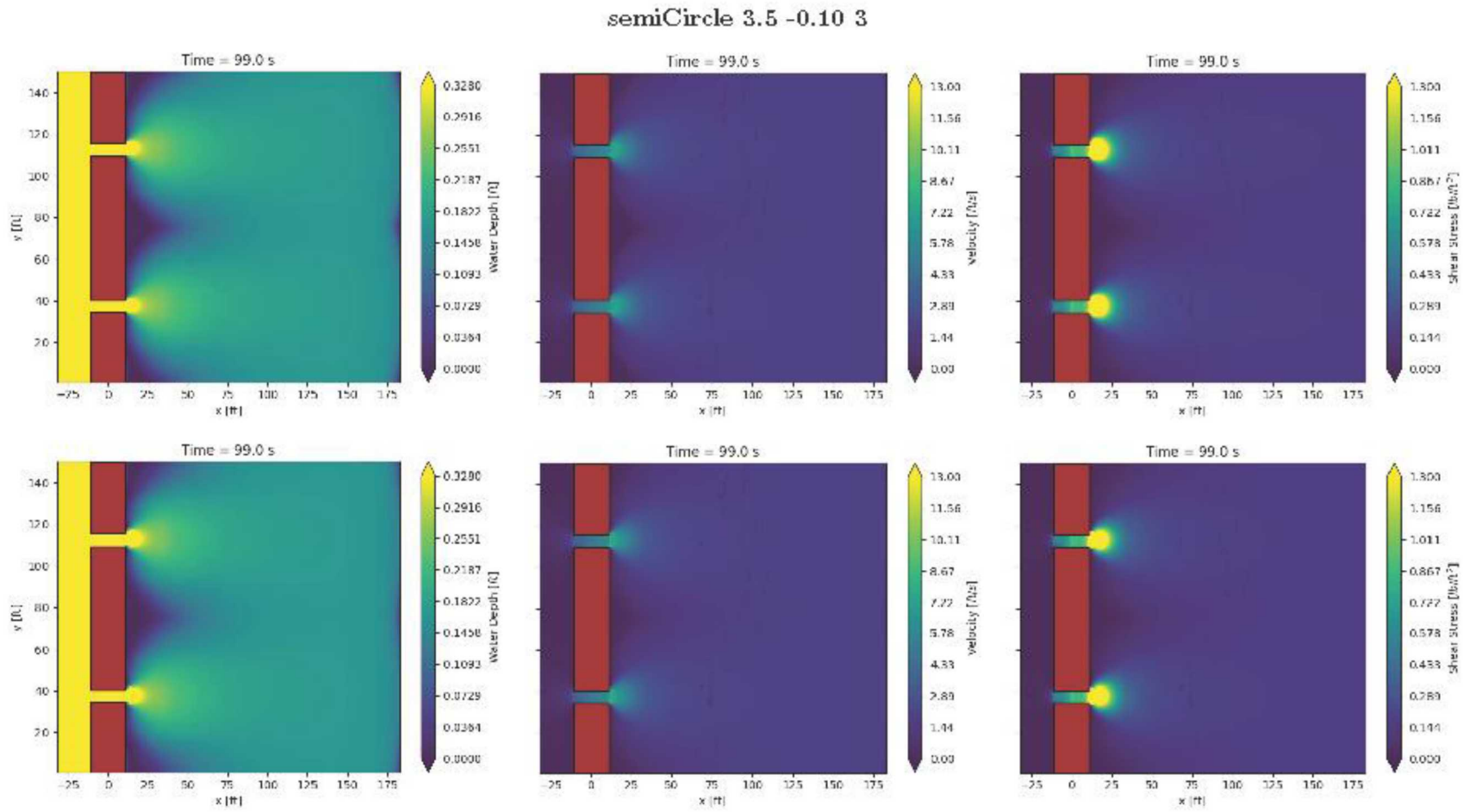

Figure 1: Top Row base case. Bottom Row semiCircle x = 3.5 m, depth = -0.10 m, diameter = 3m. Column 1: Water Depth, Column 2: Velocity Magnitude, Column 3: Bed Shear-stress

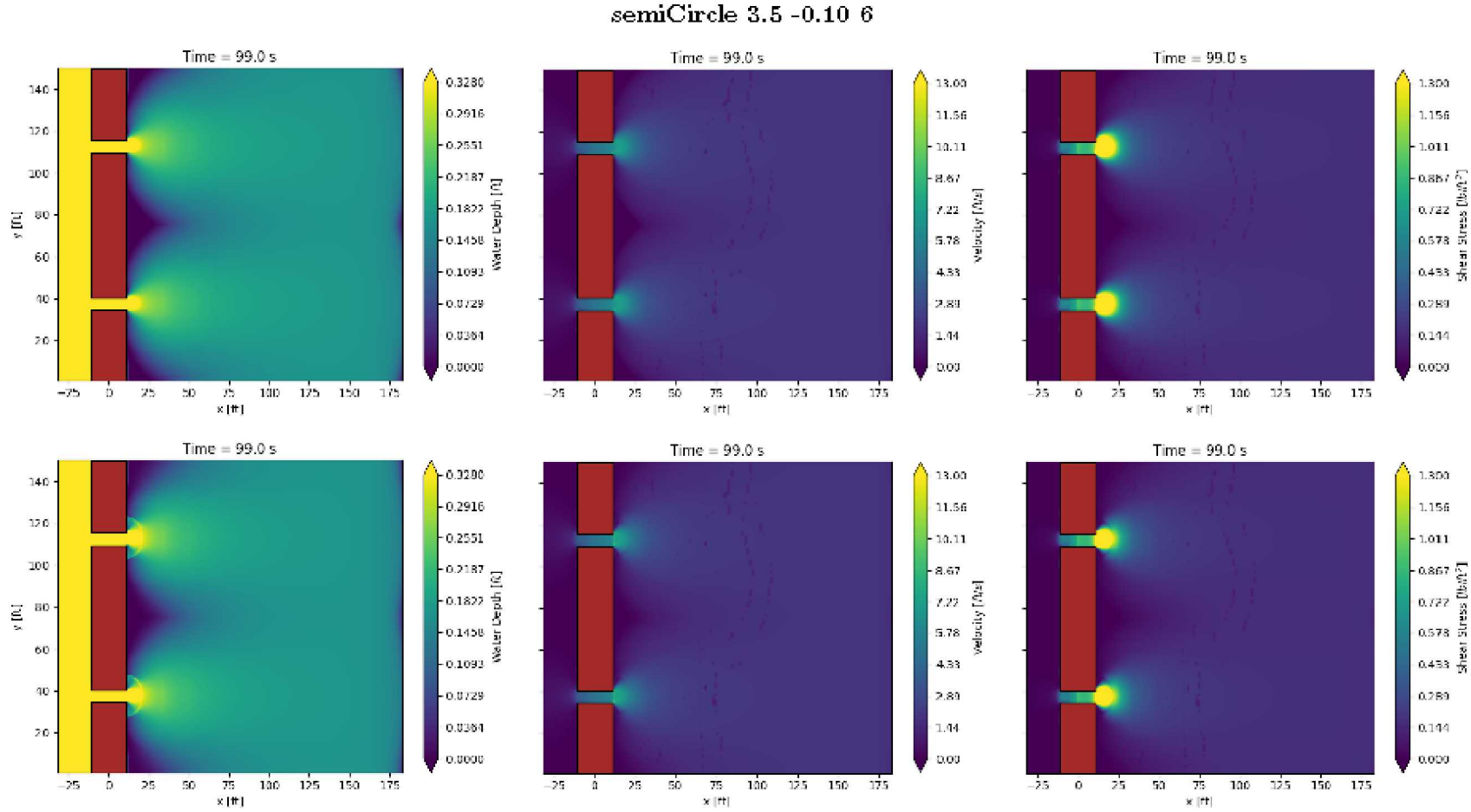

Figure 2: Top Row base case. Bottom Row semiCircle x = 3.5 m, depth = -0.10 m, diameter = 6m. Column 1: Water Depth, Column 2: Velocity Magnitude, Column 3: Bed Shear-stress

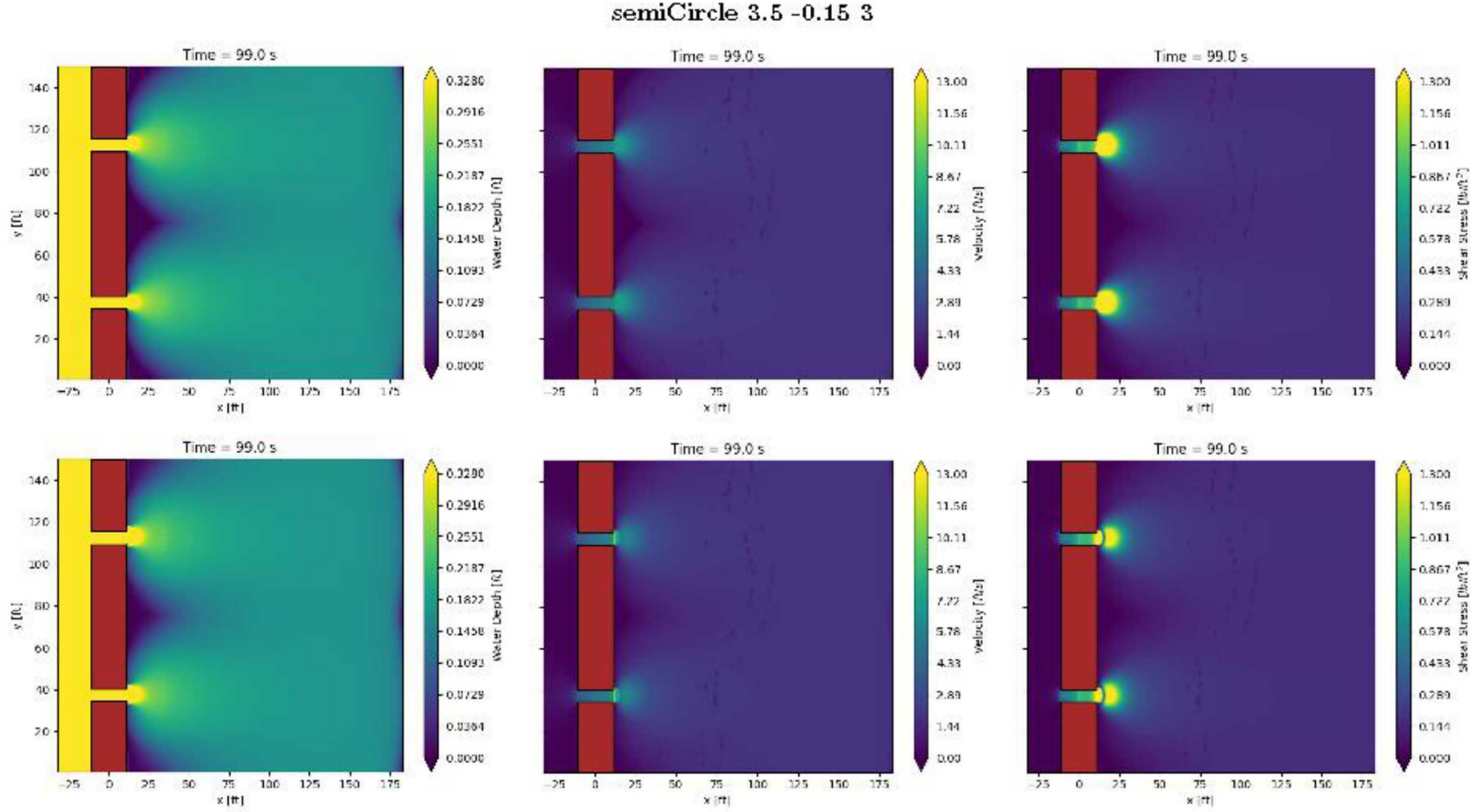

Figure 3: Top Row base case. Bottom Row semiCircle x = 3.5 m, depth = -0.15 m, diameter = 3m. Column 1: Water Depth, Column 2: Velocity Magnitude, Column 3: Bed Shear-stress

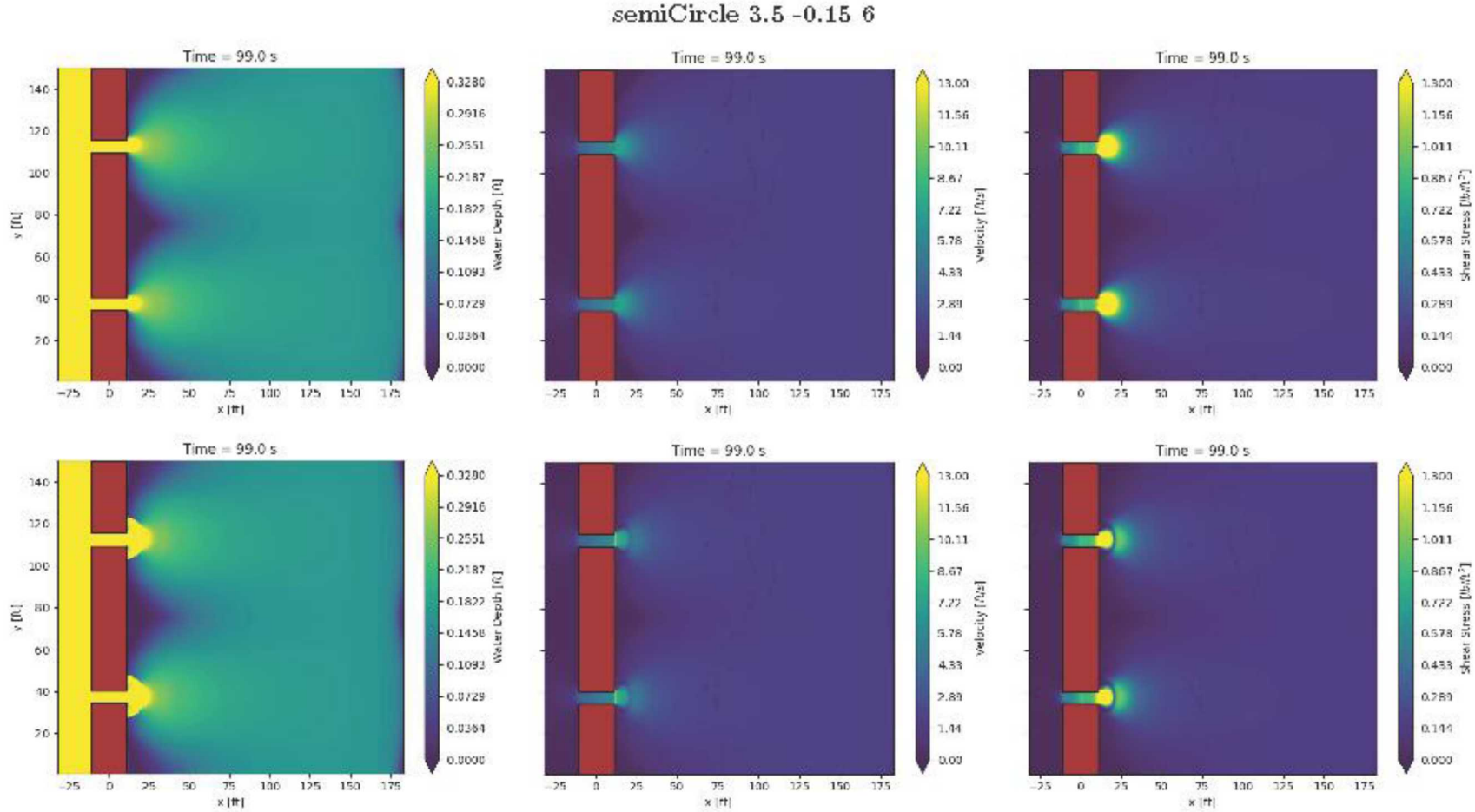

Figure 4: Top Row base case. Bottom Row semiCircle x = 3.5 m, depth = -0.15 m, diameter = 6m. Column 1: Water Depth, Column 2: Velocity Magnitude, Column 3: Bed Shear-stress

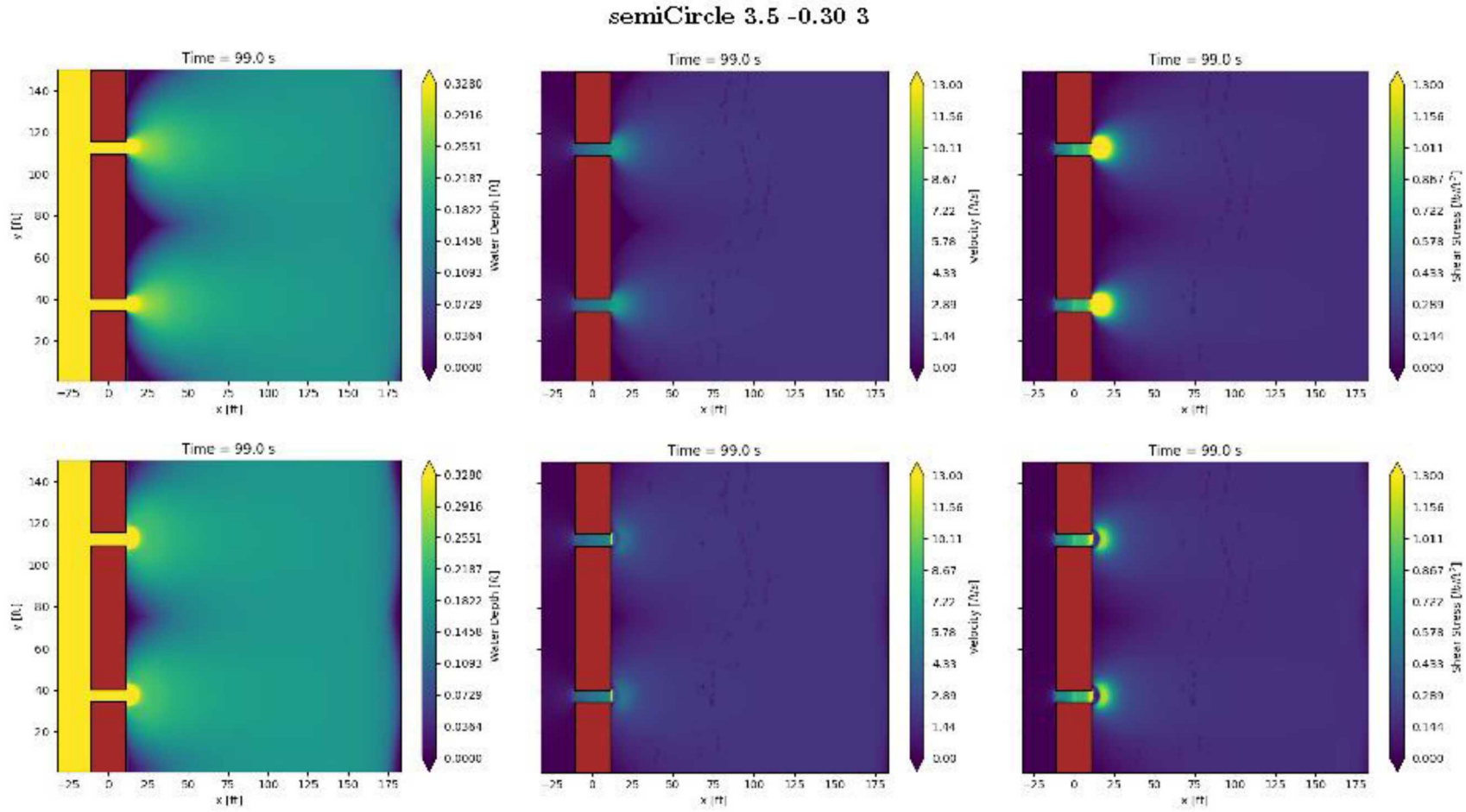

Figure 5: Top Row base case. Bottom Row semiCircle x = 3.5 m, depth = -0.30 m, diameter = 3m. Column 1: Water Depth, Column 2: Velocity Magnitude, Column 3: Bed Shear-stress

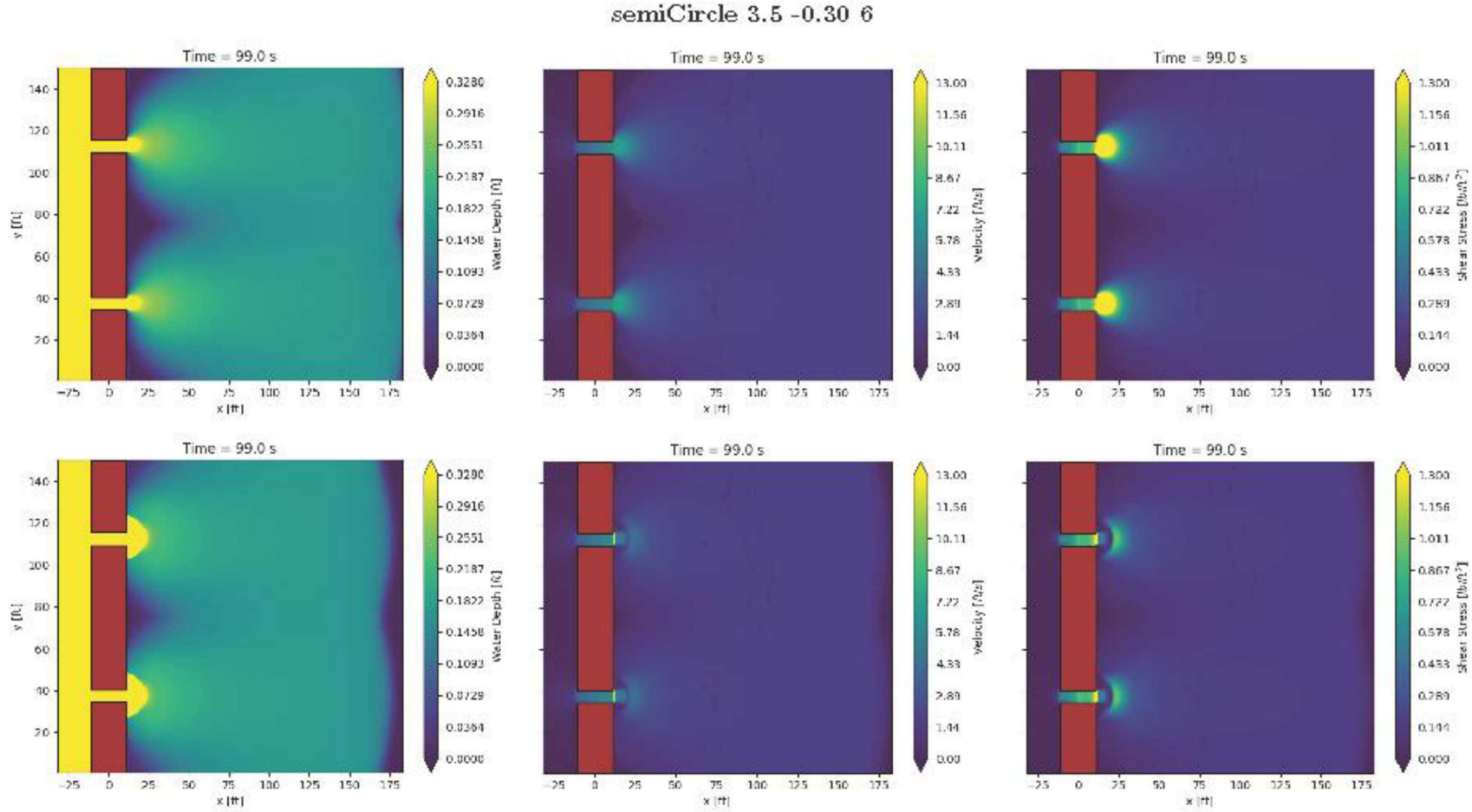

Figure 6: Top Row base case. Bottom Row semiCircle x = 3.5 m, depth = -0.30 m, diameter = 6m. Column 1: Water Depth, Column 2: Velocity Magnitude, Column 3: Bed Shear-stress

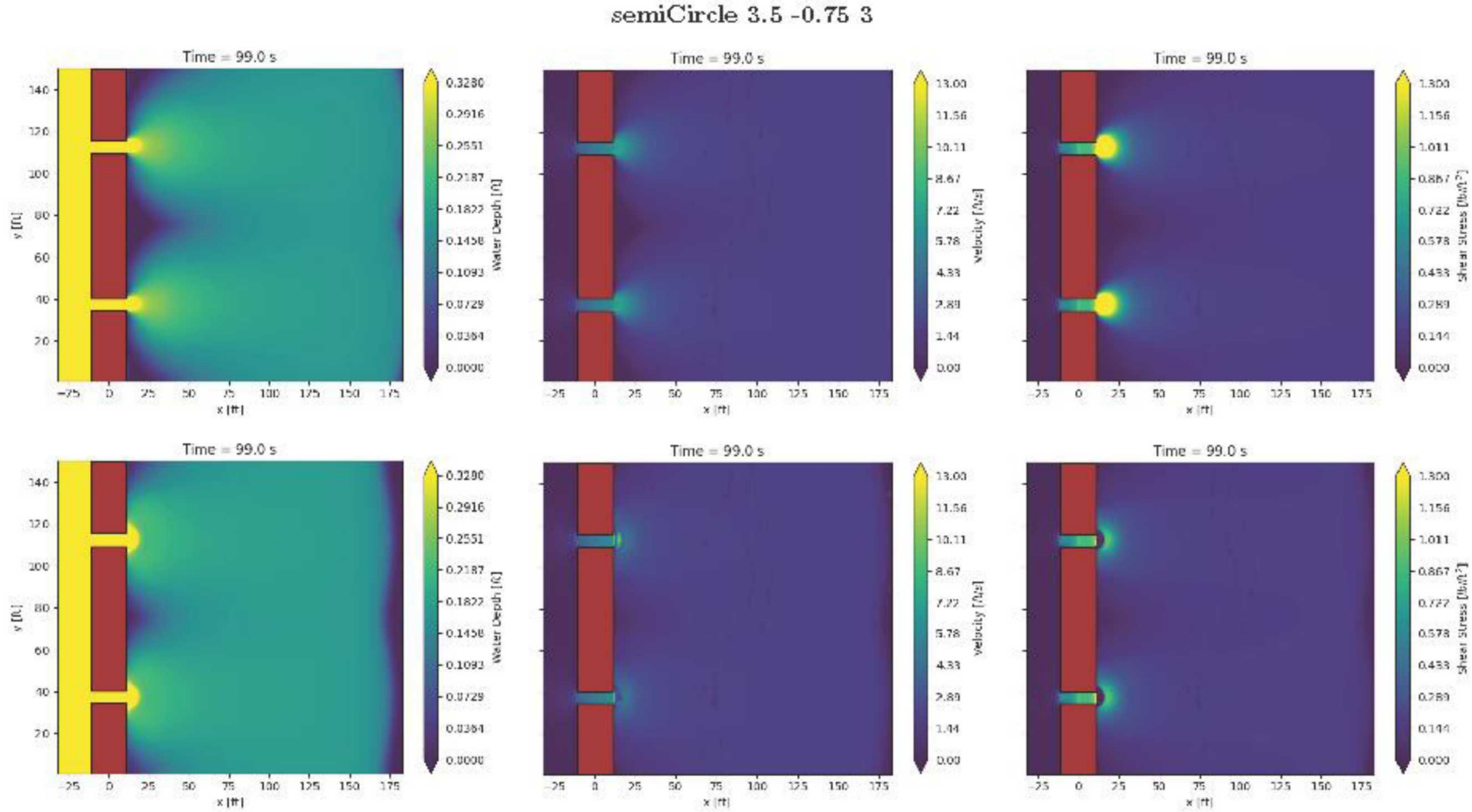

Figure 7: Top Row base case. Bottom Row semiCircle x = 3.5 m, depth = -0.75 m, diameter = 3m. Column 1: Water Depth, Column 2: Velocity Magnitude, Column 3: Bed Shear-stress

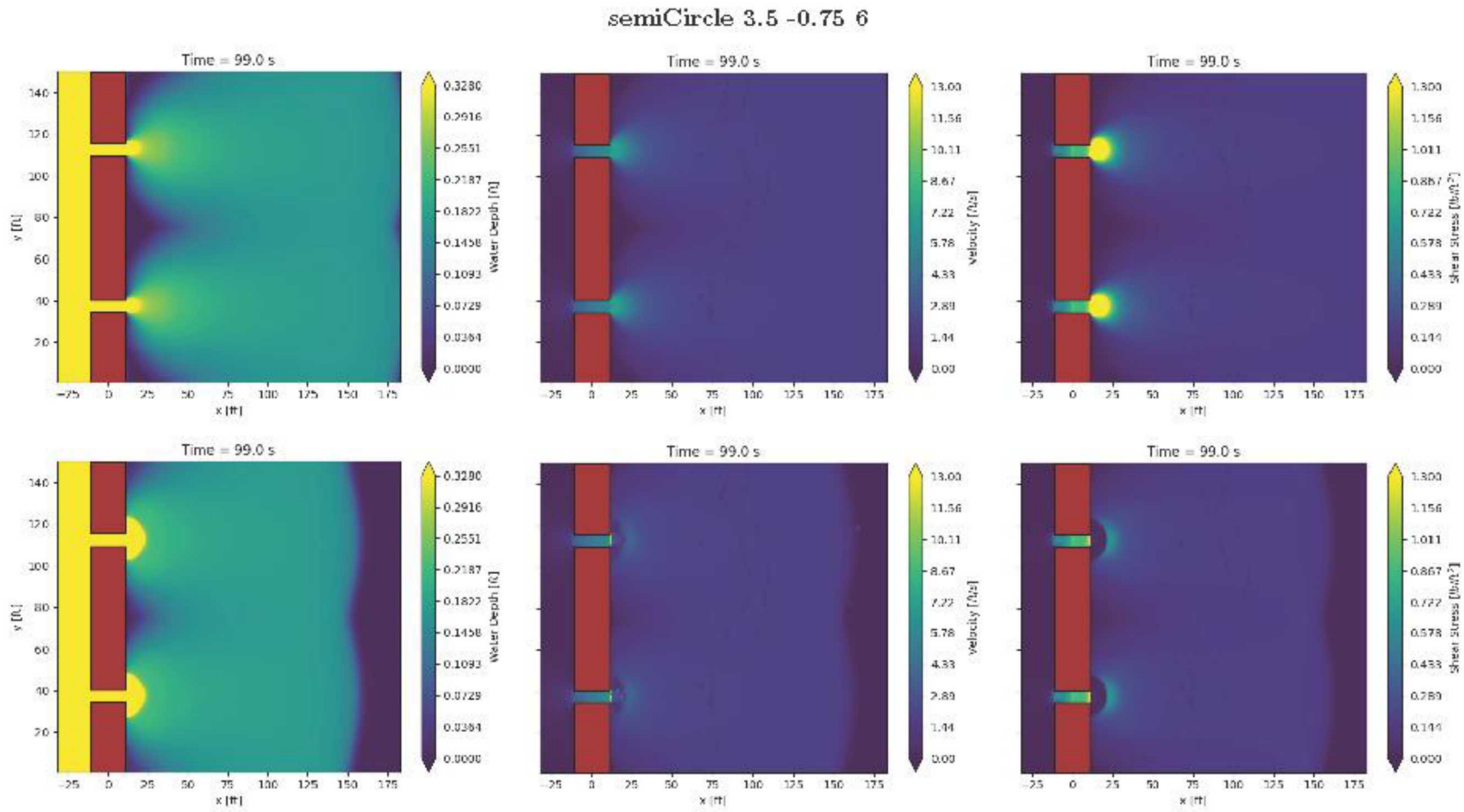

Figure 8: Top Row base case. Bottom Row semiCircle x = 3.5 m, depth = -0.75 m, diameter = 6m. Column 1: Water Depth, Column 2: Velocity Magnitude, Column 3: Bed Shear-stress

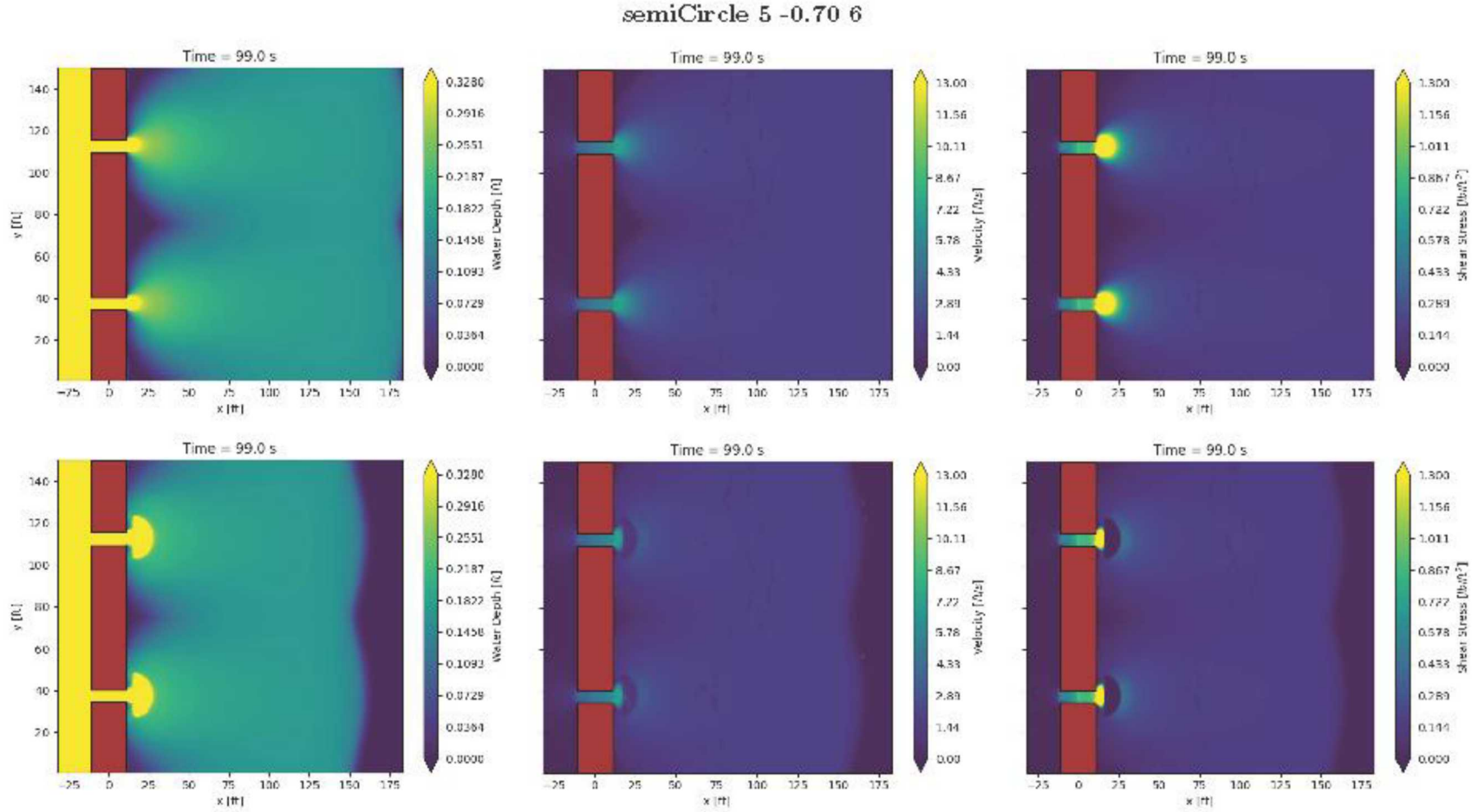

Figure 9: Top Row base case. Bottom Row semiCircle x = 5 m, depth = -0.70 m, diameter = 6m. Column 1: Water Depth, Column 2: Velocity Magnitude, Column 3: Bed Shear-stress

A.3. Gaussian Cases

A.3.1. Standard Field Cases

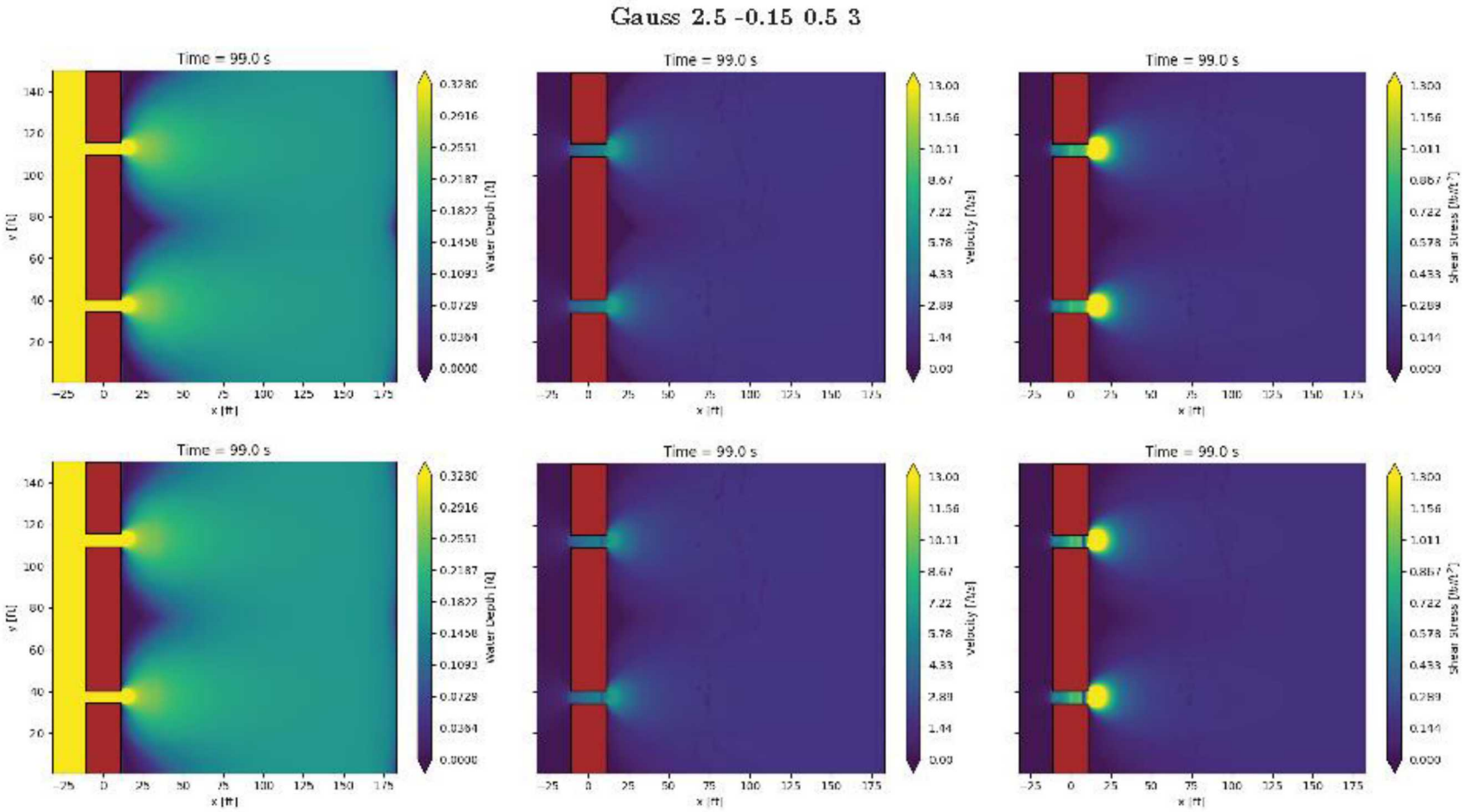

Figure 1: Top Row base case. Bottom Row Gauss x = 2.5 m, depth = -0.15 m, $FWHM_x$ = 0.5m, $FWHM_y$ = 3m. Column 1: Water Depth, Column 2: Velocity Magnitude, Column 3: Bed Shear-stress

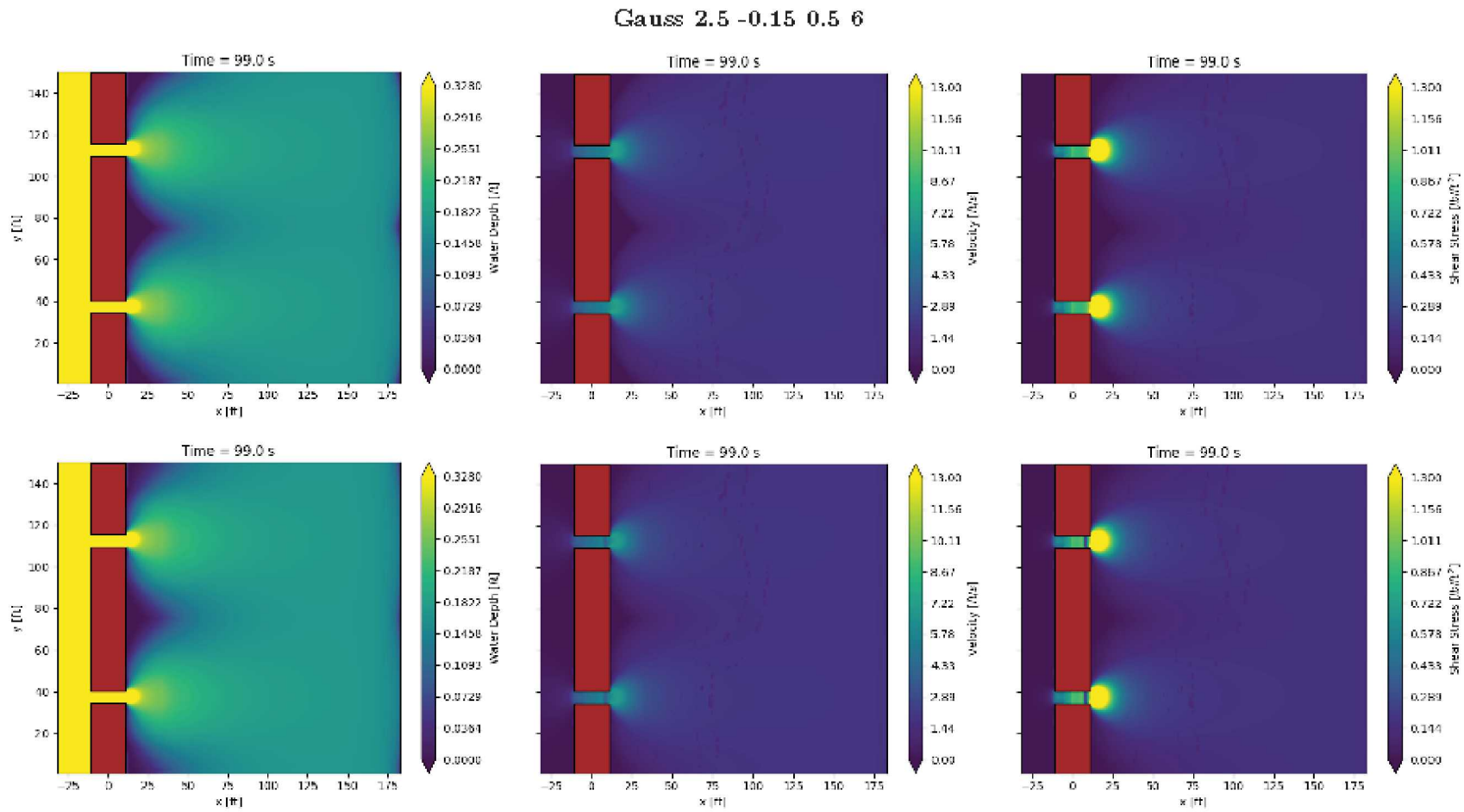

Figure 2: Top Row base case. Bottom Row Gauss x = 2.5 m, depth = -0.15 m, $FWHM_x$ = 0.5m, $FWHM_y$ = 6m. Column 1: Water Depth, Column 2: Velocity Magnitude, Column 3: Bed Shear-stress

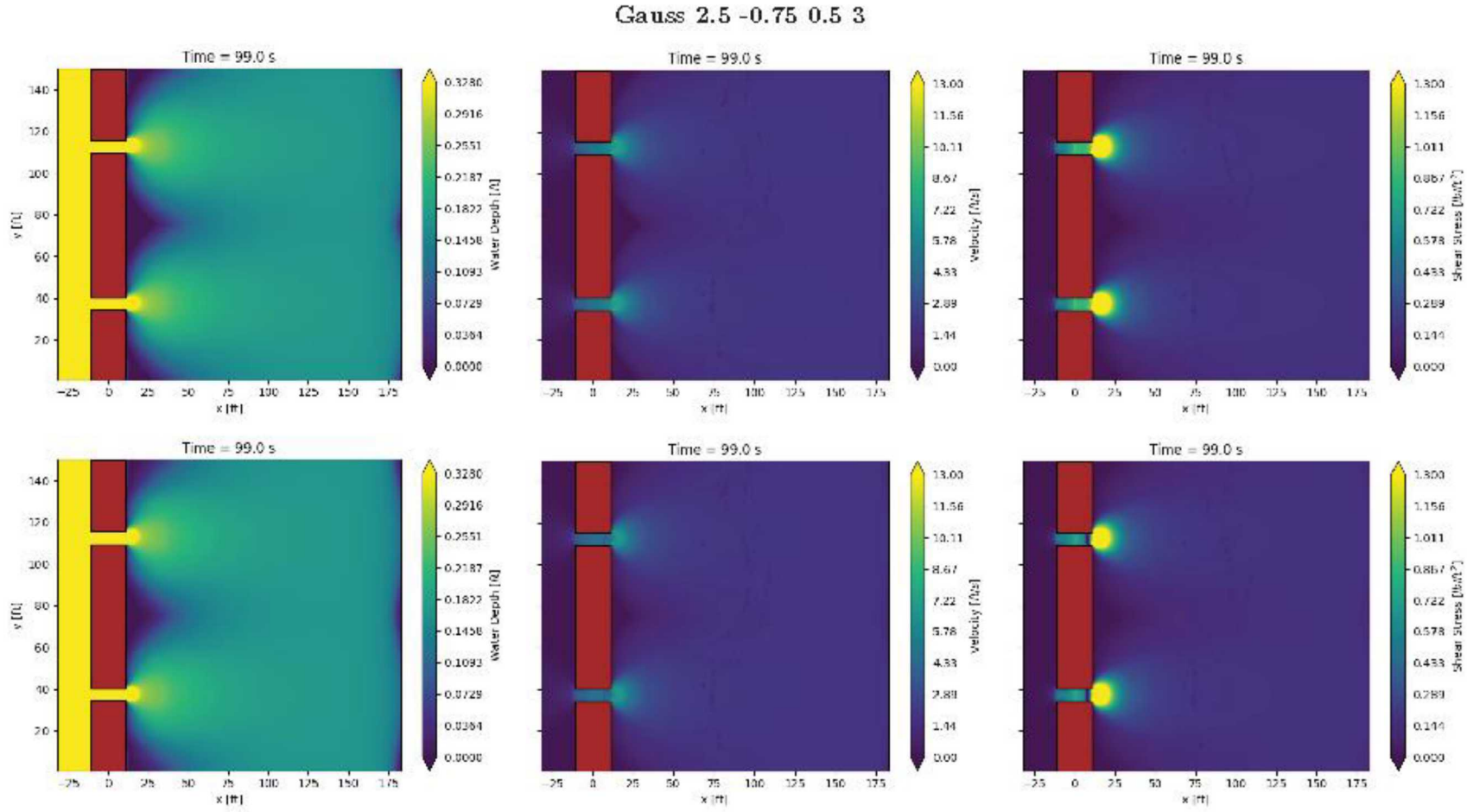

Figure 3: Top Row base case. Bottom Row Gauss x = 2.5 m, depth = -0.75 m, $FWHM_x$ = 0.5m, $FWHM_y$ = 3m. Column 1: Water Depth, Column 2: Velocity Magnitude, Column 3: Bed Shear-stress

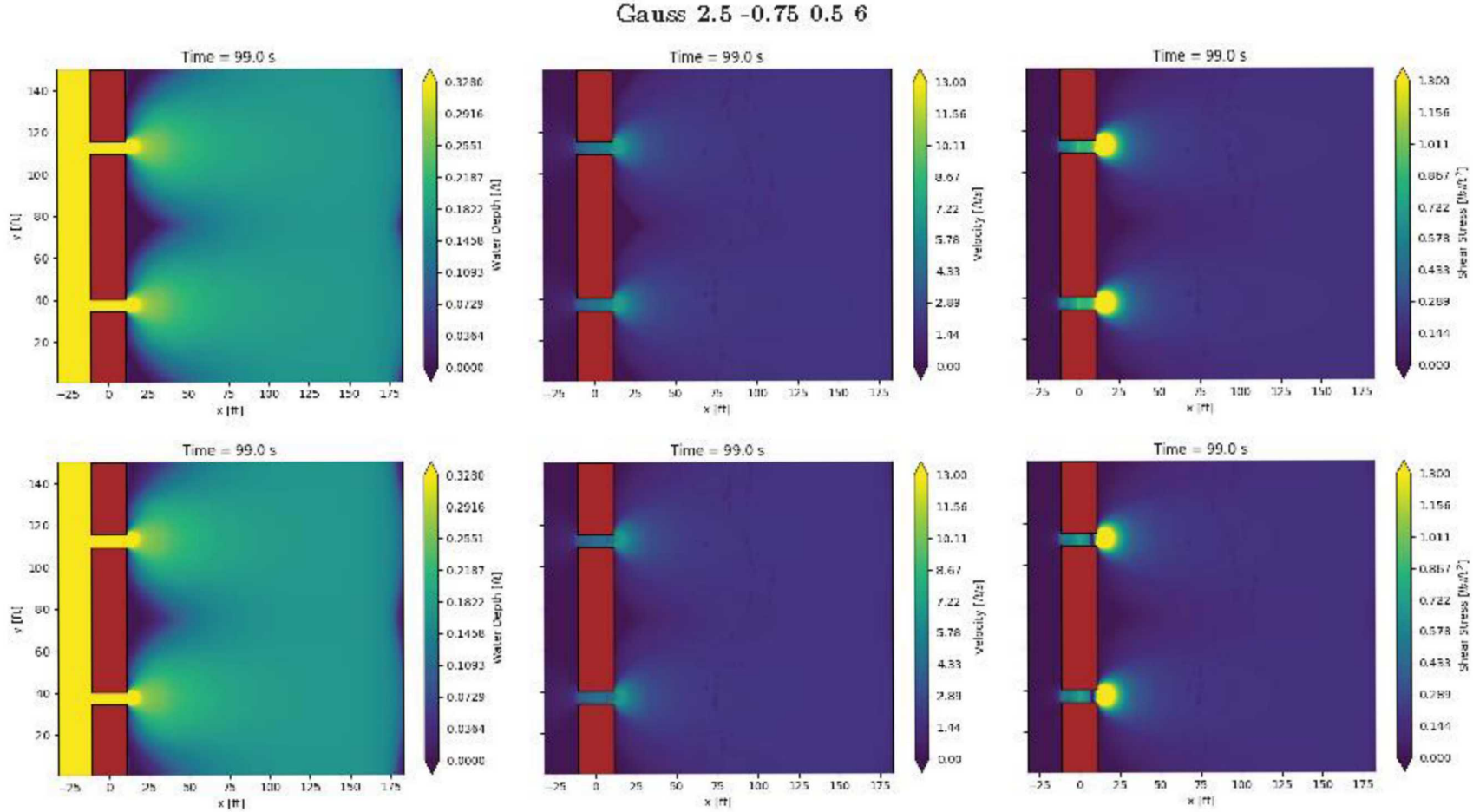

Figure 4: Top Row base case. Bottom Row Gauss x = 2.5 m, depth = -0.75 m, $FWHM_x$ = 0.5m, $FWHM_y$ = 6m. Column 1: Water Depth, Column 2: Velocity Magnitude, Column 3: Bed Shear-stress

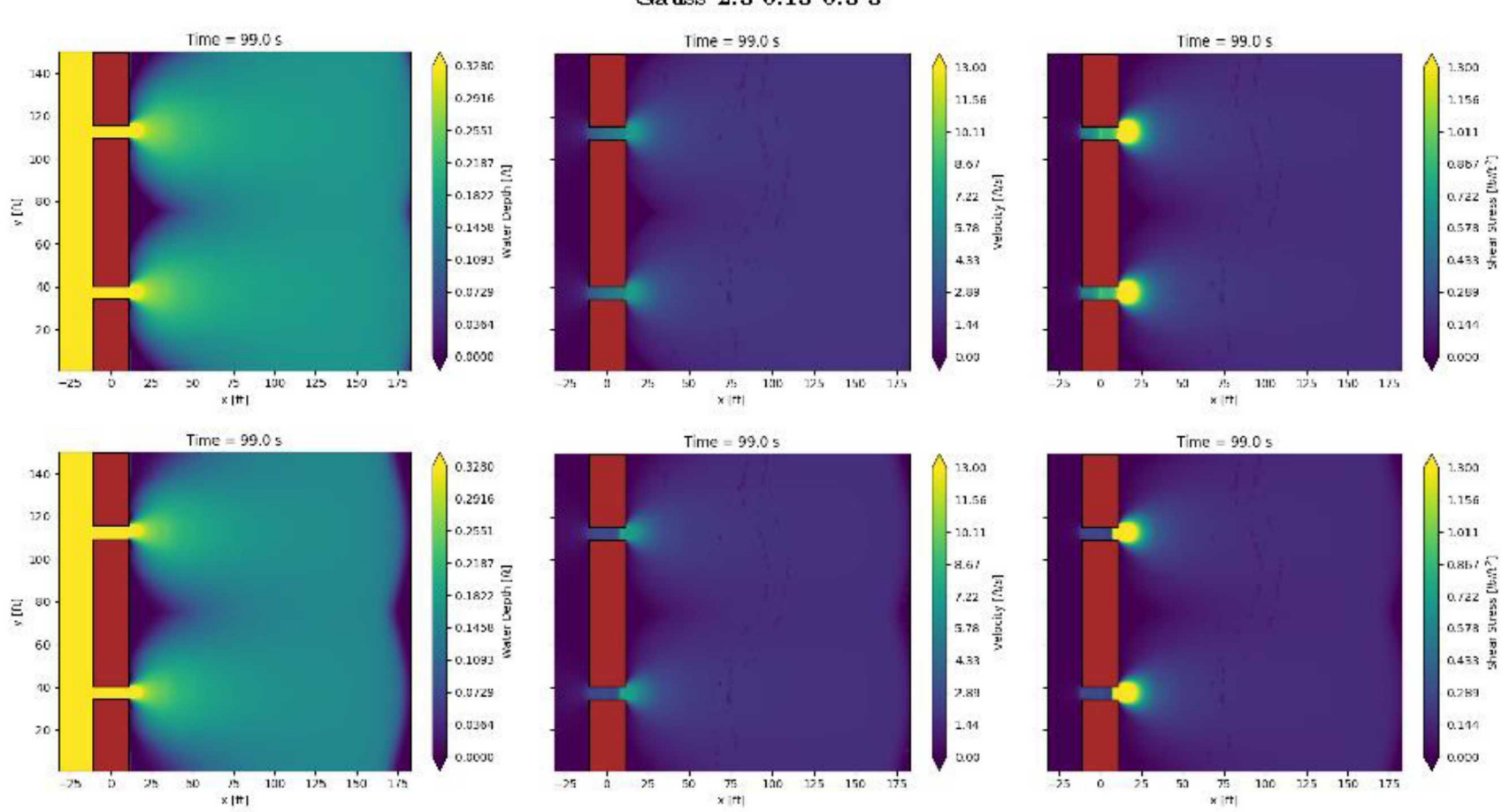

Figure 5: Top Row base case. Bottom Row Gauss x = 2.5 m, depth = 0.15 m, $FWHM_x$ = 0.5m, $FWHM_y$ = 3m. Column 1: Water Depth, Column 2: Velocity Magnitude, Column 3: Bed Shear-stress

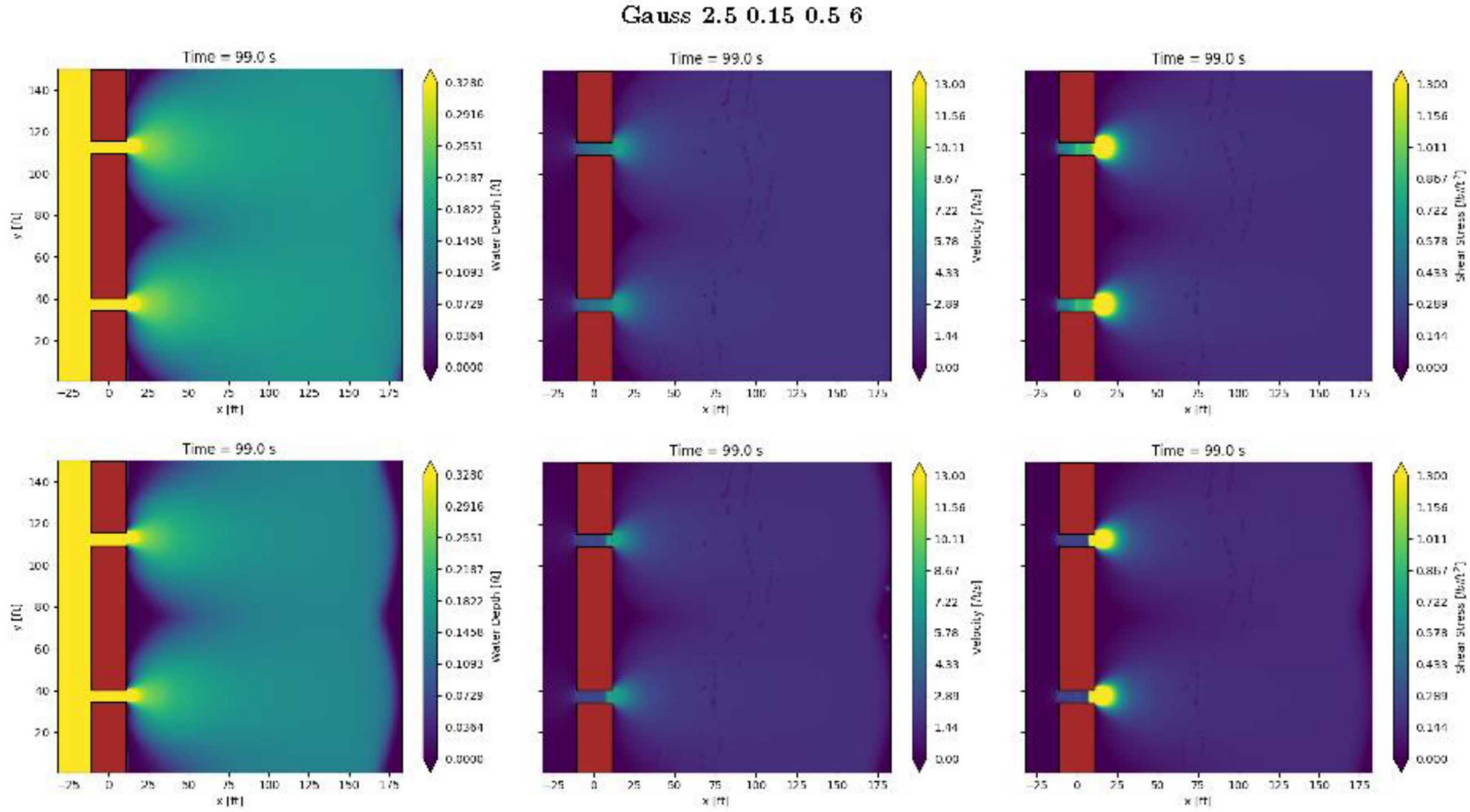

Figure 6: Top Row base case. Bottom Row Gauss x = 2.5 m, depth = 0.15 m, $FWHM_x$ = 0.5m, $FWHM_y$ = 6m. Column 1: Water Depth, Column 2: Velocity Magnitude, Column 3: Bed Shear-stress

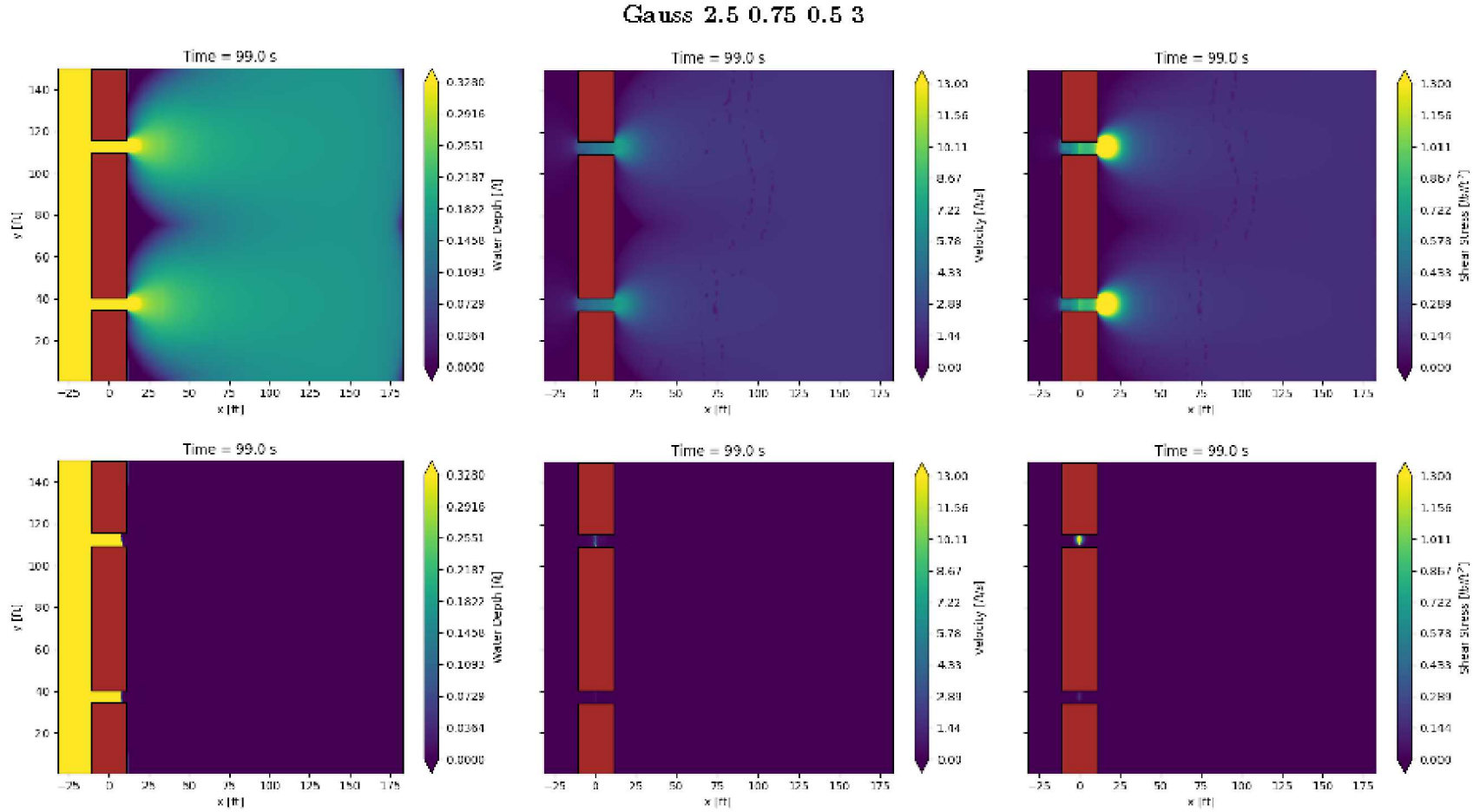

Figure 7: Top Row base case. Bottom Row Gauss x = 2.5 m, depth = 0.75 m, $FWHM_x = 0.5$m, $FWHM_y = 3$m. Column 1: Water Depth, Column 2: Velocity Magnitude, Column 3: Bed Shear-stress

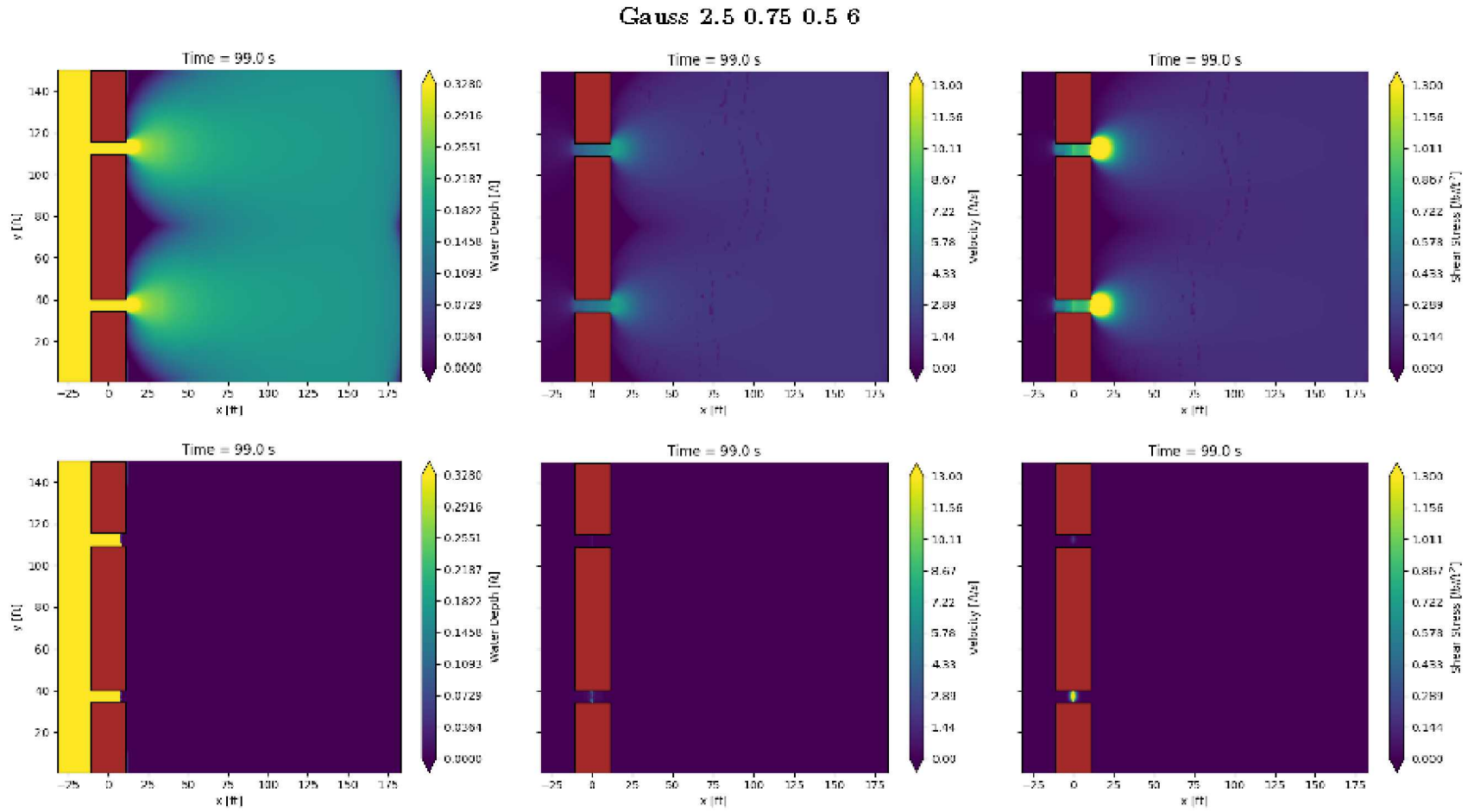

Figure 8: Top Row base case. Bottom Row Gauss x = 2.5 m, depth = 0.75 m, $FWHM_x = 0.5$m, $FWHM_y = 6$m. Column 1: Water Depth, Column 2: Velocity Magnitude, Column 3: Bed Shear-stress

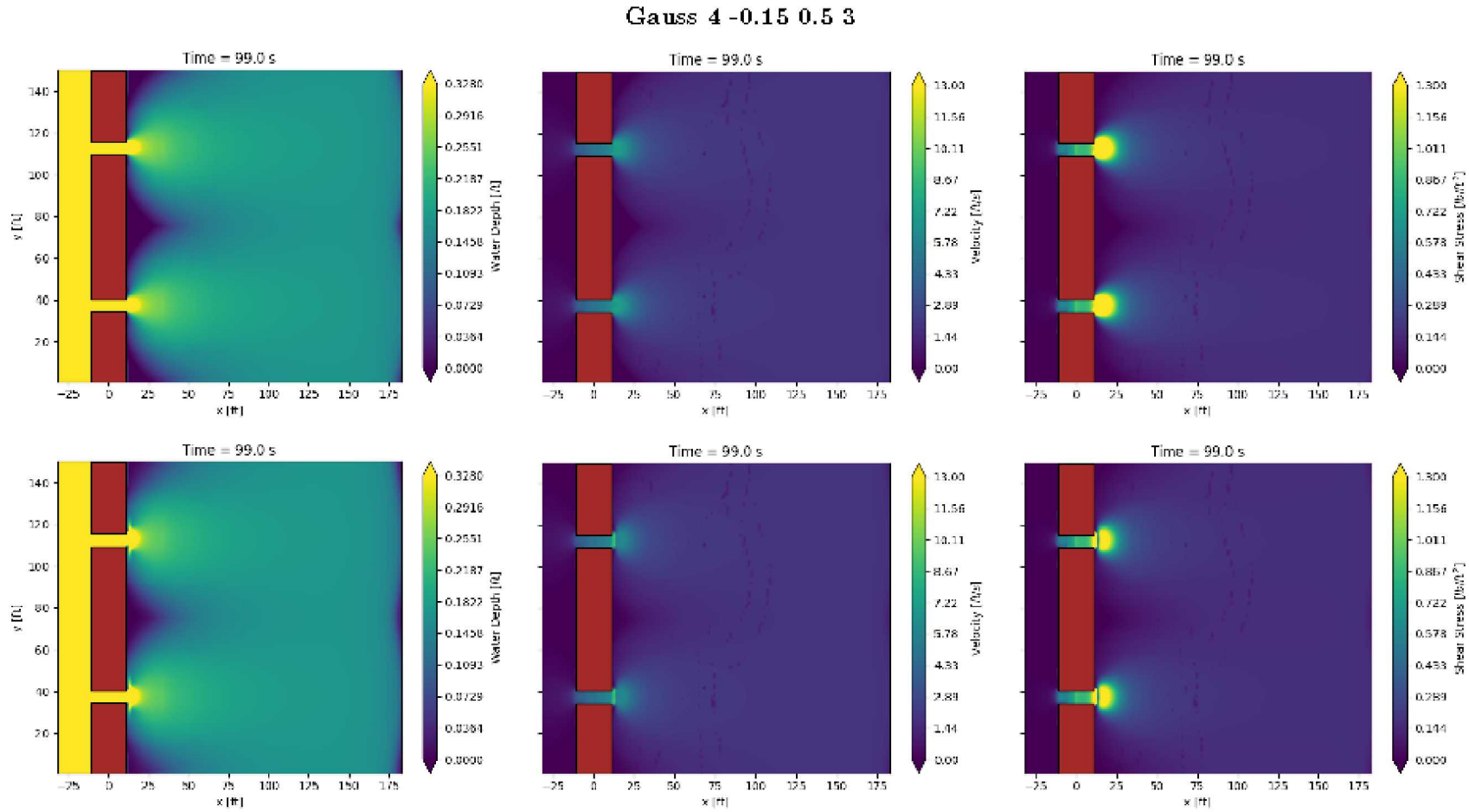

Figure 9: Top Row base case. Bottom Row Gauss x = 4 m, depth = -0.15 m, $FWHM_x$ = 0.5m, $FWHM_y$ = 3m. Column 1: Water Depth, Column 2: Velocity Magnitude, Column 3: Bed Shear-stress

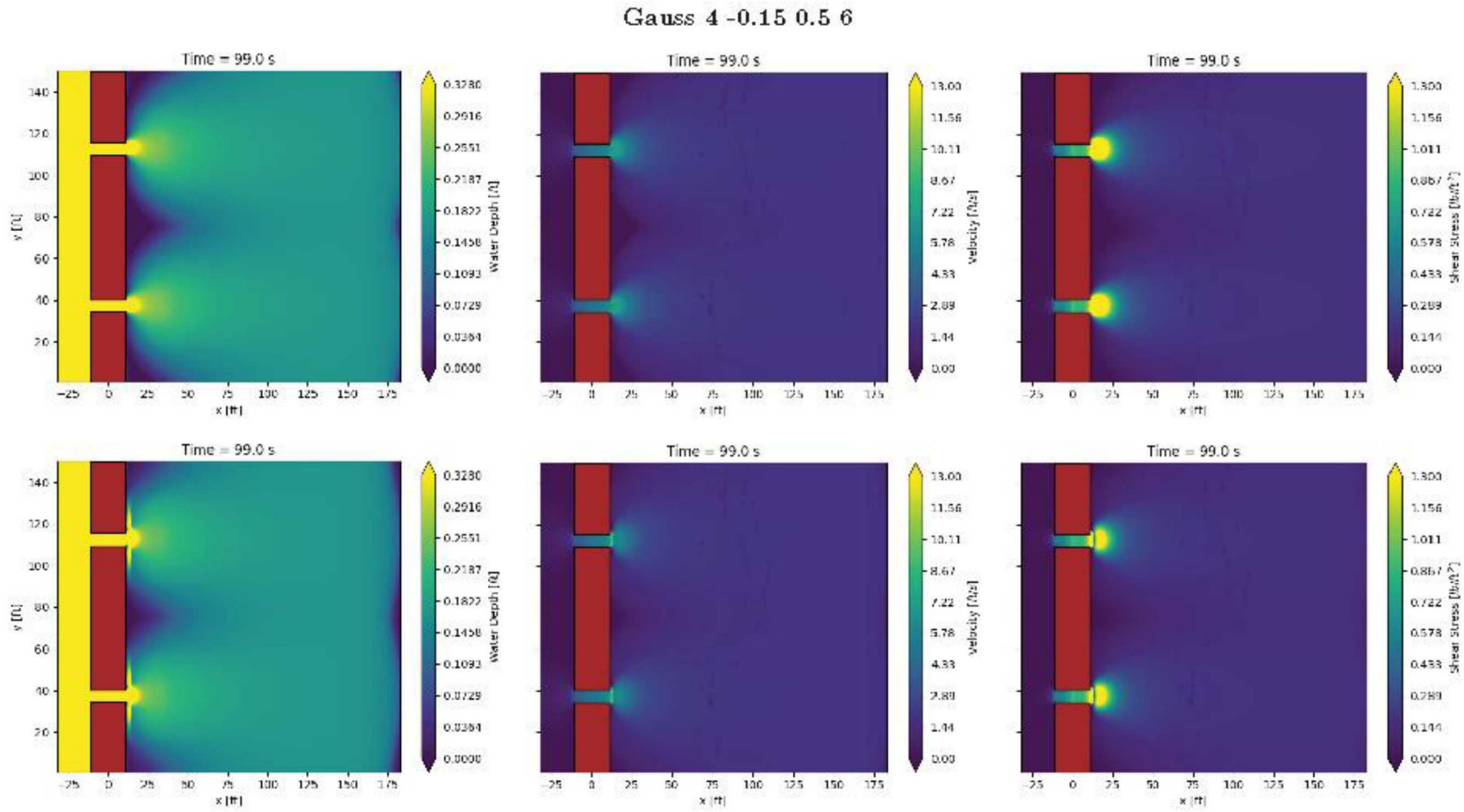

Figure 10: Top Row base case. Bottom Row Gauss x = 4 m, depth = -0.15 m, $FWHM_x = 0.5$m, $FWHM_y = 6$m. Column 1: Water Depth, Column 2: Velocity Magnitude, Column 3: Bed Shear-stress

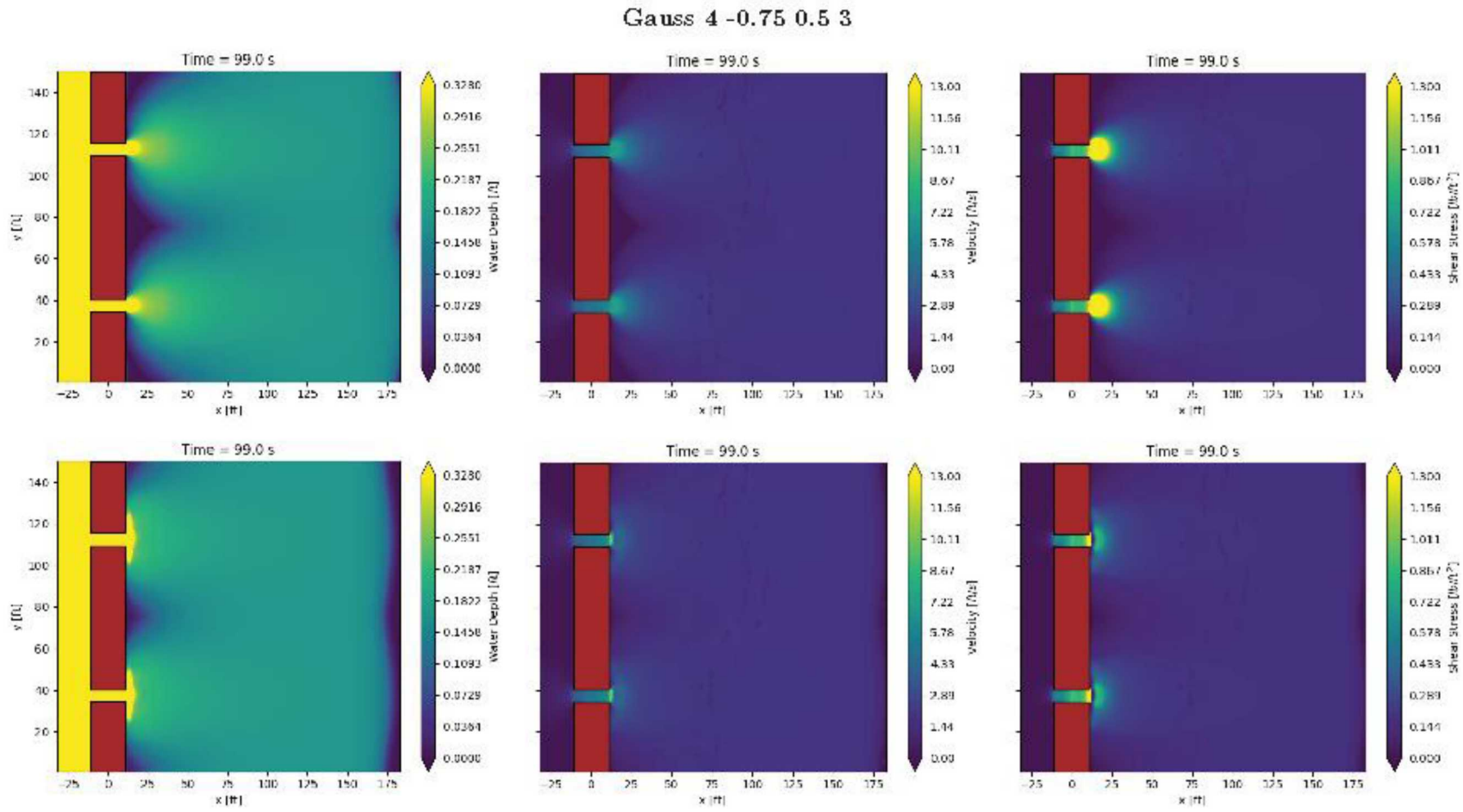

Figure 11: Top Row base case. Bottom Row Gauss x = 4 m, depth = -0.75 m, $FWHM_x = 0.5$m, $FWHM_y = 3$m. Column 1: Water Depth, Column 2: Velocity Magnitude, Column 3: Bed Shear-stress

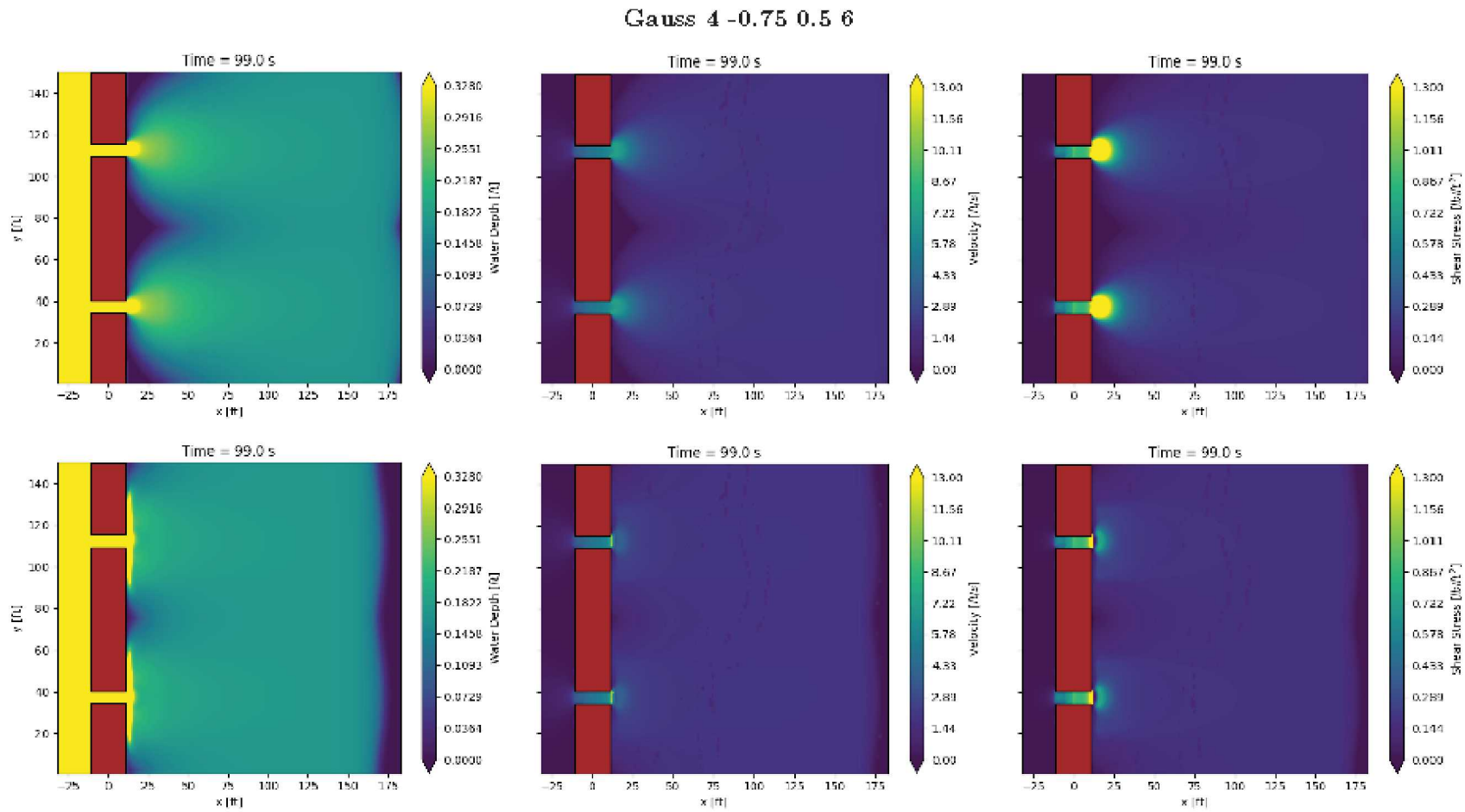

Figure 12: Top Row base case. Bottom Row Gauss x = 4 m, depth = -0.75 m, $FWHM_x$ = 0.5m, $FWHM_y$ = 6m. Column 1: Water Depth, Column 2: Velocity Magnitude, Column 3: Bed Shear-stress

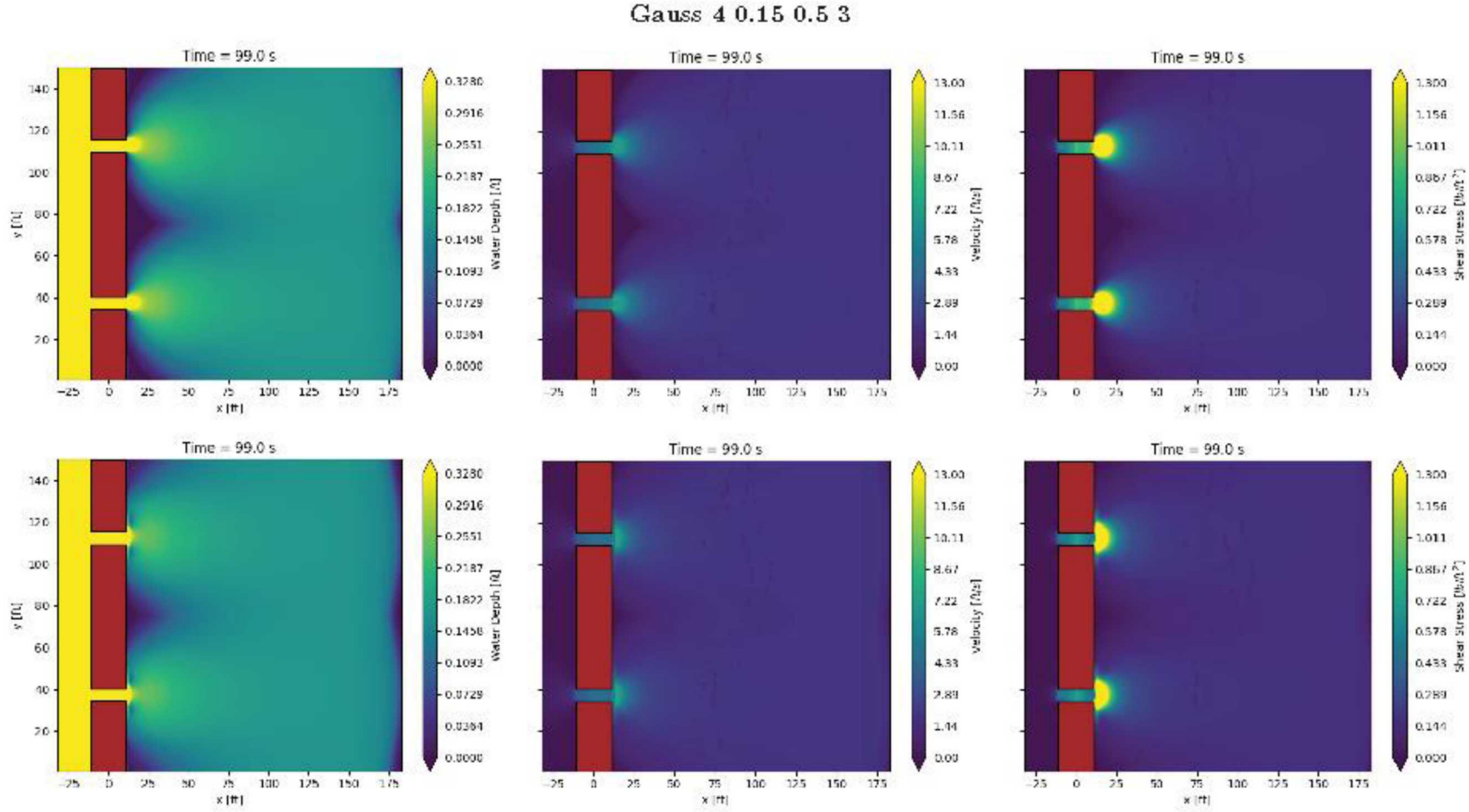

Figure 13: Top Row base case. Bottom Row Gauss x = 4 m, depth = 0.15 m, $FWHM_x = 0.5$m, $FWHM_y = 3$m. Column 1: Water Depth, Column 2: Velocity Magnitude, Column 3: Bed Shear-stress

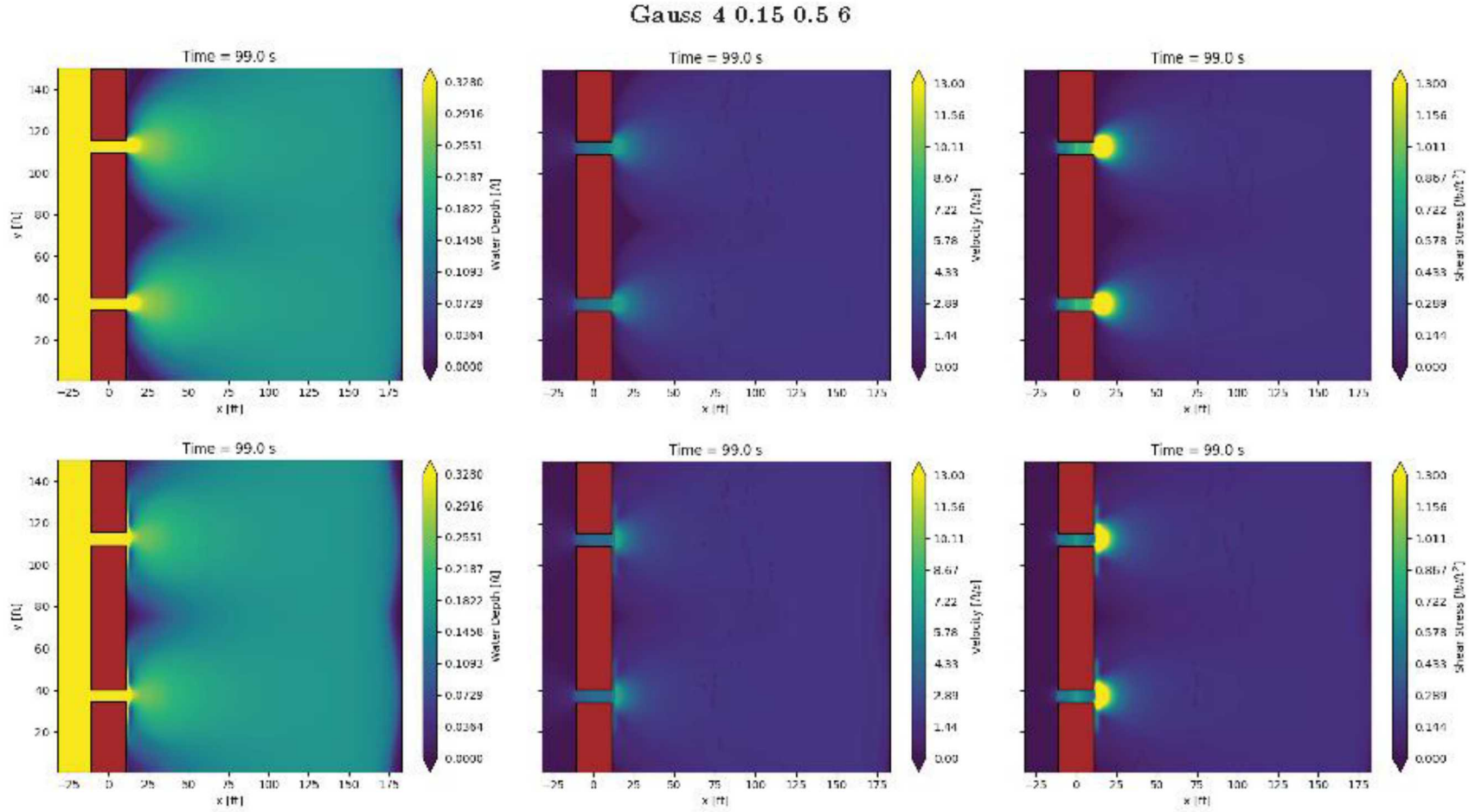

Figure 14: Top Row base case. Bottom Row Gauss x = 4 m, depth = 0.15 m, $FWHM_x = 0.5$m, $FWHM_y = 6$m. Column 1: Water Depth, Column 2: Velocity Magnitude, Column 3: Bed Shear-stress

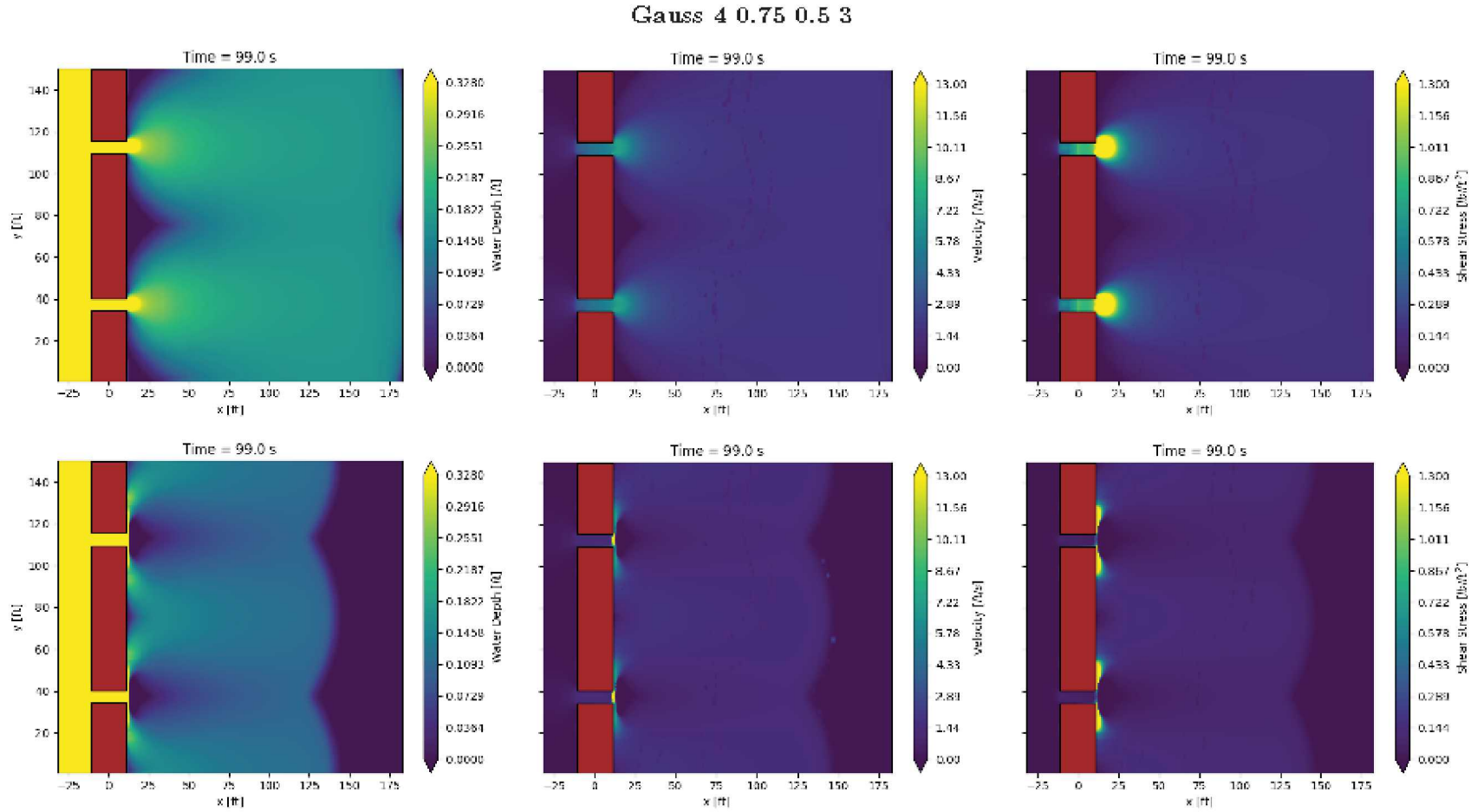

Figure 15: Top Row base case. Bottom Row Gauss x = 4 m, depth = 0.75 m, $FWHM_x = 0.5$m, $FWHM_y = 3$m. Column 1: Water Depth, Column 2: Velocity Magnitude, Column 3: Bed Shear-stress

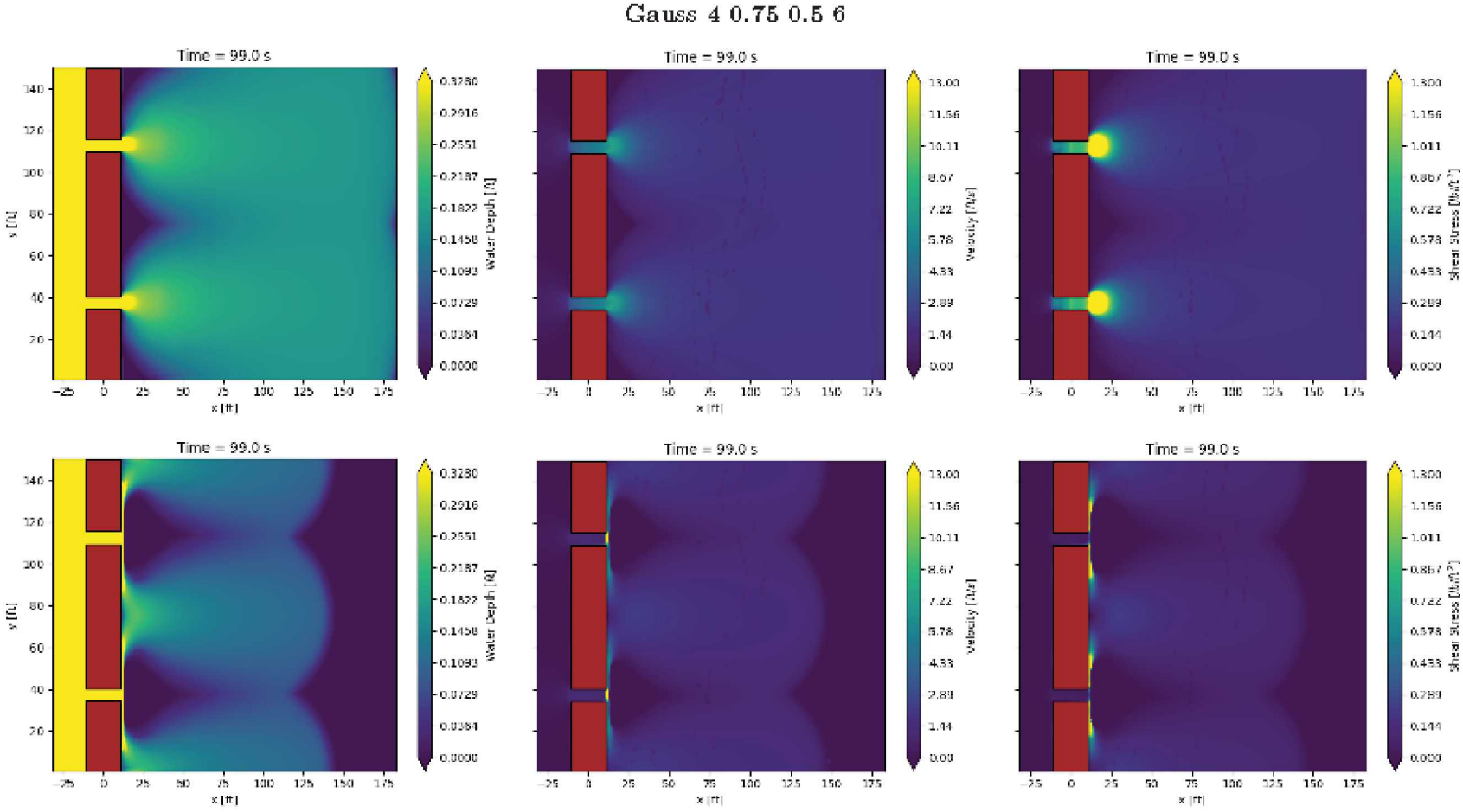

Figure 16: Top Row base case. Bottom Row Gauss x = 4 m, depth = 0.75 m, $FWHM_x = 0.5$m, $FWHM_y = 6$m. Column 1: Water Depth, Column 2: Velocity Magnitude, Column 3: Bed Shear-stress

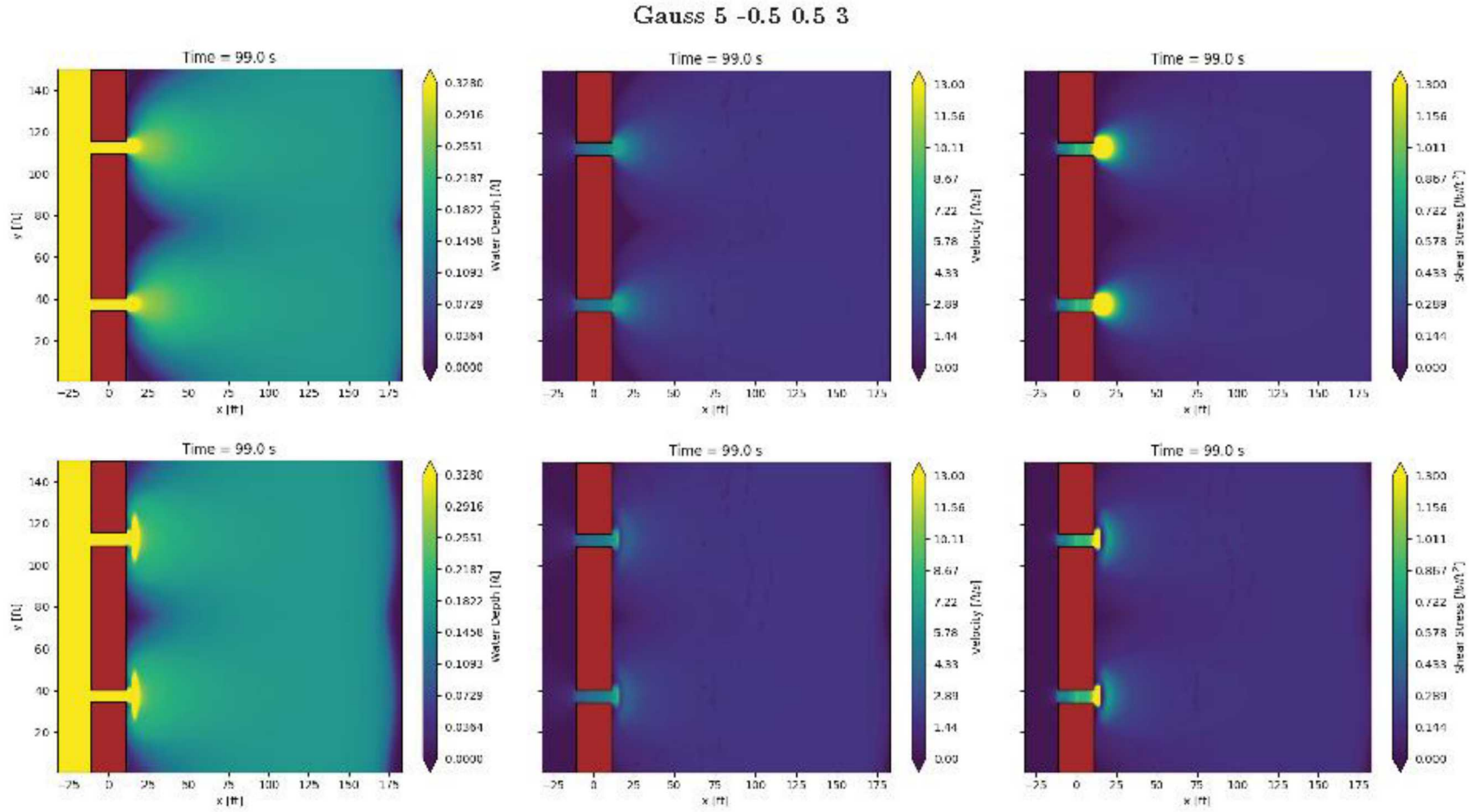

Figure 17: Top Row base case. Bottom Row Gauss x = 5 m, depth = -0.5 m, $FWHM_x$ = 0.5m, $FWHM_y$ = 3m. Column 1: Water Depth, Column 2: Velocity Magnitude, Column 3: Bed Shear-stress

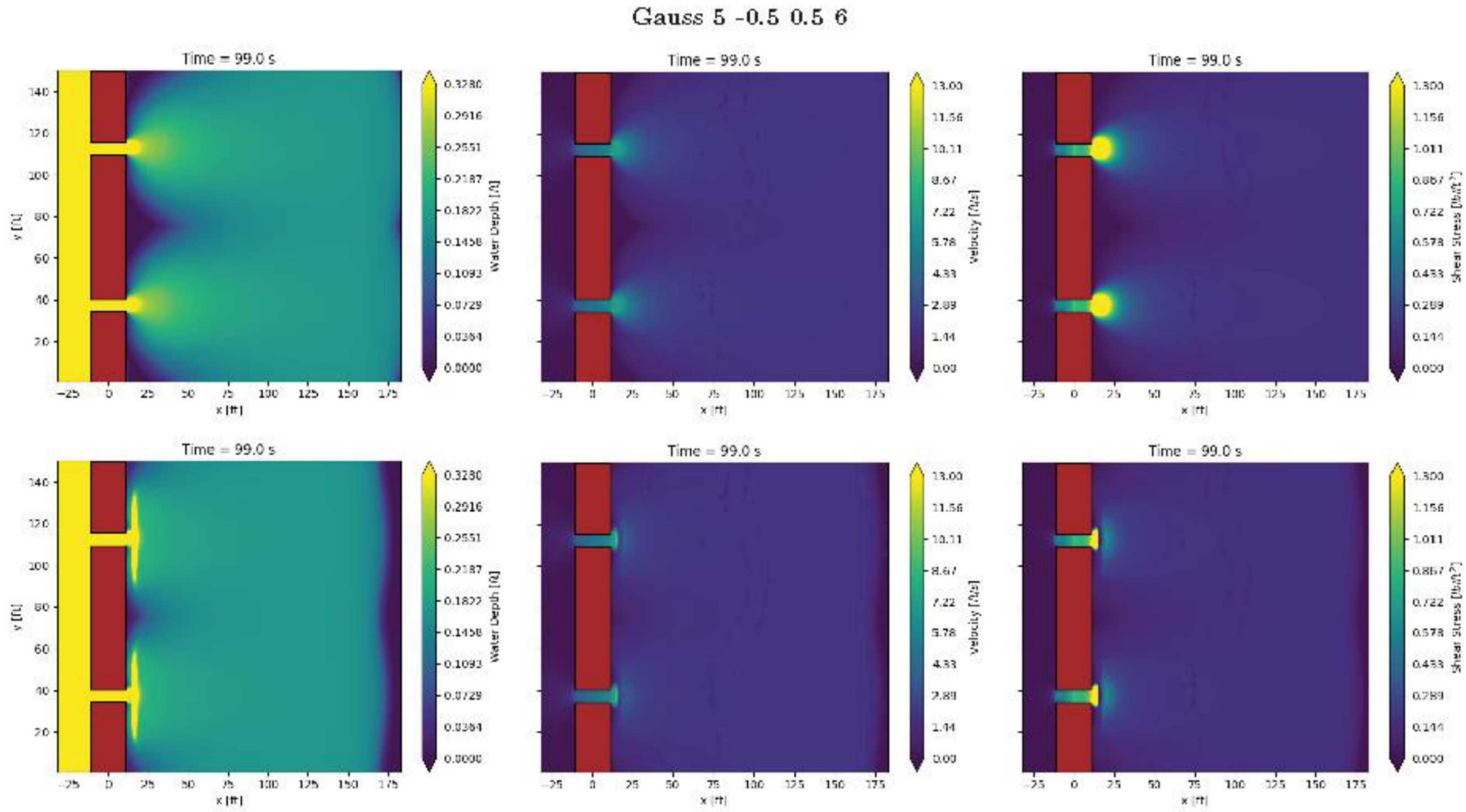

Figure 18: Top Row base case. Bottom Row Gauss x = 5 m, depth = -0.5 m, $FWHM_x$ = 0.5m, $FWHM_y$ = 6m. Column 1: Water Depth, Column 2: Velocity Magnitude, Column 3: Bed Shear-stress

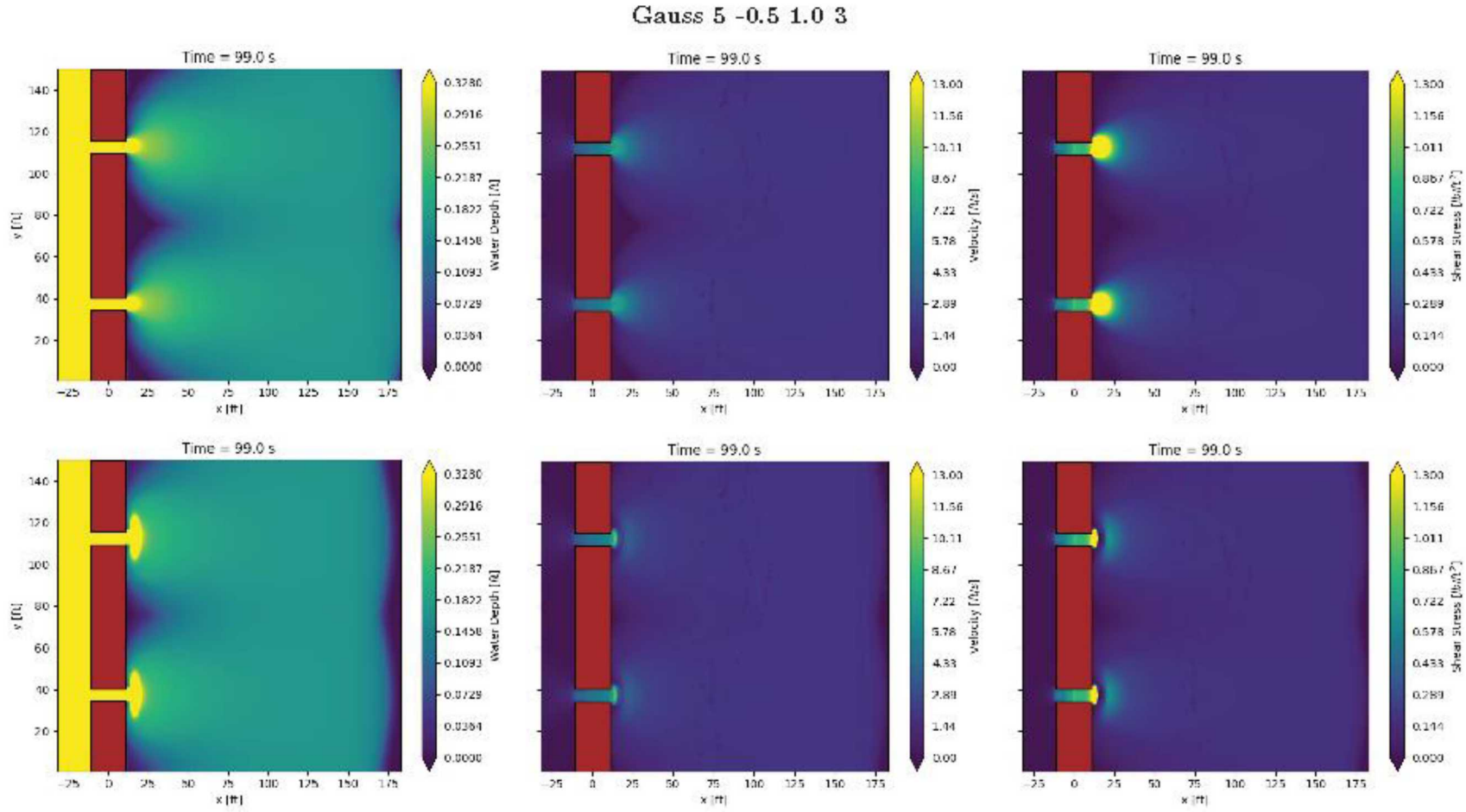

Figure 19: Top Row base case. Bottom Row Gauss x = 5 m, depth = -0.5 m, $FWHM_x = 1.0$m, $FWHM_y = 3$m. Column 1: Water Depth, Column 2: Velocity Magnitude, Column 3: Bed Shear-stress

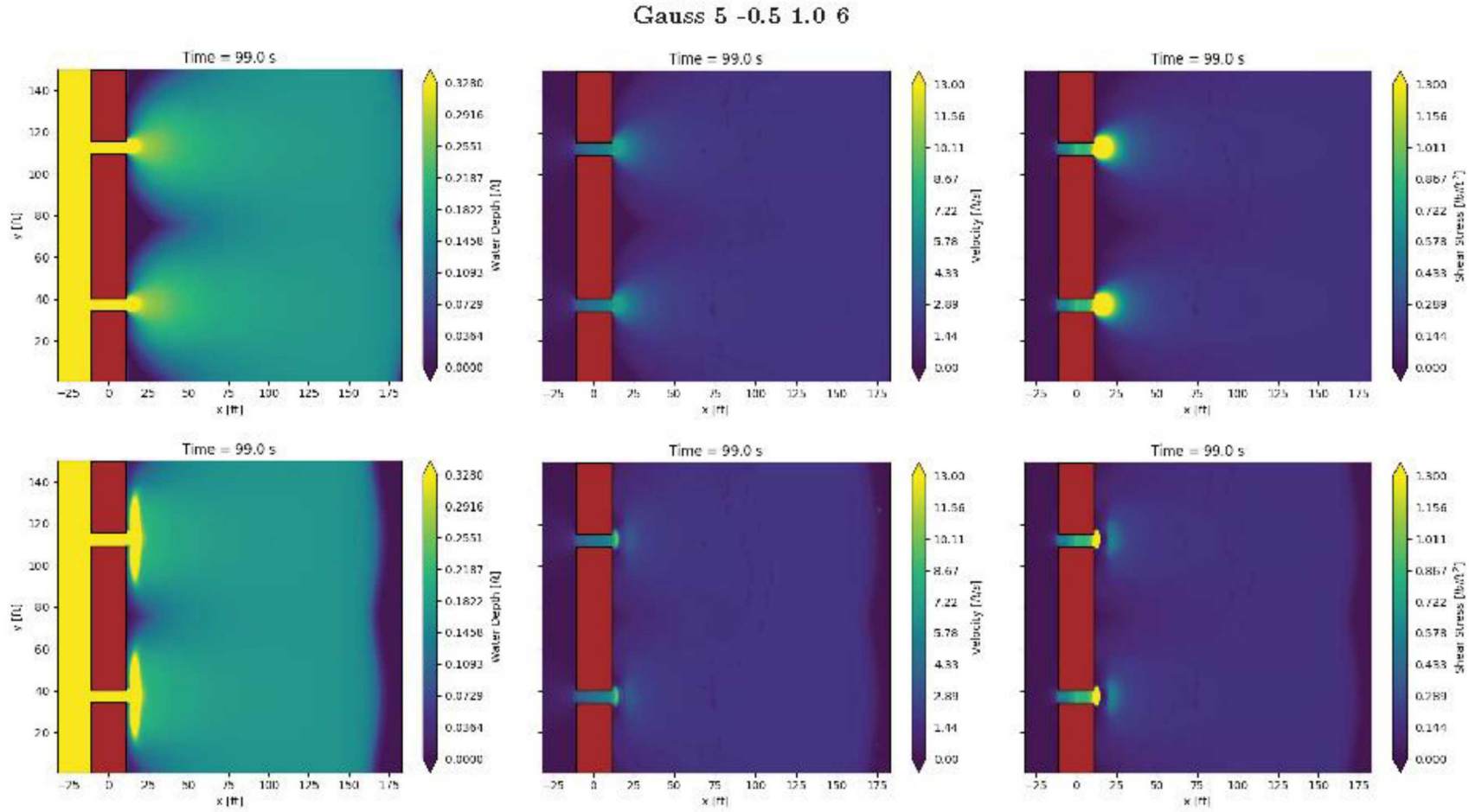

Figure 20: Top Row base case. Bottom Row Gauss x = 5 m, depth = -0.5 m, $FWHM_x = 1.0$m, $FWHM_y = 6$m. Column 1: Water Depth, Column 2: Velocity Magnitude, Column 3: Bed Shear-stress

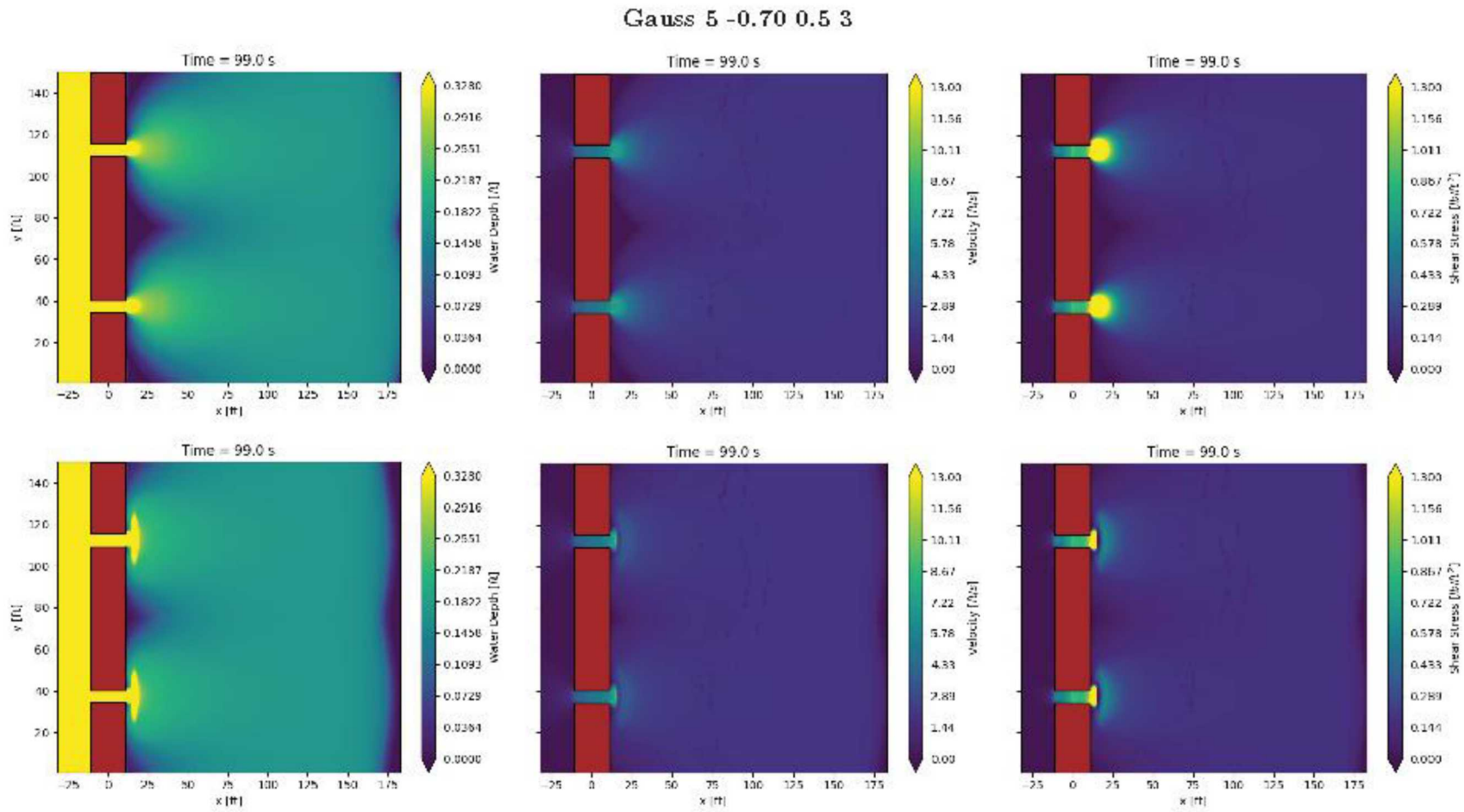

Figure 21: Top Row base case. Bottom Row Gauss x = 5 m, depth = -0.70 m, $FWHM_x$ = 0.5m, $FWHM_y$ = 3m. Column 1: Water Depth, Column 2: Velocity Magnitude, Column 3: Bed Shear-stress

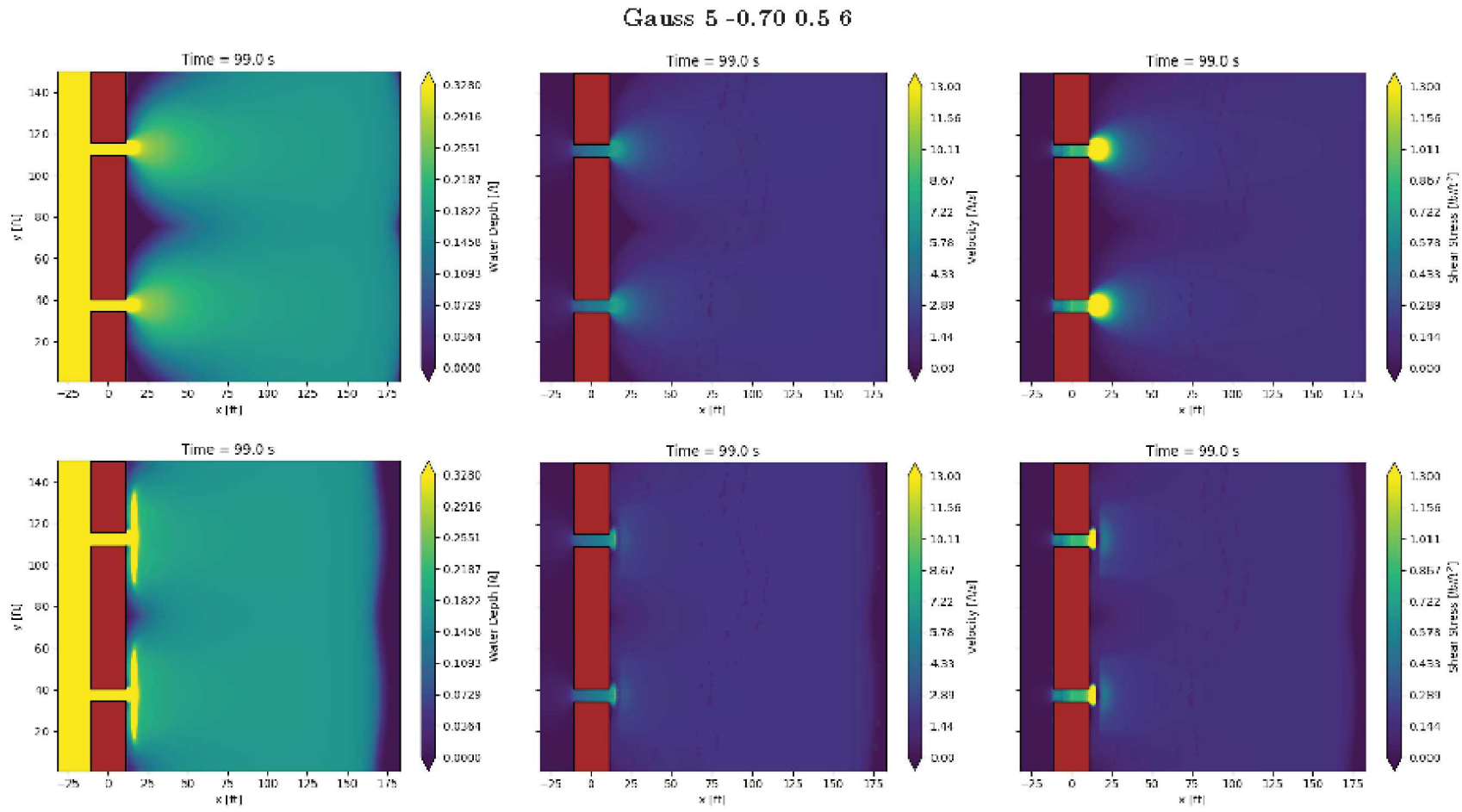

Figure 22: Top Row base case. Bottom Row Gauss x = 5 m, depth = -0.70 m, $FWHM_x = 0.5$m, $FWHM_y = 6$m. Column 1: Water Depth, Column 2: Velocity Magnitude, Column 3: Bed Shear-stress

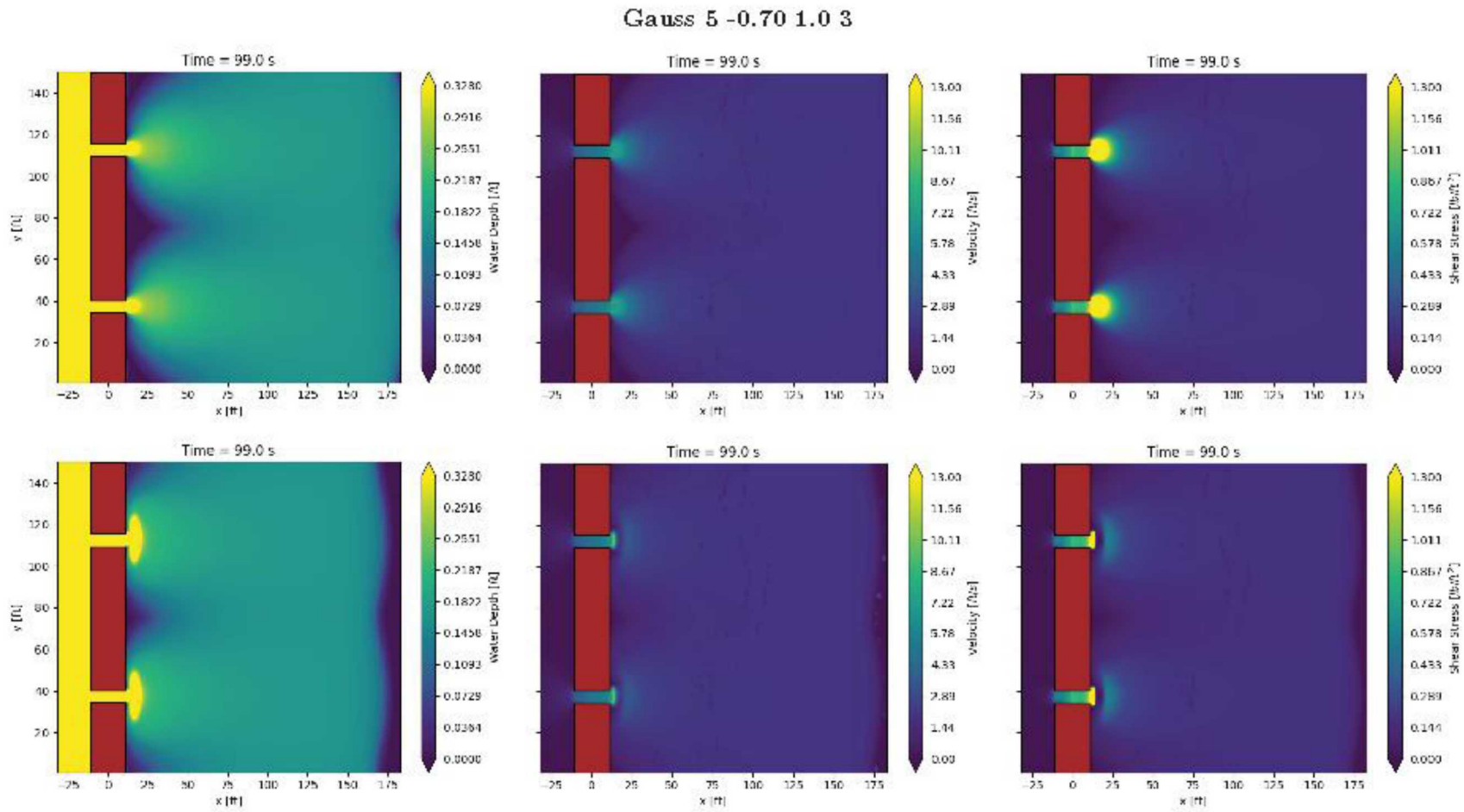

Figure 23: Top Row base case. Bottom Row Gauss x = 5 m, depth = -0.70 m, $FWHM_x = 1.0$m, $FWHM_y = 3$m. Column 1: Water Depth, Column 2: Velocity Magnitude, Column 3: Bed Shear-stress

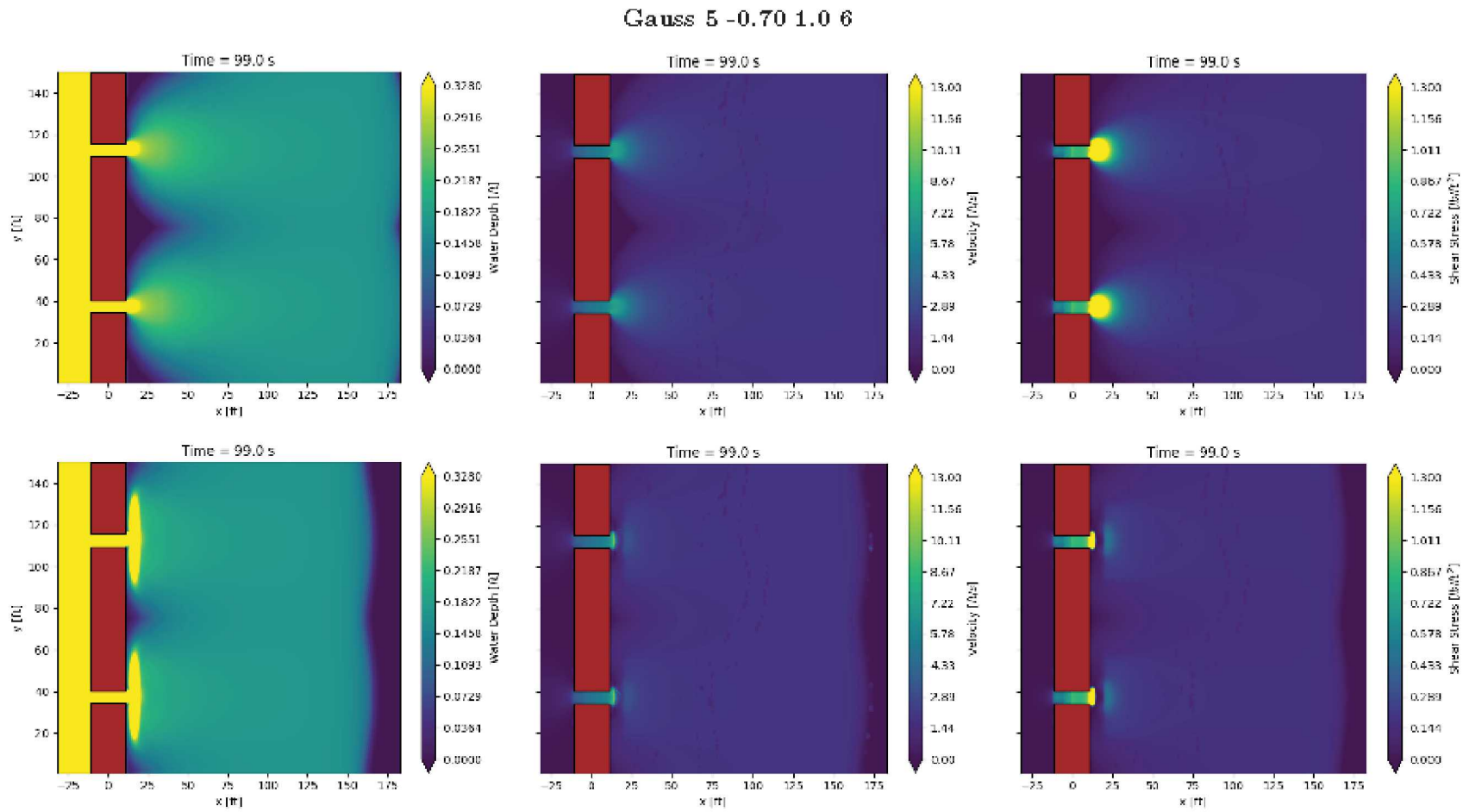

Figure 24: Top Row base case. Bottom Row Gauss x = 5 m, depth = -0.70 m, $FWHM_x = 1.0$m, $FWHM_y = 6$m. Column 1: Water Depth, Column 2: Velocity Magnitude, Column 3: Bed Shear-stress

A.3.2. Edge Field Cases

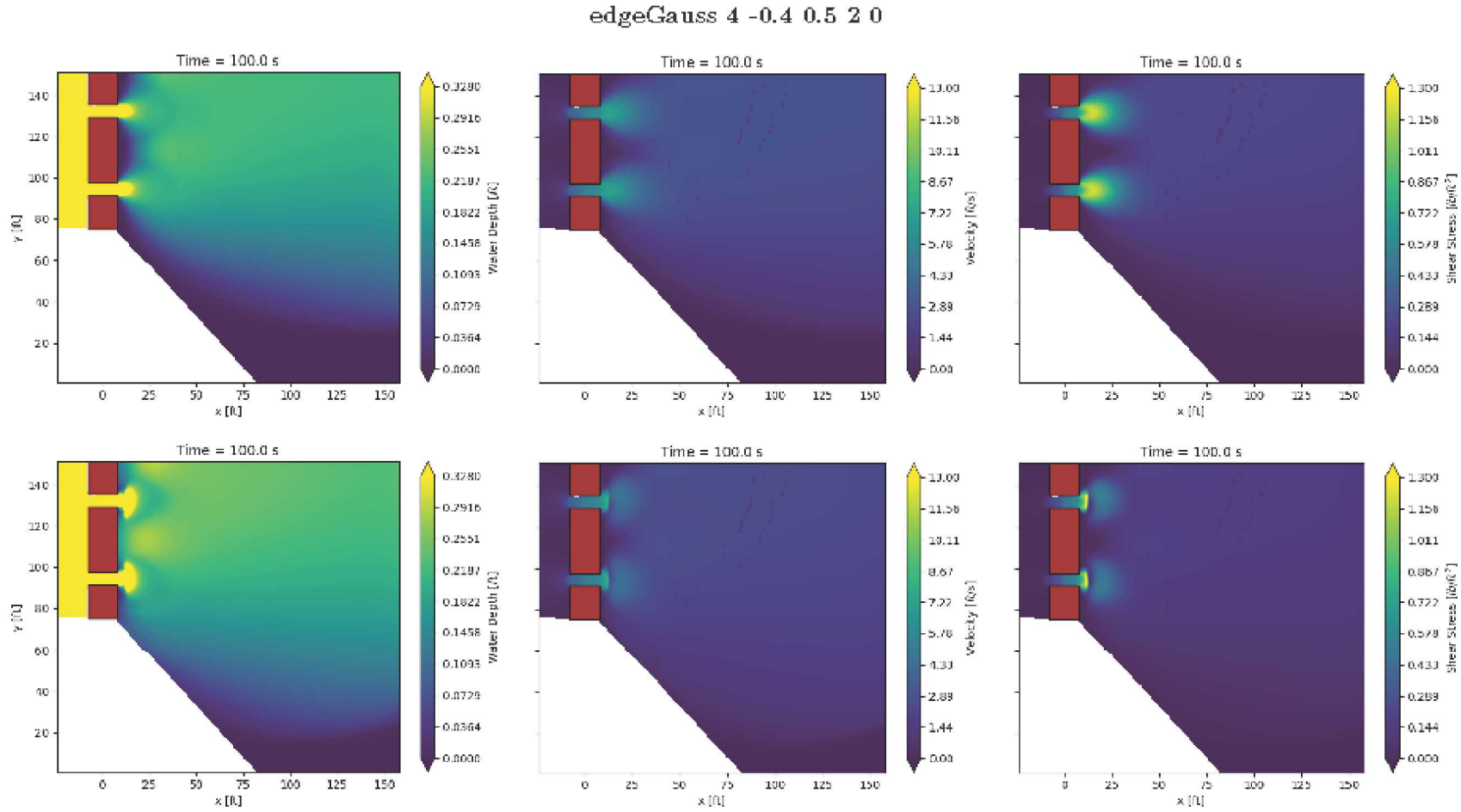

Figure 1: Top Row base case. Bottom Row edgeGauss x = 4 m, depth = -0.4 m, $FWHM_x = 0.5$m, $FWHM_y = 2$m, angle = 0 degrees counter-clockwise from the y-axis. Column 1: Water Depth, Column 2: Velocity Magnitude, Column 3: Bed Shear-stress

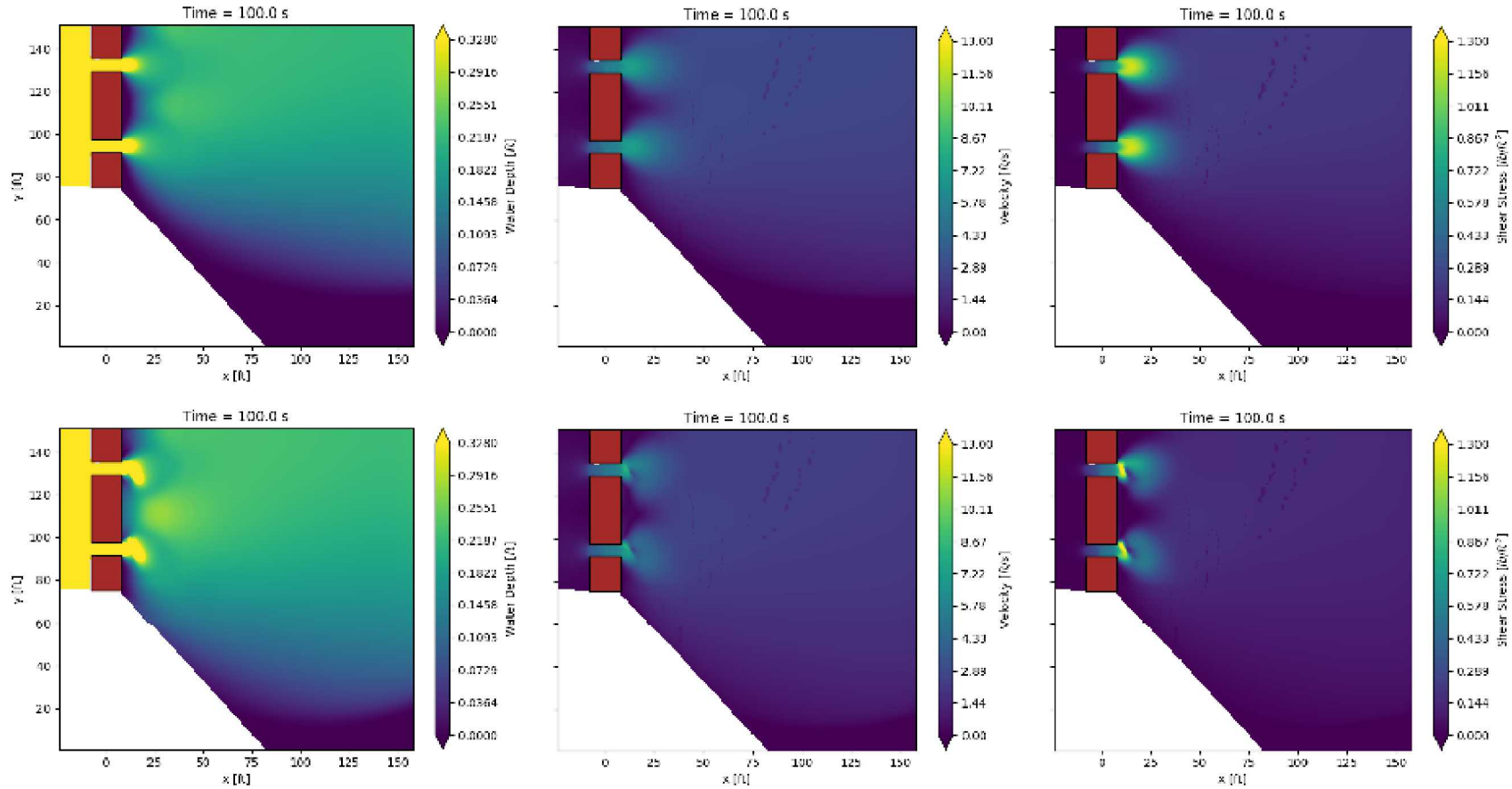

Figure 2: Top Row base case. Bottom Row edgeGauss x = 4 m, depth = -0.4 m, $FWHM_x$ = 0.5m, $FWHM_y$ = 2m, angle = 45 degrees counter-clockwise from the y-axis. Column 1: Water Depth, Column 2: Velocity Magnitude, Column 3: Bed Shear-stress

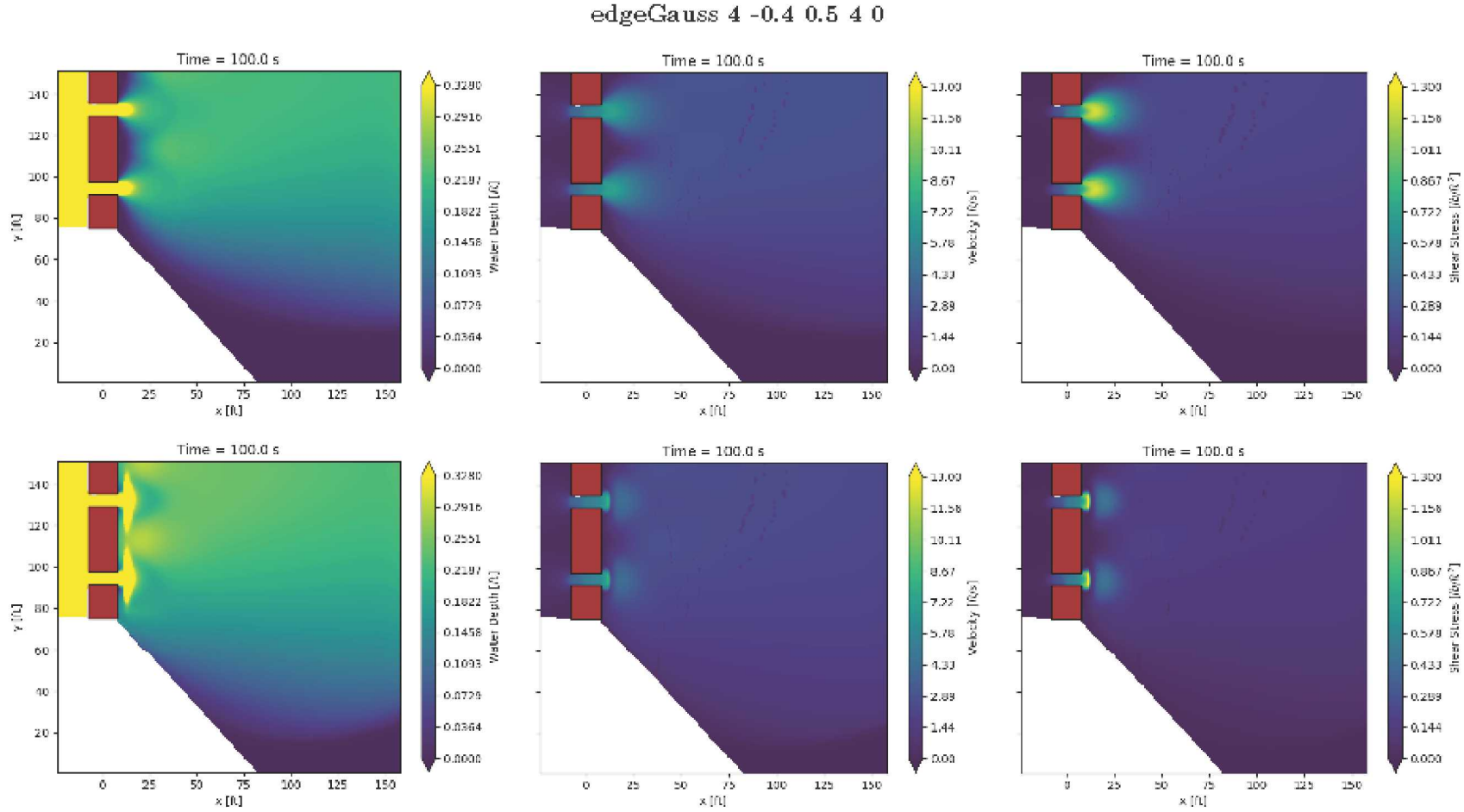

Figure 3: Top Row base case. Bottom Row edgeGauss x = 4 m, depth = -0.4 m, $FWHM_x = 0.5$m, $FWHM_y = 4$m, angle = 0 degrees counter-clockwise from the y-axis. Column 1: Water Depth, Column 2: Velocity Magnitude, Column 3: Bed Shear-stress

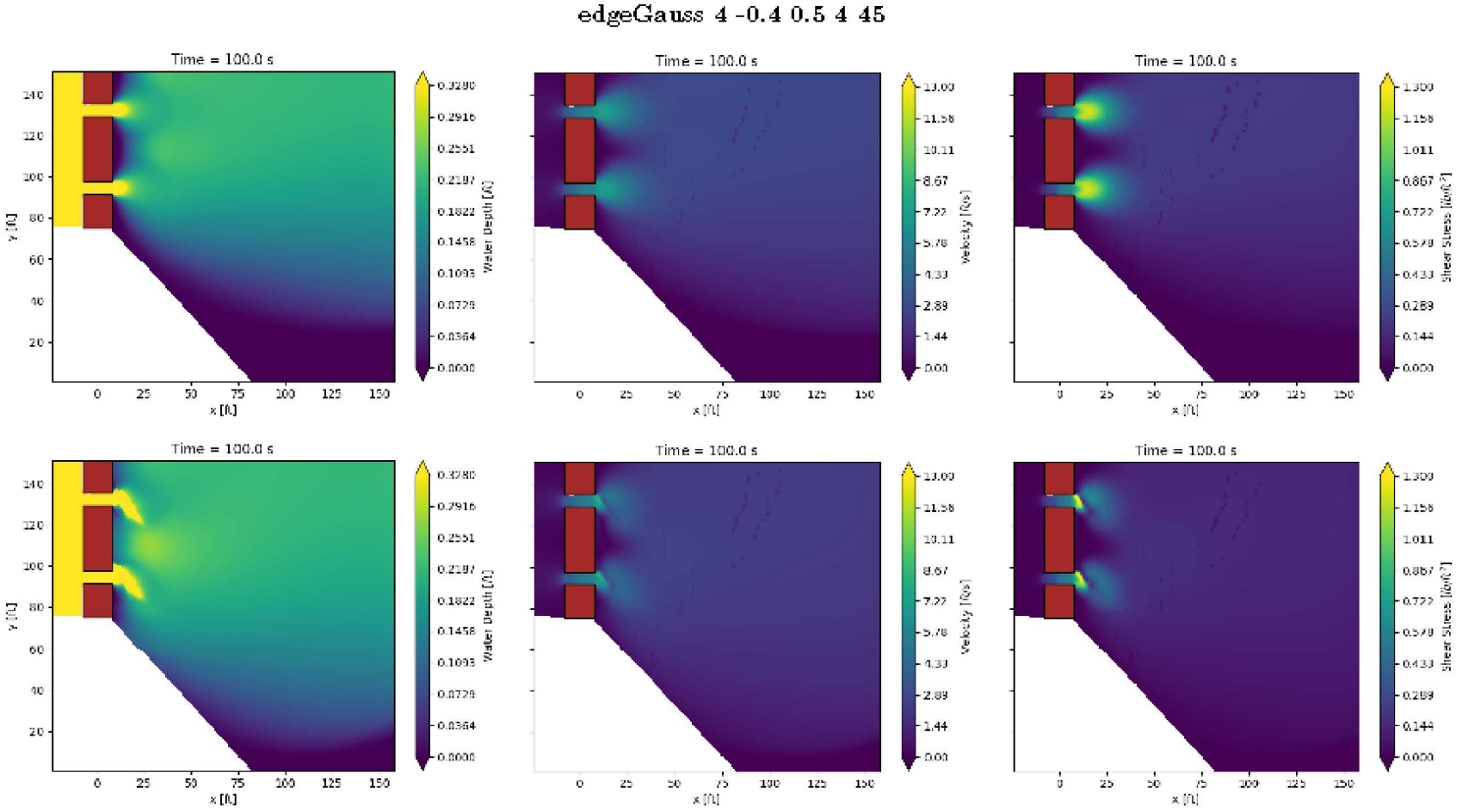

Figure 4: Top Row base case. Bottom Row edgeGauss x = 4 m, depth = -0.4 m, $FWHM_x$ = 0.5m, $FWHM_y$ = 4m, angle = 45 degrees counter-clockwise from the y-axis. Column 1: Water Depth, Column 2: Velocity Magnitude, Column 3: Bed Shear-stress

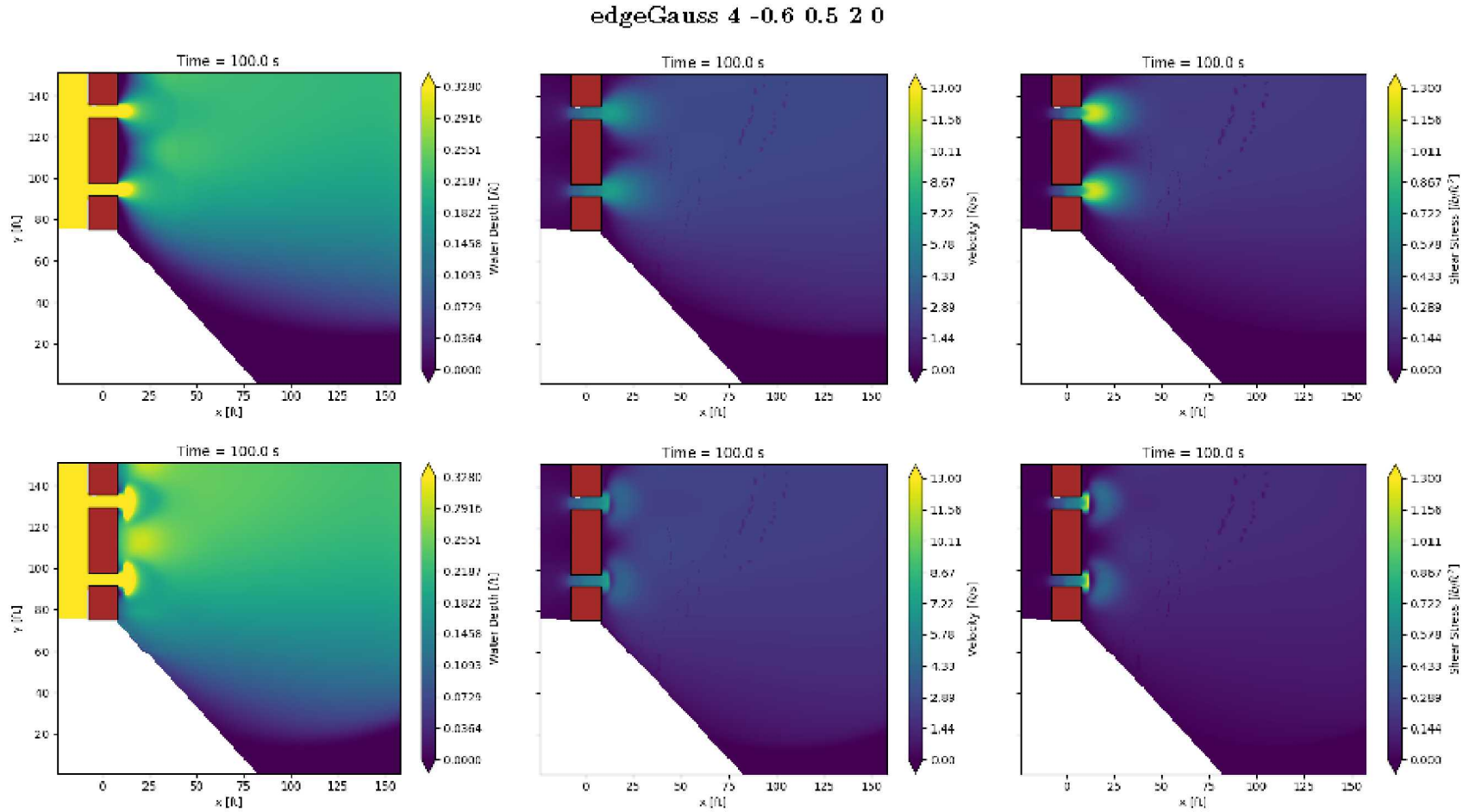

Figure 5: Top Row base case. Bottom Row edgeGauss x = 4 m, depth = -0.6 m, $FWHM_x = 0.5$m, $FWHM_y = 2$m, angle = 0 degrees counter-clockwise from the y-axis. Column 1: Water Depth, Column 2: Velocity Magnitude, Column 3: Bed Shear-stress

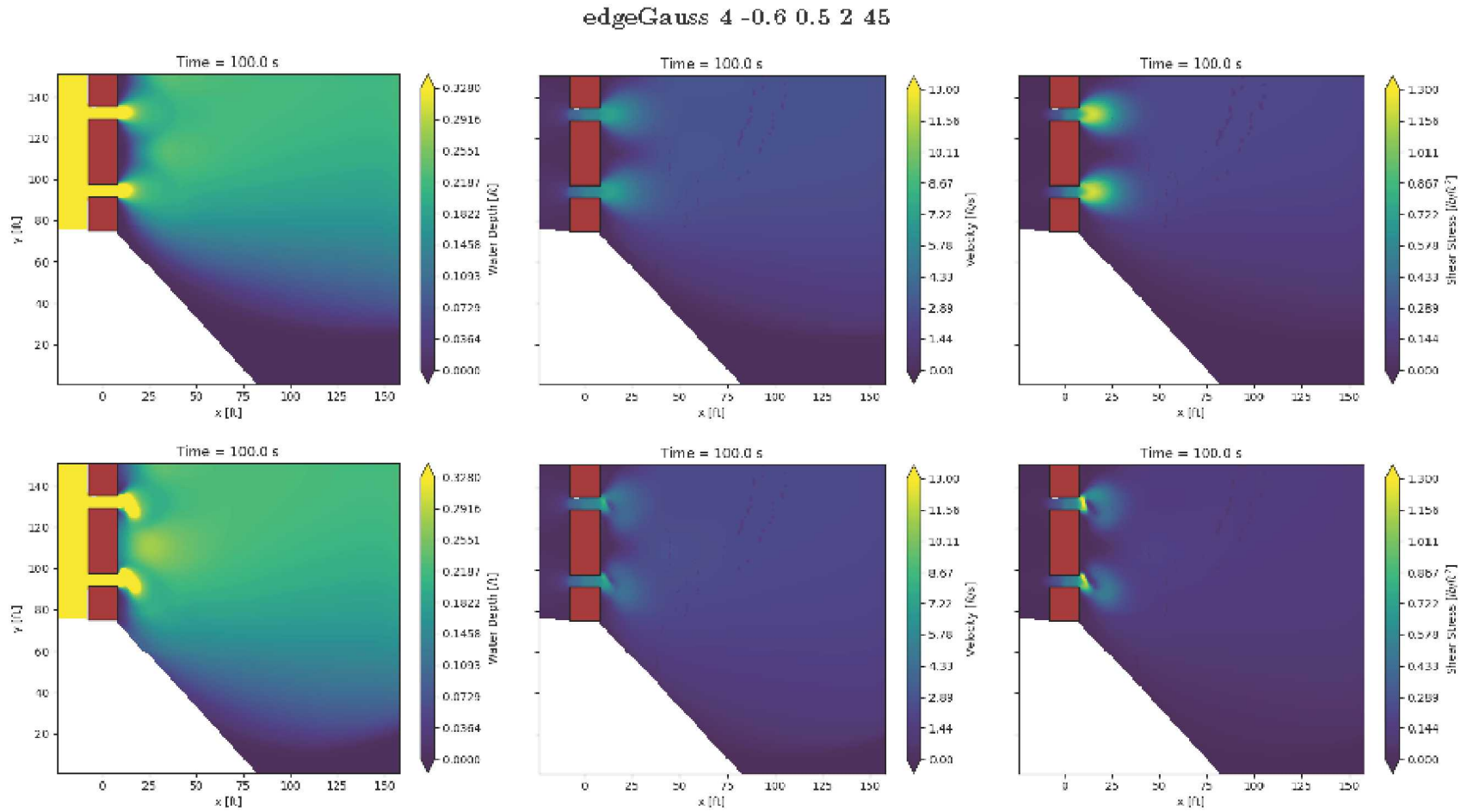

Figure 6: Top Row base case. Bottom Row edgeGauss x = 4 m, depth = -0.6 m, $FWHM_x$ = 0.5m, $FWHM_y$ = 2m, angle = 45 degrees counter-clockwise from the y-axis. Column 1: Water Depth, Column 2: Velocity Magnitude, Column 3: Bed Shear-stress

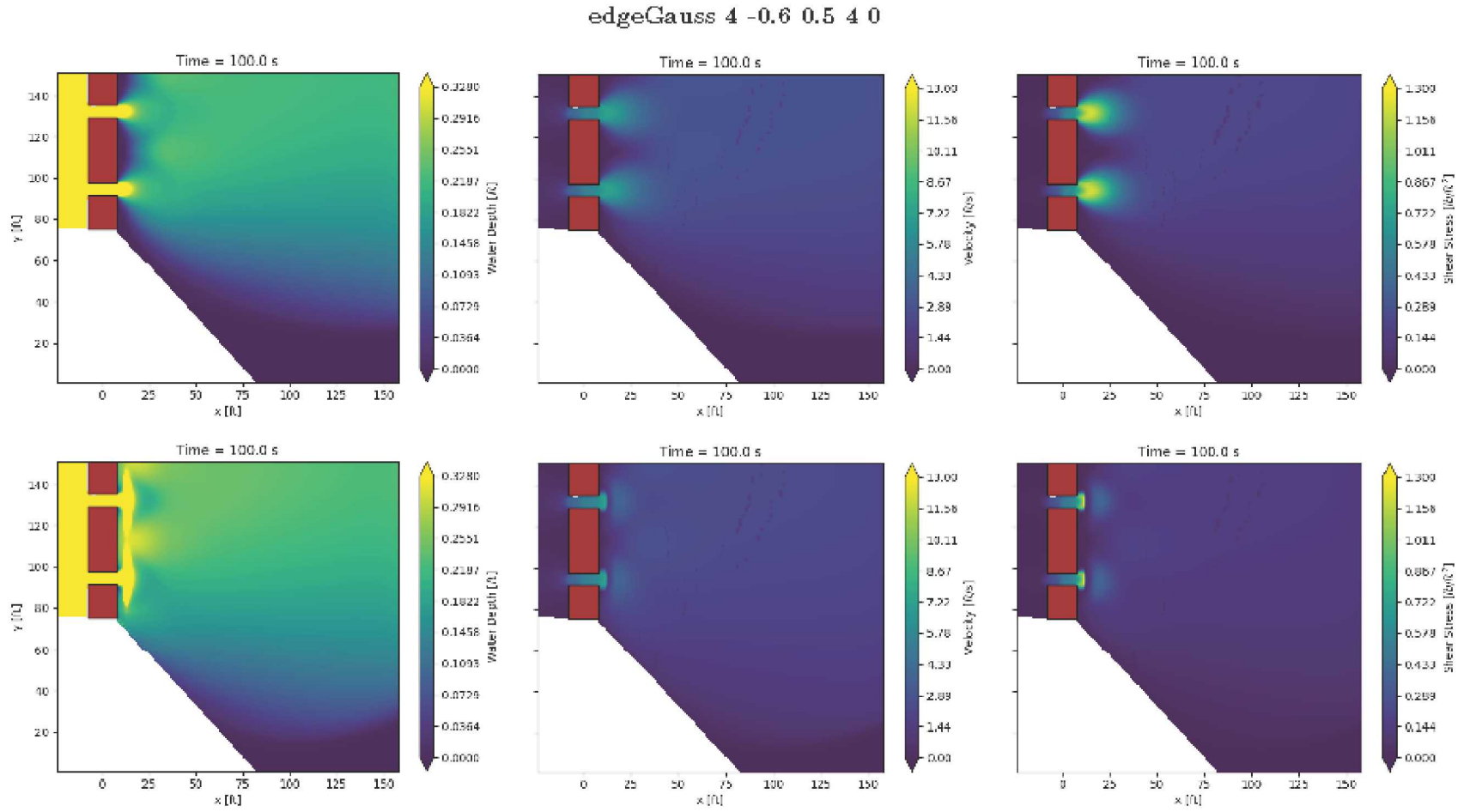

Figure 7: Top Row base case. Bottom Row edgeGauss x = 4 m, depth = -0.6 m, $FWHM_x = 0.5$m, $FWHM_y = 4$m, angle = 0 degrees counter-clockwise from the y-axis. Column 1: Water Depth, Column 2: Velocity Magnitude, Column 3: Bed Shear-stress

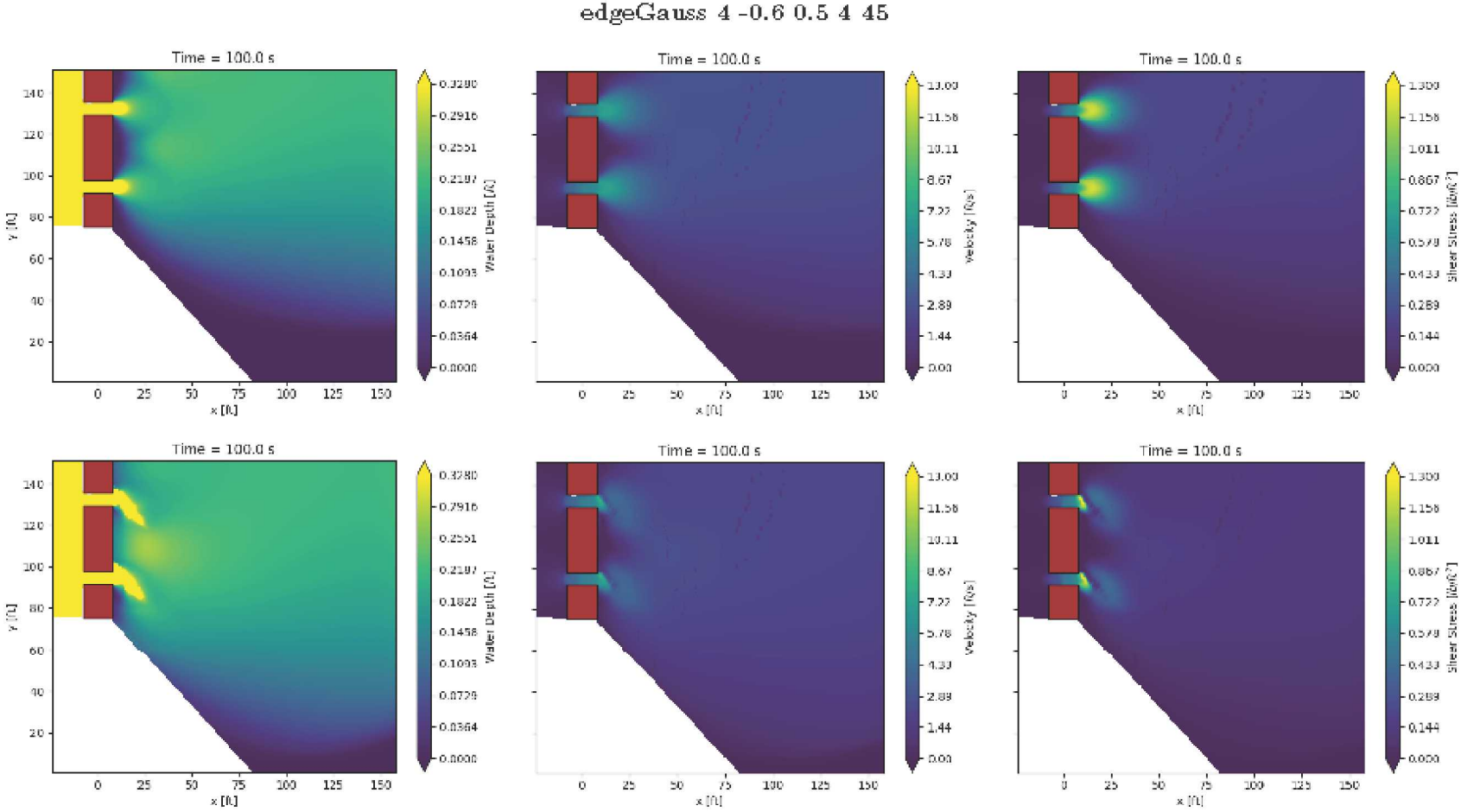

Figure 8: Top Row base case. Bottom Row edgeGauss x = 4 m, depth = -0.6 m, $FWHM_x$ = 0.5m, $FWHM_y$ = 4m, angle = 45 degrees counter-clockwise from the y-axis. Column 1: Water Depth, Column 2: Velocity Magnitude, Column 3: Bed Shear-stress

DISTRIBUTION

Email—Internal

Name	Org.	Sandia Email Address
Technical Library	01977	sanddocs@sandia.gov

This page left blank

This page left blank

Sandia National Laboratories

Sandia National Laboratories is a multimission laboratory managed and operated by National Technology & Engineering Solutions of Sandia LLC, a wholly owned subsidiary of Honeywell International Inc. for the U.S. Department of Energy's National Nuclear Security Administration under contract DE-NA0003525.